Contribution to adaptive higher order sliding mode controllers and observers : Application to energy management systems.

Hussein Obeid

SPIM

Thèse de Doctorat

école doctorale **sciences pour l'ingénieur et microtechniques**

UNIVERSITÉ DE TECHNOLOGIE BELFORT-MONTBÉLIARD

Contribution à la commande et à l'observation adaptatives par modes glissants d'ordres supérieurs - Application aux systèmes de gestion de l'énergie.

HUSSEIN OBEID

SPIM

Thèse de Doctorat

école doctorale **sciences pour l'ingénieur et microtechniques**

UNIVERSITÉ DE TECHNOLOGIE BELFORT-MONTBÉLIARD

N° | X | X | X | X |

THÈSE présentée par

HUSSEIN OBEID

pour obtenir le

Grade de Docteur de
l'Université de Technologie de Belfort-Montbéliard

Spécialité : **Automatique**

Contribution à la commande et à l'observation adaptatives par modes glissants d'ordres supérieurs - Application aux systèmes de gestion de l'énergie.

Unité de Recherche :
Femto-ST UMR CNRS

Soutenue publiquement le 05 Novembre 2018 devant le Jury composé de :

MICKAEL HILAIRET	Président	Professeur à l'IUT de Belfort-Montbéliard
JEAN-PIERRE BARBOT	Rapporteur	Professeur à l'ENSEA, Cergy-Pontoise
FRANCK PLESTAN	Rapporteur	Professeur à l'Ecole Centrale de Nantes
CHRISTOPHER EDWARDS	Examinateur	Professeur à l'Université d'Exeter, R.U
YACINE CHITOUR	Examinateur	Professeur à l'Université Paris-Sud
LEONID FRIDMAN	Co-encadrant de thèse	Professeur à l'UNAM, Mexique
MOHAMED HARMOUCHE	Co-encadrant de thèse	Ingénieur de recherche à Acitility
SALAH LAGHROUCHE	Directeur de thèse	Maître de conférences HDR, UTBM

Acknowledgment

I wish to express my gratitude to all those who helped and encouraged me during my doctoral studies. I am grateful to God for the good health and wellbeing that were necessary to complete this thesis

First of all, I would like to express my deepest gratitude to my supervisor, Salah LAGHROUCHE, for the full confidence that he has given me, and for providing me the opportunity to join his team and to work with other expert Prof. in our topic which have allowed the accomplishment of this work. I thank him for his highly professional guidance, unlimited support and unceasing encouragement. I would like to express my deepest gratitude to Leonid FRIDMAN for the great collaboration during this PhD. Since day one, he supported me and granted me his full confidence, which led to the success of this PhD. Their expertise in the domain as well as their valuable remarks have contributed the most part to the success of my PhD thesis. I highly value the friendly yet professional environment that they created during these last years of my PhD. I am extremely thankful and indebted to them for that.

Likewise, I would like to express my deepest gratitude to Mohamed HARMOUCHE for regularly discussing with me and giving me valuable advice. I highly value his patience, motivation and immense knowledge. I learned a lot from him, especially in terms of overcoming numerous obstacles that I have been facing through my research.

I would like to express my special thanks to Mr. Jean-Pierre BARBOT and Mr. Franck PLESTAN for accepting to review my PhD thesis. I would also like to thank Mr. Christopher EDWARDS, Mr. Mickael HILAIRET and Mr. Yacine CHITOUR for agreeing to examine this thesis. Their valuable remarks and hard questions helped improve the quality of this thesis.

Thank you to my childhood friends Karim and Samer. They deserve my sincerest thanks. Their friendship and assistance have meant more to me than I could ever express. My thanks also go to my friend Fouad, who gave me some useful suggestions in my daily life in France. Thank you to my colleagues and Lebanese friends inside and outside UTBM who have supported me along the way.

My wife Abir, thank you for your patience, your precious support and you believing in me. I would like to thank my uncle Ihsan and his wife Sana, who have provided me with moral and emotional support through my three years of thesis.

Last but not the least, I would like to thank my family. My parents Ayman and Nada, my brother Omar, and my sisters Sarah and Asmaa, thank you for supporting me and encouraging me. Thank you for believing in me. Thank you for asking me every single day about my progress. And thank you for being there for me anytime. I especially thank my aunts Hafsa, Samar, Amal and Hamda for supporting me spiritually through out my life. Besides, Thank you for my aunt Hind, may god have mercy on her, for accepting nothing less than excellence from me.

Contents

Abbreviations and notations

List of abbreviations

SM	Sliding Mode	BF	Barrier Function
SMC	Sliding Mode Control	PBF	Positive BF
OSM	Order Sliding Mode	PSBF	Positive Semi-definite BF
FOSMC	First Order SMC	APS	Adaptive FOSMC
HOSMC	Higher Order SMC	AST	Adaptive STC
DHOSMC	Discontinuous HOSMC	LD	Levant Differentiator
ISMC	Integral SMC	WECS	Wind Energy Conversion System
DISMC	Discontinuous ISMC	LIM	Linear Induction Motor
CISMC	Continuous ISMC	RIM	Rotary Induction Motor
ASMC	Adaptive SMC	MPPT	Maximum Point Power Tracking
AHOSMC	Adaptive HOSMC	BAFOSMC	BF-based Adaptive FOSMC
ADHOSMC	Adaptive DHOSMC	BASTC	BF-based Adaptive STC
TC	Twisting Controller	BAISMC	BF-based Adaptive ISMC
STC	Super-Twisting Controller		

List of notations

$\mathbb{R}$	Set of real numbers	$sign(.)$	The signum function
$\|\|x\|\|$	Euclidean norm of the vector x	$\lfloor x \rceil^{\gamma}$	$\|x\|^{\gamma} sign(x)$
$\|a\|$	The absolute value of the real number a		

General Introduction

The control of nonlinear physical systems in the presence of unknown external disturbances and parametric uncertainties is a hot topic of the modern control theory. Among different robust controls, the Sliding Mode/Higher Order Sliding Mode Control (SMC/HOSMC) is one of the effective techniques that handles such systems [71]. Indeed, it has proven its high efficiency due to its insensitivity to the disturbances/uncertainties and its ability to guarantee the finite-time convergence. The basic idea of this technique consists in applying discontinuous control on a system which ensures convergence of the output function (sliding variable) in a finite time to a manifold of the state-space, called the sliding manifold [74]. It has been shown in [71, 28, 66], that if the control forces the system states to remain on the sliding manifold, then their dynamics are only defined by the manifold, no longer influenced by parametric uncertainties and external disturbances in the system itself.

The implementation of SMC/HOSMC algorithms require the information of the upper bound of disturbances or the upper bound of their derivatives. In many cases, and specially in practical systems, these bounds are not constant and frequently they are unknown. Furthermore, in order to implement the SMC/HOSMC, the information about the states should be available. A well-known solution for this problem is to use the SMC algorithms to design observers that can estimate the unavailable states and/or disturbances. There again, observers and differentiators design needs the information of the upper bound of disturbances or their derivatives.

On the other hand, the SMC suffers from *chattering*; the phenomenon of finite frequency, finite-amplitude oscillations in the output which appear because the high-frequency switching excites unmodeled dynamics of the closed loop system [68]. HOSMC approaches provide chattering reduction by artificially increasing the input-output relative degree, and, consequently, are able to provide continuous control signals [28]. Nevertheless, HOSMC

algorithms include all "signum" function frequently multiplied by a gain that depends on bounds of uncertainties or bounds of their derivatives, and thus chattering is not totally deleted even by increasing the relative degree.

In some practical applications, the upper limits of disturbances or their derivatives are often difficult to calculate, or even impossible in some cases. Thus, during the control design, conservative and overestimated upper limits are used to guarantee sliding mode. As a result, this conservatism implies an overestimation of the control gain which could increase the chattering associated with unmodeled dynamics.

This problematic has motivated the researchers to develop Adaptive Sliding Mode and Higher Order Sliding Mode Controllers (ASMCs/AHOSMCs). The general goal of these techniques is to ensure a dynamical adaptation of the control gain in order to be as small as possible whereas sufficient to counteract the uncertainties/disturbances and ensures a sliding mode or a real sliding mode [58]. These techniques do not require knowledge of all or part of upper bounds of disturbances or their derivatives, while guaranteeing the convergence of the sliding variable to zero (or its neighborhood) and avoiding the overestimation of the gains.

Different ASMCs/AHOSMCs have been recently developed [70, 25, 24, 54, 7, 67, 53, 58, 64, 65]. In [70], an adaptive strategy, which is based on the concept of equivalent control [71], has been proposed to design ASMC/AHOSMC algorithms. This approach consists in increasing the gain to enforce the Sliding Mode (SM) to be reached. Then, when the SM is achieved, the equivalent control value is used in the adaptive scheme, allowing the gain to decrease to its minimal value while preserving the sliding mode (SM). However, this approach assumes that the disturbances are smooth and requires the knowledge of the minimum and the maximum allowed values of the adaptive gain. Following the concept of equivalent control, a dual-layer adaptive approach has been presented to design ASMC/AHOSMC algorithms in [25, 24]. This approach can ensure that the SM is maintained as well as the adaptive gain is as small as possible to mitigate chattering effect. Theoretically, this approach does not require any information of the disturbances or their derivatives. However, in practice, in order to design the low-pass filter to estimate the equivalent control, the filter constant should be chosen less than the inverse of the upper bound of the disturbances first derivatives (in the case of ASMC) or second derivatives (in the case of AHOSMC). This means that some information about the bounds of the disturbances or their derivatives are needed. Furthermore, to implement this strategy, the disturbances should be smooth. Another adaptive approach, which is also based on the

concept of equivalent control has been proposed to design ASMC algorithm in [54]. This approach employs a monotonically increasing gain to force the SM to be achieved. After that, the equivalent control can be used as an estimation of the disturbance. The advantages of this strategy are its simplicity and the possibility to be implemented in the case of non smooth disturbances. This adaptation does not theoretically require any information of the disturbances. However, as mentioned earlier, in practice the filter constant should be chosen less than the inverse of the upper bound of disturbances first derivatives. In [7, 67] an adaptive strategy based on the usage of discrete time criterion to verify the appearance of a real-sliding motion [71] has been developed to design ASMC/AHOSMC algorithms. In order to implement this strategy, a SM indicator which is based on the detection of real SM is introduced. The idea is to increase the control gain until the indicator reveals that the SM is reached. Then, the adaptive gain starts to decrease until the sliding mode indicator becomes negative. At this moment, the adaptive gain is increased in one impulse to ensure the achievement of SM immediately. Then, the gain decrease will take place until the SM is once more lost. This strategy can ensure the finite time convergence of the sliding variable (in the case of ASMC) and its derivative (in case of AHOSMC) to some neighborhoods of zero. However, it assumes that the disturbances are smooth and requires the knowledge of the boundaries of the disturbances's logarithmic derivatives. Moreover, when the gain reaches its minimum, it immediately jumps to its maximum value when the real SM is violated, even in the case when the change in the disturbances amplitudes is small. This adaptation mechanism can be very stressful for electromechanical systems. In [53], an adaptation of HOSMC algorithms has been presented. This adaptation consists in increasing the gain until the moment when the SM is reached, then the gain is fixed at this value, providing the convergence in a finite time of the sliding variable and its derivative to zero. The main advantage of this adaptation is that it does not require any information on the bound of disturbances or their derivatives. However, the adaptive gain in this strategy is overestimated. To overcome this problem, an approach based on increasing and decreasing the gain has been developed in [58, 64, 65] for ASMC/AHOSMC algorithms. This approach ensures the finite-time convergence of the sliding variable (in the case of ASMC) and its derivative (in case of AHOSMC) to some neighborhoods of zero. However, the sizes of these neighborhoods depend on the unknown upper bound of the disturbances or their derivatives.

This thesis deals with the development of novel strategies to adapt sliding mode and higher order sliding mode controllers and differentiators which display the following features:

- The sliding variable in case of ASMC/AHOSMC converges in a finite time to zero or to a predefined neighborhood of zero, independently of upper bounds of disturbances and their derivatives, and cannot exceed it.
- The sliding variable derivatives in the case of AHOSMC converge in a finite time to zero or to some neighborhoods of zero.
- The gains provided by proposed strategies are not overestimated.
- The proposed strategies do not theoretically require knowledge of all upper bounds of disturbances and their derivatives.

The first contribution of this thesis is the design of an adaptive strategy that can ensure the convergence of the sliding variable to a predefined neighborhood of zero without requiring any information of the disturbance or its derivative and without overestimating the adaptive gain. This adaptive strategy is then declined for the design of the first order, second order and integral sliding mode controllers, and for the Levant's differentiator. The second contribution of the thesis is the development of two adaptive strategies for discontinuous higher order sliding mode control. The proposed two algorithms can provide the achievement of n-order sliding mode despite disturbances with unknown upper bounds or with unknown upper bounds of their derivatives. Finally, in order to show the effectiveness of the proposed algorithms, they are successfully applied through simulations to control the wind energy conversion system and the linear induction motor system for cogeneration.

Organization and contributions of the thesis

Chapter 1 introduces a non-exhaustive overview of adaptive strategies to design adaptive sliding mode and higher order sliding mode controllers proposed in the scientific literature along with their advantages and disadvantages.

In **Chapter 2**, two adaptive techniques called barrier functions are presented. The main feature of these functions is that they tend to infinity when their arguments come close to some predefined limits. Based on this attractive feature, a new adaptive strategy for first order SMC is developed. The proposed adaptive algorithm can be applied to a class of first order disturbed systems whose disturbance is bounded with an unknown boundary. It can

ensure the convergence of the sliding variable and maintain it in a predefined neighborhood of zero independent of the upper bound of the disturbance, without overestimating the control gain. Then, this adaptive strategy is applied to adapt the gain of a Discontinuous Integral Sliding Mode Controller (DISMC). This adaptation allows such controller to be implemented to a class of arbitrary order disturbed systems with unknown bounded disturbance. It can ensure that the auxiliary variable belongs to a predefined neighborhood of zero starting from the initial time moment. The properties of both proposed adaptive algorithms are demonstrated through simulation examples.

Chapter 3 presents an adaptive version of Super-Twisting Controller (STC) for disturbed first order system where the disturbance is Lipschitz with unknown Lispchitz constant. The adaptation law is based on the barrier strategy introduced in the previous chapter. Unlike other adaptive versions of STC, the proposed one can ensure the convergence of the sliding variable and maintain it in a predefined neighborhood of zero independent of the upper bound of the disturbance derivative, without overestimating the control gain and without requiring neither the upper bound of the disturbance derivative nor the use of the low-pass filter. Then, based on the barrier strategy, an adaptive version of a Continuous Integral Sliding mode controller (CISMC) is proposed. This algorithm ensures that the auxiliary variable belongs to a predefined neighborhood of zero starting from the initial time moment. Moreover, it allows to avoid the reaching phase, and guarantees that the adaptive gain is not overestimated. The properties of both proposed adaptive algorithms are demonstrated through simulation examples.

In **Chapter 4** the barrier function is used to adapt Levant's Differentiator (LD). This adaptation is useful for the case when the upper bound of second derivative of base signal exists but it is unknown. Thanks to its feature, from the initial time moment it can be guaranteed that the error of estimation of the signal belongs to a predefined vicinity of zero. Moreover, the proposed adaptive strategy can ensure the convergence of LD to some vicinity of the first derivative. Then, a comparison between different adaptation strategies of LD to estimate the first derivative is drawn. Without noise, it is shown that the proposed adaptive strategy is in competition with the known strategies of adaptation. In the presence of noise, the main advantage of the proposed adaptive strategy is that it could indicate when LD does not converge. On the other hand, the other existing strategies for LD adaptation [64, 53] could converge to the sum of the derivatives of the base and noise

signals and it is impossible to identify it.

Chapter 5 proposes two different adaptive Discontinuous HOSMC (DHOSMC) strategies. These controllers are based on the adaptation of homogeneous DHOSMC strategies proposed in [22]. The first strategy consists in growing the gain until the sliding mode is achieved and it can be applied in the case of bounded disturbances with unknown upper bound. While the second strategy comprises a novel dual layer adaptation and can be applied in the case of Lipschitz disturbance with unknown Lipschitz constant.
To the best of our knowledge, the proposed adaptive DHOSMCs are the first that ensure the finite time convergence of the states to zero without requiring any information about the disturbances.

Chapter 6 addressees the active and reactive power control of a Wind-Energy Conversion System (WECS). Due to the high complexity of wind-energy conversion system which comes from the nonlinear system dynamics and parameter uncertainties, adaptive SMCs are required for this system. Then, in this chapter the adaptive first order SMC and STC are applied. These adaptive controllers can extract the maximum power and achieve the reference reactive power with predefined errors, independent of the upper bound of the disturbance/uncertainties and their derivatives. Performances of proposed controllers applied to WECS have been demonstrated and compared through simulations.

Chapter 7 focuses on the control of linear induction motor used in cogeneration system. For linear induction motor, the control objective can be summarized as driving the actual speed and flux to their desired values. Since the flux dynamics and the speed dynamics can be considered as disturbed double integrator systems where the upper bound of the disturbances and their derivatives are unknown, the adaptive SMCs are required for this system. Hence, the adaptive versions of DISMC, CISMC and the adaptive DHOSMCs are applied. Moreover, their performances are compared.

In the end, some concluding remarks and perspectives on expansion of the work are presented in the chapter **Conclusion and perspectives**.

Some of the results presented in this thesis have been published or are under revision process for publication in journals and conferences.

Peer-reviewed journal papers

- H. Obeid, L. Fridman, Salah Laghrouche, M. Harmouche, M. Ali Golkani, *Adaptation of Levant's Differentiator Based on Barrier Function*, International journal of control, DOI: 10.1080/00207179.2017.1406149.

- H. Obeid, L. Fridman, S. Laghrouche, Mohamed Harmouche, *Barrier Function-Based Adaptive Sliding Mode Control*, Automatica, DOI: 10.1016/j.automatica.2018.03.078.

Journal papers submitted for peer-review

- H. Obeid, L. Fridman, S. Laghrouche, Mohamed Harmouche, *Barrier Function-Based Adaptive Super-Twisting Controller*, Submitted to IEEE Transactions on Automatic Control.

Peer-reviewed international conference papers

- H. Obeid, L. Fridman, S. Laghrouche, M. Harmouche, *Barrier Adaptive First Order Sliding Mode Differentiator*, IFAC World Congress, Toulouse, France, 2017.

- H. Obeid, L. Fridman, S. Laghrouche, M. Harmouche, *Barrier Function-Based Adaptive Twisting Controller*, 15^{th} International Workshop on Variable Structure Systems and Sliding Mode Control (VSS18), Graz Universitiy of Technology, Austria, 2018.

- H. Obeid, L. Fridman, Salah Laghrouche, M. Harmouche, *Barrier Function-Based Adaptive Integral Sliding Mode Control*, 57^{th} IEEE Conference on Decision and Control (CDC 2018), Fontainebleau, Miami Beach, USA, 2018.

Chapter 1

State-of-Art on adaptive sliding mode control

Nonlinear dynamic physical systems suffer from parametric uncertainty and are difficult to characterize. Parametric uncertainty arises from varying operating conditions and external disturbances that affect the physical characteristics of systems. The variation limits or the bounds of this uncertainty might be known or unknown. This needs to be considered during control design so that the controller counteracts the effect of variations and guarantees desired performances under different operating conditions. Sliding Mode and Higher Order Sliding Mode control (SMC/HOSMC) [71] is a well-known method for control of nonlinear systems, renowned for its insensitivity to parametric uncertainty and external disturbances. This technique is based on applying discontinuous control on a system which ensures a convergence of the output function (sliding variable) in a finite time to a manifold of the state-space, called the sliding manifold [74].

The implementation of SMC/HOSMC algorithms requires the information of the upper bound of the disturbances or the upper bound of their derivatives. For instance, the implementation of the Super-Twisting Control (STC) requires the knowledge of the upper bound of disturbances derivatives. In many cases, these bounds are not constant and, moreover, frequently they are unknown.

On the other hand, the SMC suffers from *chattering*; the phenomenon of finite-frequency, finite-amplitude oscillations in the output which appear because the high-frequency switching excites unmodeled dynamics of the closed loop system [68]. HOSMC is an effective method for chattering attenuation [28]. Indeed HOSM controllers [63] provide

chattering attenuation across artificially increasing the input-output relative degree, and, consequently, are able to produce continuous control signals. However, SMC/HOSMC algorithms contain "signum" multiplied by a control gain that depends on the upper bound of disturbances or their derivatives, and therefore chattering is not totally eliminated even in the case where HOSMC algorithms are used.

During the last decade several control strategies have been published on adaptive sliding mode and higher order sliding mode control (ASMC/AHOSM). The objective of these strategies is to adapt the gains of controllers in such a way that the sliding mode (or the real sliding mode [45]) is achieved in a finite time with non-overestimation of control gains, while eliminating or decreasing the required information of the bounds of the disturbances and their derivatives.

In this chapter a descriptive, non-exhaustive overview of ASMC/AHOSMC strategies proposed in the scientific literature is presented. This chapter is organized as follows: we first recall definitions of an ideal and a real sliding mode. Then, non-exhaustive adaptive strategies to design adaptive ASMCs/AHOSMCs are presented along with their advantages and disadvantages.

1.1 Preliminaries

Consider the perturbed chain of integrators of order n

$$\begin{aligned} \dot{x}_1(t) &= x_2(t) \\ &\vdots \quad \vdots \quad \vdots \\ \dot{x}_n(t) &= u(t) + \delta(t), \\ s(t) &= x_1(t), \end{aligned} \tag{1.1}$$

with $x = [x_1, \ldots, x_n]^T \in \mathcal{X} \subset \mathbb{R}^n$ is the state vector ($\mathcal{X}$ is a bounded subset of $\mathbb{R}^n$), $u \in \mathbb{R}$ is the control input, $\delta(t)$ is an unknown disturbance, and $s(t)$ is a measured smooth output-feedback function, named sliding variable. The control task is to make $s(t)$, vanish in a finite time and to keep it at zero afterwards.

System (1.1) has a relative degree n with respect to $s(t)$. It means [37] that for the first time the control explicitly appears in the nth total time derivative of s, i.e.

$$s^{(n)}(t) = u(t) + \delta(t). \tag{1.2}$$

The assumptions on the disturbance $\delta(t)$ will depend on each adaptive algorithm, therefore they will be presented in each section. Before describing each adaptive algorithm, the definitions of an ideal and a real sliding mode are given.

Definition 1.1.1. *[63] Consider system* (1.1) *with the sliding variable* $s(t)$*. Then, if*

1. *the successive time derivatives* $s, \dot{s}, \cdots, s^{(n-1)}$ *are continuous functions;*

2. *the set*

$$\left\{x \in \mathcal{X} \,|\, s = \dot{s} = \cdots = s^{(n-1)} = 0\right\} \tag{1.3}$$

   is a nonempty integral set;

3. *the Filippov set of admissible velocities at the* n*-sliding points* (1.3) *contains more than one vector;*

the motion on the set (1.3) *is said to exist in an ideal* n^{th}*-order sliding mode (*n*-OSM). The set* (1.3) *is called the* n*-OSM set.*

Definition 1.1.2. *[45] Consider system* (1.1) *and the sliding variable* $s(t)$*. Assume that the successive time derivatives* $s,\ \dot{s}, \cdots,\ s^{(n-1)}$ *are continuous functions. The manifold defined as (*τ *being the sampling period of the control law)*

$$\left\{x|\ |s| \leq \mu_0 \tau^n, \cdots, |s^{(n-1)}| \leq \mu_{n-1}\tau\right\} \tag{1.4}$$

with $\mu_i \geq 0$ *(with* $0 \leq i \leq n-1$*), is called a real* n*-OSM set, which is nonempty and is locally an integral set in the Fillipov sense. The motion on this manifold is called a real* n*-OSM with respect to the sliding variable* $s(t)$*.*

1.2 Utkin's adaptation

This adaptation is based on the concept of equivalent control [71]. It consists in increasing the gain to enforce SM to be reached. Then, when the SM is achieved, the equivalent control value is used in the adaptive scheme, allowing the gain to decrease to its minimal value while preserving the SM. Hence, it reduces the amplitude of the chattering. This adaptation has been applied to adapt FOSMC and STC [70] as will be shown in the next subsections.

1.2.1 FOSMC based on Utkin's adaptation

Consider the sliding variable dynamic (1.2) with $n = 1$ under the assumption that the disturbance satisfies $|\delta(t)| < \delta_{max}$ and $|\dot{\delta}(t)| < M$, where δ_{max} and M are finite and known. The Utkin's adaptive FOSMC takes the following form

$$u = -K(t)sign(s), \tag{1.5}$$

where

$$\dot{K}(t) = \rho K(t)sign(\zeta(t)) - N[K(t) - K^+]_+ + N[\mu - K(t)]_+, \tag{1.6}$$

with

$$[z]_+ := \begin{cases} 1 & if\ z \geq 0 \\ 0 & if\ z < 0 \end{cases}, \quad N > \rho K^+, \quad K^+ > \delta_{max}, \quad \rho > 0. \tag{1.7}$$

and

$$\zeta(t) = |[sign(s(t))]_{eq}| - \alpha, \quad \alpha \in (0, 1). \tag{1.8}$$

The function $[sign(s(t))]_{eq}$ is the average value (equivalent control) of the discontinuous signal $sign(s(t))$ which can be obtained by the following low-pass filter

$$\frac{d}{dt}[sign(s(t))]_{eq} = \frac{1}{\tau}\Big(sign(s(t)) - [sign(s(t))]_{eq}\Big), \tag{1.9}$$

with $\tau > 0$ is the filter time constant.

The objective here is to first achieve ideal 1-OSM. Then to decrease $|[sign(s(t))]_{eq}|$ until it becomes close to 1. This leads to maintaining ideal 1-OSM as well as decreasing the amplitude of $K(t)$ (i.e. amplitude of chattering). However, even this adaptation can maintain ideal 1-OSM, it can be only applied in the case when the bounds of the disturbance and its derivative are known.

1.2.2 Application of Utkin's adaptation to STC

Consider the sliding variable dynamic in (1.2) with $n = 1$ and under the assumption that the disturbance satisfies $|\ddot{\delta}(t)| < M^*$ where M^* is finite and it is known. The Utkin's adaptive STC is defined as

$$\begin{cases} u(t) = -\bar{\alpha}|s|^{\frac{1}{2}}sign(s) + u_2(t) \\ \dot{u}_2 = -K(t)sign(s), \end{cases} \tag{1.10}$$

with $\bar{\alpha} > 0$ is chosen sufficiently large, and

$$\dot{K}(t) = \begin{cases} \gamma_0 k(t) sign(\zeta(t)) - N[K(t) - K^+]_+ + N[\mu - K(t)]_+ & \text{if } 0 < \mu \leq K(t) \leq K^+, \\ 0 \quad \text{otherwise,} \end{cases} \tag{1.11}$$

where $\gamma_0 > M^*/\mu$, $\mu > 0$ is a preselected minimal value of $K(t)$ and K^+ is a sufficient value for enforcing SM.

The objective of this adaptation is to minimize the magnitude of the discontinuous input $K(t)sign(s)$ while providing ideal 2-OSM. Although, it can achieve this objective, this adaptation requires the knowledge of the minimum and maximum allowed values of the adaptive gain.

1.3 Edwards & Shtessel's adaptation

Inspired by Utkin's adaptation, this strategy has been developed in order to overcome the requirement of information about the disturbance bounds. As Utkin's idea, this strategy uses the concept of equivalent control in the adaptation process. Moreover, it is based on a dual layer adaptive structure which can ensure that the SM is maintained as well as the adaptive gain is as small as possible to mitigate chattering effect.
The application of this adaptation to design FOSMC and STC and continuous HOSMC [25, 24] are studied in the following subsections.

1.3.1 Application to FOSMC

Consider the sliding mode Eq. (1.2) with $n = 1$ and with the disturbance $\delta(t)$ which satisfies $|\delta(t)| < \delta_{max}$ and $|\dot{\delta}(t)| < M$, where δ_{max} and M are finite. The control law is defined as

$$u(t) = -(K(t) + \nu) sign(s), \tag{1.12}$$

where ν is a small positive constant and $K(t)$ is the adaptive control gain. Before defining explicitly the dynamic of $K(t)$, it is assumed that there exists a finite time $t_f > 0$, such that $\forall t > t_f$ the following inequality holds

$$||\bar{u}_{eq}(t) - u_{eq}(t)|| < \varepsilon_1 |u_{eq}(t)| + \varepsilon_0, \tag{1.13}$$

where $||.||$ represents the Euclidean norm, $1 > \varepsilon_1 > 0$, $\varepsilon_0 > 0$ are scalars, $u_{eq}(t)$ is the so-called equivalent control obtained during the sliding motion (i.e. when $s = \dot{s} = 0$) and given

by $u_{eq}(t) = -\delta(t)$, and $\bar{u}_{eq}(t)$ is the approximation in a real-time by low-pass filtering of the switching signal $u(t)$ and it satisfies

$$\dot{\bar{u}}_{eq}(t) = \frac{1}{\tau}\Big(-(K(t)+\nu)sign(s) - \bar{u}_{eq}(t)\Big), \tag{1.14}$$

with $\tau > 0$ is the filter time constant.
Under this assumption, the adaptive gain dynamic $K(t)$ is given by

$$\dot{K}(t) = -\rho(t)sign(\zeta(t)), \tag{1.15}$$

where

$$\rho(t) = r_0 + r(t), \tag{1.16}$$

with r_0 is a fixed positive scalar, $r(t)$ follows a differential equation that will be defined later (in accordance with the assumption on M), and $\zeta(t)$ is described by

$$\zeta(t) = K(t) - \frac{1}{\alpha}|\bar{u}_{eq}(t)| - \varepsilon, \tag{1.17}$$

where $0 < \alpha < 1$ and $\varepsilon > 0$ are design scalars to ensure that $\bar{u}_{eq}(t)$ satisfies

$$\frac{1}{\alpha}|\bar{u}_{eq}(t)| + \varepsilon/2 > |u_{eq}(t)|. \tag{1.18}$$

Now, in order to define $r(t)$, two cases will be considered: firstly the case when M is known, and secondly when it is unknown.

1.3.1.1 Case when the bound M is known

In this case, $r(t)$ is computed through

$$\dot{r}(t) = \gamma|\zeta(t)| + r_0\sqrt{\gamma}sign(e(t)), \tag{1.19}$$

where $\gamma > 0$ is a design scalar and $e(t)$ satisfies

$$e(t) = q\frac{M}{\alpha} - r(t), \tag{1.20}$$

with $q > 1$ is chosen to ensure that $\frac{d}{dt}|(\bar{u}_{eq}(t))| < qM$.
This dual layer adaptive scheme (1.15)-(1.19) forces $\zeta(t) = 0$ in finite time. Consequently, it ensures the achievement of ideal 1-OSM (i.e. $s = 0$), since $\zeta(t) = 0$ yields

$$K(t) = \frac{1}{\alpha}|\bar{u}_{eq}(t)| + \varepsilon > |u_{eq}(t)| = |\delta(t)|, \tag{1.21}$$

which is exactly the condition necessary to maintain 1-OSM. However, in this case it is supposed that M is known and only δ_{max} is unknown.

1.3.1.2 Case when the bound M is unknown

In this case, it is assumed that both δ_{max} and M are unknown. The dynamics of $r(t)$ is defined now as

$$\dot{r}(t) = \begin{cases} \gamma|\zeta(t)| & \text{if } |\zeta(t)| > \zeta_0 \\ 0 & \text{otherwise,} \end{cases} \tag{1.22}$$

where ζ_0 is a design scalar.

This dual layer adaptive scheme given by (1.15)-(1.27) also ensures the achievement in finite time of ideal 1-OSM. However, in both cases, the disturbance should be smooth. Moreover, the filter time constant used in the estimation of u_{eq} should be chosen much less than the inverse of the upper bound of the first derivative of the disturbance. This latter is unknown.

1.3.2 Application to STC (Adaptation of one gain)

Consider once again the sliding mode Eq. (1.2) with $n = 1$, but now under the assumption that $|\dot{\delta}(t)| \leq M$ where $M > 0$ and $|\ddot{\delta}(t)| < M^*$. The control law is given by

$$\begin{aligned} u(t) &= -\lambda|s|^{1/2} sign(s) + u_2(t), \\ \dot{u}_2(t) &= -K(t) sign(s), \end{aligned} \tag{1.23}$$

where $\lambda > 0$ is chosen sufficiently large, and $K(t)$ is to be adapted. Suppose that $\phi(t) = u_2(t) + \delta(t)$ and $\omega(t) = K(t) sign(s)$, then the dynamic of the first order system can be expressed as

$$\begin{cases} \dot{s}(t) = -\lambda|s|^{\frac{1}{2}}(t) sign(s) + \phi(t), \\ \dot{\phi}(t) = -\omega(t) + \dot{\delta}(t). \end{cases} \tag{1.24}$$

Here, the equivalent control $\omega_{eq}(t)$ is obtained when ideal 2-OSM is achieved (i.e. $s = \phi = 0$) and given by $\omega_{eq}(t) = \dot{\delta}(t)$. Moreover, as in the previous subsection, $\bar{\omega}_{eq}(t)$ is available by low-pass filtering $w(t)$ and satisfies similar bounds with respect to $\omega_{eq}(t)$ as in (1.18). Again, in order to define $r(t)$, two cases will be considered: first the case when the bound M^* is known, and second when the bound M^* is unknown.

1.3.2.1 Case when the bound M^* is known

In this case, the dual layer scheme is given by (1.15)-(1.16)-(1.19) where

$$\zeta(t) = k(t) - \frac{1}{\alpha}|\bar{w}_{eq}(t)| - \varepsilon, \tag{1.25}$$

with $0 < \alpha < 1$, $\varepsilon > 0$ is a small real number, and

$$e(t) = \bar{q}M^*/\alpha - r(t), \tag{1.26}$$

where $\bar{q} > 1$ represents a user defined gain.
This dual-layer scheme for STC provides in finite time an ideal 2-OSM.

1.3.2.2 Case when the bound M^* is unknown

In this case, the dual layer scheme is defined in (1.15)-(1.16) where

$$\dot{r}(t) = \begin{cases} \gamma|\zeta(t)| & \text{if } |\zeta(t)| > \zeta_0 \\ 0 & \text{otherwise,} \end{cases} \tag{1.27}$$

with γ and ζ_0 are positive scalars, and $\zeta(t)$ satisfies (1.25). This dual-layer scheme for STC also provides in finite time an ideal 2-OSM.

It is important to note that in both cases, the dual layer scheme is applied to adapt one gain of STC while the other gain λ is supposed to be sufficiently large (i.e. overestimated). Therefore, this adaptation can increase the amplitude of chattering.

1.3.3 Application to STC (Adaptation of both gains)

To deal with the above problem (i.e. adaptation of one gain), the same dual layer strategy has been employed to adapt both gains of STC instead of only one gain. The system in Eq. (1.2) is considered with $n = 1$, under the assumption that $|\dot{\delta}(t)| \leq M$ where $M > 0$ and $|\ddot{\delta}(t)| < M^*$. The STC structure is now modified and a new additional time varying gain is introduced within as follows

$$\begin{aligned} u(t) &= -\lambda(t)sign(s(t))|s(t)|^{1/2} + u_2(t) - s(t)\dot{K}(t)/K(t) \\ \dot{u}_2(t) &= -\beta(t)sign(s(t)), \end{aligned} \tag{1.28}$$

where

$$\lambda(t) = \sqrt{K(t)}\lambda_0, \quad \beta(t) = K(t)\beta_0, \tag{1.29}$$

with λ_0 and $\beta_0 > 1$ are fixed positive scalars and $K(t) > 0$ is the adaptive gain. Now $K(t)$ follows (1.15)-(1.16) with

$$\dot{r}(t) = \gamma|\zeta(t)|, \tag{1.30}$$

where γ is positive scalar, and $\zeta(t)$ satisfies (1.25).

This algorithm ensures in finite time that $K(t) > |\dot{\delta}(t)|$, which leads the achievement of ideal 2-OSM. However, it requires that the two following constraints are satisfied $|\dot{\delta}(t)| \leq M$ and $|\ddot{\delta}(t)| < M^*$. Moreover, in the application, the filter constant should be chosen less than the inverse of the upper bound of the second derivative of the disturbance.

1.3.4 Continuous HOSMC based on Edwards & Shtessel's adaptation

Now consider the sliding mode Eq. (1.2) with $n > 2$ and with the disturbance $\delta(t)$ satisfies the assumptions that $|\dot{\delta}(t)| \leq M$ where $M > 0$ and $|\ddot{\delta}(t)| < M^*$. The control law is now chosen as a combination of two terms

$$u = -u_n(t) - u_\sigma(t), \tag{1.31}$$

where

$$u_n(.) = \gamma_1 |s|^{\alpha_1} sign(s) ... + \gamma_n |s^{(n-1)}|^{\alpha_n} sign(s^{(n-1)}), \tag{1.32}$$

and

$$u_\sigma(t) = \lambda |\sigma|^{\frac{1}{2}}(t) sign(\sigma) + \int_0^t K(\tau) sign(\sigma(\tau)) d\tau, \tag{1.33}$$

where $\sigma(t)$ is the auxiliary variable defined as

$$\sigma(t) = s^{(n-1)}(t) - \int_0^t u_n(\tau) d\tau, \tag{1.34}$$

Proposition 1.3.1. *[10] Consider system* (1.2) *under the assumption that* $\delta(t) = 0$. *If the scalars* $\gamma_1,\ \gamma_2, ...,\ \gamma_n$ *are chosen such that the polynomial* $p^n + \gamma_n p^{n-1} + ... + \gamma_2 p + \gamma_1$ *is Hurwitz and the scalars* $\alpha_1,\ \alpha_2, ...,\ \alpha_n$ *are chosen recursively as*

$$\alpha_{i-1} = \frac{\alpha_i \alpha_{i+1}}{2\alpha_{i+1} - \alpha_i}, \quad i = 2, ..., n \tag{1.35}$$

with $\alpha_{n+1} = 1$ *and* $\alpha_n = \bar{\alpha}$. *Then, there exists an* $\varepsilon_b \in (0, 1)$ *such that for every* $\bar{\alpha} \in (1 - \varepsilon_b, 1)$, *the continuous controller* $u_n(t)$ (1.32) *drives in finite time* $s, \dot{s}, ..., s^n$ *to the origin.*

If $u_\sigma(t)$ is chosen according to (1.23), and $u_n(t)$ follows proposition 1.3.1, then he proposed combination (1.31) provides in a finite time the convergence of $s,\ \dot{s}, ...,\ s^n \rightarrow 0$ (i.e. ideal n-OSM) despite the presence of disturbance with unknown bounded derivatives $|\dot{\delta}(t)| \leq M$ and $|\ddot{\delta}(t)| < M^*$. Therefore, it is called adaptive continuous HOSMC.

As mentioned before, the main drawback of this adaptation is that the filter constant should be chosen less than the inverse of the upper bound of the disturbance second derivative. This means that some information about the bounds of the disturbance are needed.

1.4 Oliveira & Hsu's adaptation

Utkin's adaptation and Edwards & Shtessel's adaptation assume that the disturbance is smooth. To overcome this constraint, Oliveira and co-authors [54] proposed adaptive law which employs a monotonically increasing gain to force the SM to be achieved. After that, the equivalent control can be used as an estimation of the disturbance. This adaptation has been only applied to design adaptive FOSMC [54]. In what follows, we will the principles of this method.

1.4.1 Application to FOSMC

Consider the sliding variable dynamic in (1.2) with $n = 1$ and suppose that the disturbance satisfies $|\delta(t)| \leq \delta_{max}$, where $\delta_{max} > 0$ is unknown. The Oliveira & Hsu's adaptive FOSMC is given by

$$u = -K(t)sign(s), \tag{1.36}$$

where

$$\dot{K}(t) = -\lambda_f K(t) + c_f(|u_{av}| + \zeta), \quad K(0) \geq 0, \tag{1.37}$$

with $\zeta > 0$ is a constant which guaranties a desired minimum control level, λ_f and c_f are two constants satisfying the inequalities

$$c_f > \lambda_f > 0, \tag{1.38}$$

and u_{av} is the average control, obtained by low-pass filter

$$\tau \dot{u}_{av} = -u_{av} + u_{eq}, \tag{1.39}$$

where $\tau > 0$ is the filter time constant, and $u_{eq} = -K(t)sign(s)$.

This algorithm ensures the finite time convergence of s to zero (i.e. 1-OSM). However, as mentioned before, to be able to estimate u_{eq}, the filter constant should be chosen much less than the inverse of the upper bound of the first derivative of disturbance.

1.5 Bartolini, Levant, Plestan's adaptation

This adaptation is based on the usage of discrete time criterion to verify the appearance of a real-sliding motion [71]. Hence, a SM indicator which is based on the detection of the real SM is introduced. The idea is to increase the control gain until the indicator

reveals that the SM is reached. Then, the adaptive gain starts to decrease until the sliding mode indicator becomes negative. At this moment, the adaptive gain is increased in one impulse to ensure the achievement of SM immediately. Then, the gain decrease will take place until the SM is once more lost.
In what follows the application of this adaptation to FOSMC and Twisting Control (TC) [7, 67] are presented.

1.5.1 Application to FOSMC

Consider the sliding variable dynamic in (1.2) with $n = 1$ and suppose that there exist some positive constant δ_d, δ_{dm}, δ_m that satisfy the following inequalities

$$|\dot{\delta}/\delta| \leq \delta_d \quad \text{with} \quad |\delta(t)| \geq \delta_m, \quad |\dot{\delta}(t)/\delta(t)| \leq \delta_{dm} \quad \text{with} \quad |\delta(t)| \leq \delta_m. \tag{1.40}$$

Only δ_d is supposed to be known. Note that in this case the disturbance can be unbounded. The control is given in the following form

$$u = -K(t)sign(s), \tag{1.41}$$

where the adaptation law is

$$\dot{K} = \begin{cases} -\alpha\lambda K & \text{if } K > K_m, \\ -\alpha\lambda_m & \text{if } K_{mm} < K \leq K_m, \quad K(0) \geq K_{mm}, \\ \lambda_m & \text{if } K \leq K_{mm}, \end{cases} \tag{1.42}$$

with $\alpha(t)$ is the indicator, (λ, λ_m) are positive adaptation parameters, and (K_m, K_{mm}) are constants satisfying

$$K_m \geq K_{mm} > 0. \tag{1.43}$$

Now, the indicator $\alpha(t)$ for the detection of a real 1-OSM will be designed. Let $\tau > 0$ is the sampling period, N_t is a natural number, $\mu > 0$, and $t \in [t_i, t_{i+1})$. Then the indicator $\alpha(t)$ is given by

$$\alpha(t) = \begin{cases} 1 & \text{if } \forall t_j \in [t - N_t\tau, t]: \ |s(t_j)| \leq \mu K(t_j)\tau, \\ -1 & \text{if } \exists t_j \in [t - N_t\tau, t]: \ |s(t_j)| > \mu K(t_j)\tau, \end{cases} \tag{1.44}$$

where t_j are the sampling instants, $t_0 = 0$. The real 1-OSM indicator is considered satisfied if $\alpha = 1$, i.e. $|s(t_j)| \leq \mu K(t_j)\tau$. This inequality is designed since the accuracy of the sliding variable provided by FOSMC is proportional to τ.

In addition, an instant increment is implemented at each sampling instant t_i if the 1-OSM indicator is violated

$$K(t_i) = \begin{cases} qK(t_i - 0) & \text{if } \alpha(t_{i-1}) = 1 \ \& \ \alpha(t_i) = -1, \\ K(t_i - 0) & \text{if } \alpha(t_{i-1}) \neq 1 \text{ or } \alpha(t_i) \neq -1. \end{cases} \tag{1.45}$$

with $q > 1$ is constant.

If $\lambda > \delta_d$, this algorithm ensures in a finite time a real 1-OSM (i.e. $|s| \leq \eta\tau K(t)$ with $\eta > 0$).

The presented strategy assumes that the disturbance is smooth and requires the knowledge of the boundary of the disturbance's logarithmic derivative. Moreover, after the adaptive gain attains its minimal value, the gain has to jump to its maximum value when a real 1-OSM is violated, even in the case when the change in the disturbance amplitude is small. This mechanism can be very stressful for electromechanical systems.

1.5.2 Application to TC

Now, consider the sliding variable dynamic in (1.2) with $n = 2$ and suppose the same above assumption (1.40) for the disturbance. The control law is chosen as

$$u = -K(t)(sign(s) + \beta sign(\dot{s})), \quad 0.5 < \beta < 1, \tag{1.46}$$

where β is a constant control parameter, and $K(t)$ is the adaptive gain. Here, the adaptive gain and the instant increment are chosen as in (1.42)-(1.45) with the constants K_m, K_{mm}, q which satisfy

$$K_m \geq K_{mm} > 0, \ q > \frac{1+\beta}{1-\beta}, \tag{1.47}$$

and the indicator is designed to detect real a 2-OSM instead of real a 1-OSM. Hence,

$$\alpha(t) = \begin{cases} 1 & \text{if } \forall t_j \in [t - N_t\tau, t] : \ |s(t_j)| \leq \mu K(t_j)\tau^2, \\ -1 & \text{if } \exists t_j \in [t - N_t\tau, t] : \ |s(t_j)| > \mu K(t_j)\tau^2, \end{cases} \tag{1.48}$$

where t_j are the sampling instants. The real 2-OSM indicator is considered satisfied if $\alpha = 1$, i.e. $|s(t_j)| \leq \mu K(t_j)\tau^2$. Once again, this inequality is designed given that the accuracy of the sliding variable provided by TC is proportional to τ^2.

If $\lambda > \delta_d$, this algorithm ensures in a finite time a real 2-OSM (i.e. $|s| \leq \eta_1\tau^2 K(t)$, $|\dot{s}| \leq \eta_2\tau K(t)$ with $\eta_1 > 0$, $\eta_2 > 0$).

However, as in the adaptation of FOSMC, it is assumed that the disturbance is smooth and requires the knowledge of the boundary of the disturbance's logarithmic derivative. Furthermore, the mechanism of jumping can be damaging for electromechanical systems.

1.6 Moreno's adaptation

This adaptation consists in increasing the gain until the moment when the SM is reached. Then the gain is fixed at this value, ensuring an ideal SM for some interval of time. When the disturbance grows, the SM can be lost, therefore the gain increases to reach it again. Note that this adaptation is inspired by [36], in which it has been applied to adapt the gain of FOSMC.
The application of this adaptation to STC and TC [53] are given in the following subsections.

1.6.1 Application to STC

Consider the sliding mode dynamic in (1.2) with $n = 1$ under the assumption that the disturbance satisfies $|\delta(t)| \leq \delta_{max}$ where $\delta_{max} > 0$ is unknown. The structure of Moreno's adaptive STC is given as

$$\begin{cases} u(t) = -h_1 K(t)|s|^{\frac{1}{2}} sign(s) + u_2(t) \\ \dot{u}_2(t) = -h_2 K^2(t) sign(s), \end{cases} \tag{1.49}$$

where $h_1 = 1.5$, $h_2 = 1.1$ and the adaptive gain $K(t)$ is computed through

$$\dot{K}(t) = \begin{cases} \bar{k}, & \text{if } |s| > \varepsilon \\ 0, & \text{if } |s| \leq \varepsilon, \end{cases}, \quad K(0) > 0, \tag{1.50}$$

with $\bar{k}$ and ε are positive constants to be selected.

This algorithm ensures the convergence of s and $\dot{s}$ in finite time to zero, i.e. achievement of ideal 2-OSM. However, the adaptive gain $K(t)$ can only increase, which leads to the overestimation of the control gain resulting in a larger amplitude of chattering.

1.6.2 Application to TC

In this subsection, consider the sliding mode dynamic in (1.2) with $n = 2$ and under the same assumption as in the previous subsection, i.e. the disturbance satisfies $|\delta(t)| \leq \delta_{max}$ where $\delta_{max} > 0$ is unknown. The Moreno's adaptive TC is described by

$$u(t) = -K(t)(sign(s) + 0.5 sign(\dot{s})), \tag{1.51}$$

where the adaptive gain $k(t)$ is obtained through

$$\dot{K}(t) = \begin{cases} \bar{k}, & \text{if } ||s, \dot{s}|| > \varepsilon \\ 0, & \text{if } ||s, \dot{s}|| \leq \varepsilon \end{cases}, \quad K(0) > 0, \tag{1.52}$$

with $\bar{k}$ and ε are positive constants to be selected.

This algorithm drives s and $\dot{s}$ in a finite time to zero and provides ideal 2-OSM. However, as in Moreno's adaptive STC, this interesting behavior comes at the cost of gain overestimation, resulting in a high level of chattering.

1.7 Shtessel & Plestan's adaptation

To overcome the problem of gain overestimation, this adaptation has been developed. Indeed, this adaptation allows the gain to increase and decrease. The idea of this adaptation is to increase the control gain until the SM is reached. Then, the gain starts to decrease. This decrease will be reversed as soon as the SM is lost.
The application of this adaptation to FOSMC, STC and TC [58, 64, 65] are given in the following subsections.

1.7.1 Application to FOSMC

Consider the sliding mode dynamic in (1.2) with $n = 1$ and under the assumption that the disturbance satisfies $|\delta(t)| \leq \delta_{max}$ where $\delta_{max} > 0$ is unknown. The Shtessel & Plestan's adaptive FOSMC is given by

$$u = -K(t)sign(s), \tag{1.53}$$

where the gain $K(t)$ satisfies the following dynamic

$$\dot{K} = \begin{cases} \bar{K}|s|sign(|s| - \epsilon) & , \quad K > \mu \\ 0 & , \quad K \leq \mu \end{cases} \tag{1.54}$$

where $\bar{K}$, ε and μ are positive constants to be selected.

This controller ensures the finite-time convergence of the sliding variable s to some neighborhood of zero (i.e. real 1-OSM) without big overestimation of the gain. The main drawback of this approach is that the size of the above mentioned neighborhood depends on the unknown upper bound of disturbance, i.e. it is unknown apriori.

1.7.2 Application to STC

In this application, consider the sliding mode dynamic in (1.2) with $n=1$ and under the assumption that the disturbance satisfies $|\dot{\delta}(t)| \leq M$ where $M>0$ is unknown. The Shtessel & Plestan's adaptive STC is written as

$$\begin{cases} u(t) = -\alpha(t)|s|^{\frac{1}{2}} sign(s) + u_2(t), \\ \dot{u}_2(t) = -\dfrac{\beta(t)}{2} sign(s), \end{cases} \tag{1.55}$$

with $\beta = 2\mu\alpha$, and the adaptive gain α is obtained through

$$\dot{\alpha} = \begin{cases} w_1 \sqrt{\dfrac{\gamma_1}{2}} sign(|s| - \varepsilon), & \text{if } \alpha > \alpha_m \\ \nu, & \text{if } \alpha \leq \alpha_m \end{cases} \tag{1.56}$$

where μ, w_1, γ_1, ε, α_m, and ν are positive constants to be selected.

This controller can guarantee the convergence in finite time of s and $\dot{s}$ to some neighborhood of zero, i.e. there exists a finite time $t_f > 0$, such that $\forall t \geq t_f$, $|s| \leq \eta_1$ and $|s| \leq \eta_2$, where $\eta_1 \geq \varepsilon$, $\eta_2 \geq 0$. However, as in Shtessel & Plestan's adaptive FOSMC, the sizes of η_1 and η_2 depend on the unknown upper bound of disturbance derivative, i.e. they are unknown apriori.

1.7.3 Application to TC

In this application, consider the sliding mode dynamic in (1.2) with $n=2$ and under the assumption that the disturbance satisfies $|\delta(t)| \leq \delta_{max}$ where $\delta_{max} > 0$ is unknown. This adaptive TC takes the following form

$$u = -K(t)\left(sign(s) + 0.5 sign(\dot{s})\right), \tag{1.57}$$

where $K(t)$ is the adaptive gain. Before describing its dynamic, it is assumed that there exist

1. A sufficiently large apriori known parameter $K^* > 0$ so that $K^* - 2\varepsilon_0 > 2M$.

2. A parameter γ_1 that satisfies the condition

$$\frac{1}{4} \leq \gamma_1 < \frac{\varepsilon_0^2}{\max_{s,\dot{s},\Omega}(2\alpha s^2 + |s|\dot{s}^2) + \Delta_{\gamma_1}}, \quad K \leq K^* - \varepsilon_0$$

   where $\varepsilon_0 > 0$ is selected accordingly, $\Omega \subset \mathbb{R}^2$ is a compact set for which the interior contains the origin, and Δ_{γ_1} is a regularization term.

Under these two assumptions, the adaptive gain $K(t)$

$$\dot{K} = \begin{cases} \frac{\frac{w_1}{\sqrt{2\gamma_1}}}{\frac{1}{\gamma_1} - \frac{2\alpha s^2 + |s|\dot{s}^2}{(K^* - K)^3}} sign(V_0(s,\dot{s}) - \varepsilon), & \text{if } K > K_{\min} \\ \chi, & \text{if } K \leq K_{\min} \end{cases} \tag{1.58}$$

with

$$V_0(s,\dot{s}) = K^2 s^2 + \gamma |s|^{\frac{3}{2}} sign(s)\dot{s} + K|s|\dot{s}^2 + \frac{1}{4}\dot{s}^4 \tag{1.59}$$

where w_1, ε, χ, $K_{\min}$, Δ_{γ_1} are positive constants to be selected, and $|\gamma| \in (0, 2\alpha_{\min}^{\frac{3}{2}})$.

The controller aims to ensure the finite time convergence of $V_0(s,\dot{s})$ to the domain $V_0(s,\dot{s}) \leq \varepsilon$, i.e. the convergence of s and $\dot{s}$ to some neighborhoods of zero. Although it can achieve this aim, this adaptation has two main drawbacks. On one hand it assumes the knowledge of maximal actuator capacity K^*, and on the other hand the sizes of the above mentioned neighborhoods depend on the unknown upper bound of disturbance, i.e. they are unknown apriori.

1.8 Summary

In this chapter, an overview of ASMC/AHOSMC algorithms were presented. Their advantages and disadvantages were discussed.

The first family of adaptation is based on the usage of the equivalent control value as an estimation of the disturbance. To realize this strategy a low-pass filtered approximation of the equivalent control were proposed. However, during the realization, the filter constant should be chosen much less than the inverse of the upper bound of the first or the second derivative of the disturbance. This means that some information about the bounds of the disturbance are needed.

The second family of adaptation is based on the usage of discrete time criterion to verify the appearance of real-sliding motion. The idea of this strategy is to increase the control gain until the indicator reveals that the SM is reached. Then, the adaptive gain starts to decrease until the sliding mode indicator becomes negative. This approach ensures the finite time achievement of real SM. However, it assumes that the disturbance is smooth and requires the knowledge of the boundary of the disturbance logarithmic derivative. Moreover, after the adaptive gain attains its minimal value, the gain has to jump to its maximum value when the SM is violated, even in the case when the change in the

disturbance amplitude is small. This mechanism can be very stressful for electromechanical systems.

The third family of adaptation consists in increasing the gain until the moment when the SM is reached, and then the gain is fixed at this value, ensuring an ideal SM for some interval of time. When the disturbance grows, the SM can be lost, therefore the gain increases to reach it again. However, the control gain in this strategy is overestimated and one cannot be sure that the SM will not be lost in the future.

To overcome this problem, a strategy based on increasing and decreasing the gain has been developed. This approach ensures the finite-time convergence of the sliding variable to some neighborhood of zero without big overestimation of the gain. The main drawback of this approach is that the size of the above-mentioned neighborhood and the time of convergence depend on the unknown upper bound of disturbance, i.e. they are unknown apriori and one can never be sure that SM will never be lost for bigger values of time.

Chapter 2

Design of Adaptive FOSMC and DISMC

2.1 Introduction

For systems with matching disturbances, the sliding mode control has proven its high efficiency [71]. Indeed, it provides a closed-loop insensitivity to these disturbances and guarantees the finite-time convergence. In the case of systems with relative degree one affected by bounded disturbance, the First Order Sliding Mode Controllers (FOSMCs) can be applied. They can guarantee the convergence of the sliding variable to the origin in a finite-time by using a discontinuous control signal.

One the other hand, for systems with arbitrary relative degree affected by bounded disturbance, the FOSMC can be implemented in combination with a nominal control. Such combination is called Integral Sliding Mode Control (ISMC). Note that ISMC is a special kind of sliding mode control with two main properties:

- It ensures robustification of predesigned nominal control keeping its dimension.
- It does not have a reaching phase, i.e. it allows robustification starting from the initial time moment.

The traditional ISMC ensures the compensation of the disturbance from the initial time moment by using the FOSMC, i.e. a discontinuous control. Hence, it is called a Discontinuous ISMC (DISMC) [69, 42]. Due to the discontinuity of the overall controller for systems with fast actuators, it could provide big undesired chattering effect [11, 57].

To implement the FOSMC, the knowledge of the upper bound of disturbance is required. In practice, this bound is not constant and, moreover, frequently it is unknown. This means that the gains of the FOSMCs are overestimated. This is a main obstacle in the FOSMCs implementation leading to the growth of the undesired chattering [11]. Note that this obstacle also affects the DISMC since the FOSMC is a part of the overall control structure. So the interesting problem for the FOSMC and the DISMC consists in developing an adaptive strategy which can adjust the control gains, this means reduce the chattering effect.

The different known adaptive strategies for FOSMC and their drawbacks have already been presented in chapter 1. Recall that in [58], an adaptive FOSMC strategy has been developed. This strategy can ensure the finite time convergence of the sliding variable to some neighborhood of zero without big overestimation of the gain. The main drawback of this approach is that the size of the above-mentioned neighborhood depends on the unknown upper bound of disturbance, i.e. it is unknown apriori. In order to overcome this drawback, a novel adaptive strategy for FOSMC will be introduced.

The first contribution of this chapter consists in presenting a new adaptive strategy for FOSMC. This adaptive strategy can achieve the convergence of the sliding variable and maintain it in a predefined neighborhood of zero, with a control gain that is not overestimated, and without using any information about the upper bound of the disturbance or its derivative, nor the use of the low pass filter. To achieve the convergence, the adaptive strategy proposes the use of increasing gain strategy. Once the convergence is reached, and in order to maintain the sliding variable in a predefined neighborhood of zero, the proposed adaptive strategy applies the Barrier Functions (BFs). In this current chapter, two different classes of BFs are used: the positive semi-definite BF and the positive definite BF.

The second contribution of this chapter is the application of this adaptive strategy to design adaptive DISMC. The resulting controller ensures that the auxiliary variable belongs to a prescribed vicinity of zero starting from the initial time moment despite disturbances with unknown upper bound.

2.2 Barrier Function-Based adaptive FOSMC

2.2.1 Problem Formulation

Consider the first order system

$$\dot{s}(t) = u(t) + \delta(t), \tag{2.1}$$

where $s(t) \in \mathbb{R}$ is the sliding variable, $u(t)$ is the FOSMC and $\delta(t)$ is a disturbance. Here $\delta(t)$ is bounded function with unknown bound, i.e. $|\delta(t)| \leq \delta_{max}$. The bound $\delta_{max} > 0$ exists but is not known.

In this context, the gain of the FOSMC is to be adapted in accordance with the adaptive strategy defined later. The idea behind the proposed adaptive strategy is to first increase the adaptive gain until the sliding variable reaches a small neighborhood of zero $\frac{\varepsilon}{2}$ at time $\bar{t}$ by using a constant derivative gain as in [58]. Secondly, for $t > \bar{t}$, the adaptive gain switches to a BF that can maintain the sliding variable in the predefined neighborhood of zero $|s(t)| < \varepsilon$.

2.2.2 Preliminaries

2.2.2.1 Barrier Functions (BFs)

Definition 2.2.1. *Let us suppose that some $\varepsilon > 0$ is given and fixed, the BF can be defined as an even continuous function $K_b : x \in]-\varepsilon, \varepsilon[\rightarrow K_b(x) \in [b, \infty[$ strictly increasing on $[0, \varepsilon[$.*

- $\lim_{|x| \rightarrow \varepsilon} K_b(x) = +\infty$.
- *$K_b(x)$ has a unique minimum at zero and $K_b(0) = b \geq 0$.*

In this work, the following two different classes of BFs are considered;

- Positive definite BFs (PBFs): $K_{pb}(x) = \dfrac{\varepsilon \bar{F}}{\varepsilon - |x|}$, i.e. $K_{pb}(0) = \bar{F} > 0$.
- Positive Semi-definite BFs (PSBFs): $K_{psb}(x) = \dfrac{|x|}{\varepsilon - |x|}$, i.e. $K_{psb}(0) = 0$.

The PBF $K_{pb}(x)$ and the PSBF $K_{psb}(x)$ are illustrated in Fig. 2.1.

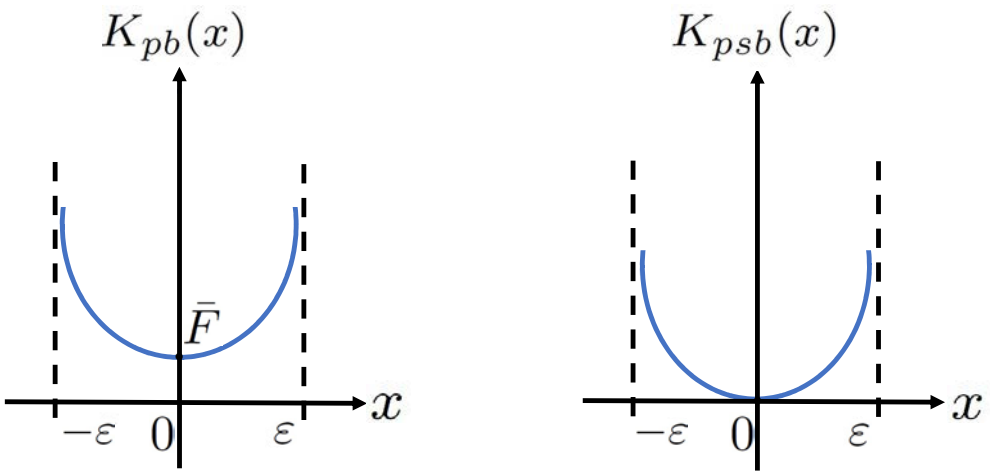

(a) $K_{pb}(x)$ (b) $K_{psb}(x)$

Figure 2.1. *Schematic illustrations of* $K_{pb}(x)$ *and* $K_{psb}(x)$.

2.2.3 Main results

The following theorem is true for both possible FOSMC gains design: using $K_B(s(t)) = K_{pb}(s(t))$ and $K_B(s(t)) = K_{psb}(s(t))$.

Theorem 2.2.2. *Consider system* (2.1) *with bounded disturbance* $\delta(t)$ *with the controller*

$$u(t) = -K(t, s(t))sign(s(t)), \tag{2.2}$$

and with the adaptive control gain $K(t, s)$

$$K(t, s(t)) = \begin{cases} K_a(t), \dot{K}_a(t) = \bar{K}|s(t)|, & \text{if } 0 < t \le \bar{t} \\ K_B(s(t)), & \text{if } t > \bar{t} \end{cases} \tag{2.3}$$

where $\bar{K}$ *to be arbitrary positive constant.*

Then, for any $s(0)$ *and* $\varepsilon > 0$, *there exists* $\bar{t}$ *the smallest root of equation* $|s(t)| \le \frac{\varepsilon}{2}$ *such that for all* $t \ge \bar{t}$, *the inequality* $|s(t)| < \varepsilon$ *holds.*

The proof of Theorem 2.2.2 is given in appendix A.

Remark 2.2.3. *Note that this strategy allows the adaptive gain to increase and decrease based on the current value of the sliding variable. When the sliding variable is going to zero, the adaptive gain decreases until the value which allows to compensate the disturbance.*

On the other hand, when the disturbance grows and the control gain is less than the absolute value of disturbance, the sliding variable grows and the control gain can grow if it is necessary until the level ensuring that the system solution will never leave the ε vicinity of zero.

Remark 2.2.4. *Theoretically, the apriori knowledge of actuator capacity P is not required, but it should be supposed that the actuator is able to compensate the disturbance. However, in practice, an actuator is used and its capacity P is known. In this case for discrete implementation of the proposed algorithm, the sampling step τ should be chosen as $\tau << \varepsilon/P$. Otherwise, the attractive feature of the BF will be lost, and the sliding variable will leave the predefined neighborhood of zero.*

The behavior of each barrier function PBF and PSBF, and the achievement of real or ideal SM in a finite time, together with the continuity or discontinuity of the control signal are discussed in the subsections 2.2.3.1 and 2.2.3.2.

2.2.3.1 Adaptation with PBF

Consider the adaptation with PBF. In this case, $K_{pb}(s(t))$ has a lower bound $\bar{F}$ when $s(t) = 0$. Therefore, when $|\delta(t)| < \bar{F}$ the adaptive gain is overestimated. In this case, this strategy provides an ideal 1-OSM. In order to attenuate this overestimation, $\bar{F}$ can be chosen small enough. The usage of PBF when the bound of the disturbance is less than $\bar{F}$ will provide a discontinuous control signal leading to the chattering whose amplitude is proportional to the choice of $\bar{F}$.

2.2.3.2 Adaptation with PSBF

Consider now the adaptation with PSBF. In this case, $K_{psb}(s(t))$ tends to zero when $s(t) \to 0$. Hence, $K_{psb}(s(t))$ has the same behavior as $\dfrac{|s(t)|}{\varepsilon}$ in the neighborhood of zero, i.e. $\dfrac{|s(t)|}{\varepsilon} << 1 \rightarrow K_{psb}(s(t)) = \dfrac{|s(t)|}{\varepsilon - |s(t)|} \approx \dfrac{|s(t)|}{\varepsilon}$.

This means that if $\delta(t)$ and $s(t)$ tend monotonically to zero, consequently the adaptive gain $K_{psb}(s(t))$ will go to zero. The discontinuity of the control signal can appear only once at time $\bar{t}$, when the adaptive gain switches to PSBF. It is necessary to note that starting from time $\bar{t}$, the control signal becomes continuous.

2.2.4 Simulation results

Two cases are considered carrying out simulations in order to show two main advantages of the proposed adaptive strategy over the adaptive algorithm presented in [58].

TABLE 2.1: *Parameter values of the PBF, PSBF and APS for adaptive FOSMCs*

	PBF	PSBF	APS
Parameter values	$\bar{K} = 1000,\ \varepsilon = 0.02,$ $\bar{F} = 0.1,\ K_a(0) = 10$	$\bar{K} = 1000,\ \varepsilon = 0.02,$ $K_a(0) = 10$	$\bar{K} = 1000,\ \varepsilon = 0.02,$ $\mu = 0.1\ ,\ K(0) = 10$

For the barrier strategy, the adaptive gain is given by (2.3) with $K_B(s(t))$ once defined as PBF and then as PSBF. In contrast, for the adaptive algorithm in [58], referred to as (APS), the adaptive gain is computed through

$$\dot{K}(t) = \begin{cases} \bar{K}|s(t)|sign(|s(t)| - \varepsilon), & \text{if } K > \mu \\ \mu, & \text{if } K \leq \mu \end{cases} \tag{2.4}$$

where $\bar{K}$, ε and μ are positive constants to be selected.

Consider the first order system (2.1) with the initial value as $s(0) = 0.04$. Table 2.1 contains the parameter values of PBF, PSBF and APS, where the parameter ε is selected as $\varepsilon = 0.02$, while all the others are set according to [58]. The attention will be focused on the behavior of each adaptation for $t > \bar{t}$, since starting from this moment the adaptive gain switches to the BFs.

2.2.4.1 Case of increasing disturbance amplitude

In this subsection, the disturbance is given by

$$\delta(t) = \begin{cases} 0.3sin(t), & \text{if } t \leq 100\ s \\ 1.4sin(t), & \text{if } 100\ s < t \leq 200\ s \\ 6.2sin(t), & \text{if } t > 200\ s. \end{cases}$$

This means that the disturbance amplitude is $\delta_{max} = 0.3$ for $t \leq 100\ s$, $\delta_{max} = 1.4$ for $100 < t \leq 200\ s$, and $\delta_{max} = 6.2$ for $t > 200\ s$ (see Fig. 2.2(a)). The zoomed-in plots of the sliding variable $s(t)$ with PBF, PSBF and APS are depicted in Figs. 2.2(b)-2.2(c)-2.2(d). It can be noticed in Figs. 2.2(b)-2.2(c) that for both barrier functions PBF and PSBF, the sliding variable does not exceed the predefined neighborhood of zero $\varepsilon = 0.02$. On the other hand, it can be seen in Fig. 2.2(d) that the size of the neighborhood of zero to which

converges $s(t)$ with APS is changing together with the amplitude of disturbance δ_{max} (for $t \leq 100\ s$, $|s(t)| \leq 0.024$, for $100 < t \leq 200\ s$, $|s(t)| < 0.029$, and for $t > 200\ s$ $|s(t)| \leq 0.031$). Therefore, it cannot be predefined. Also, it is worth noting that when the amplitude of disturbance suddenly increases to a big value, the sliding variable will also jump to a big value ($t = 200\ s$, $|s(t)| > 0.04$).

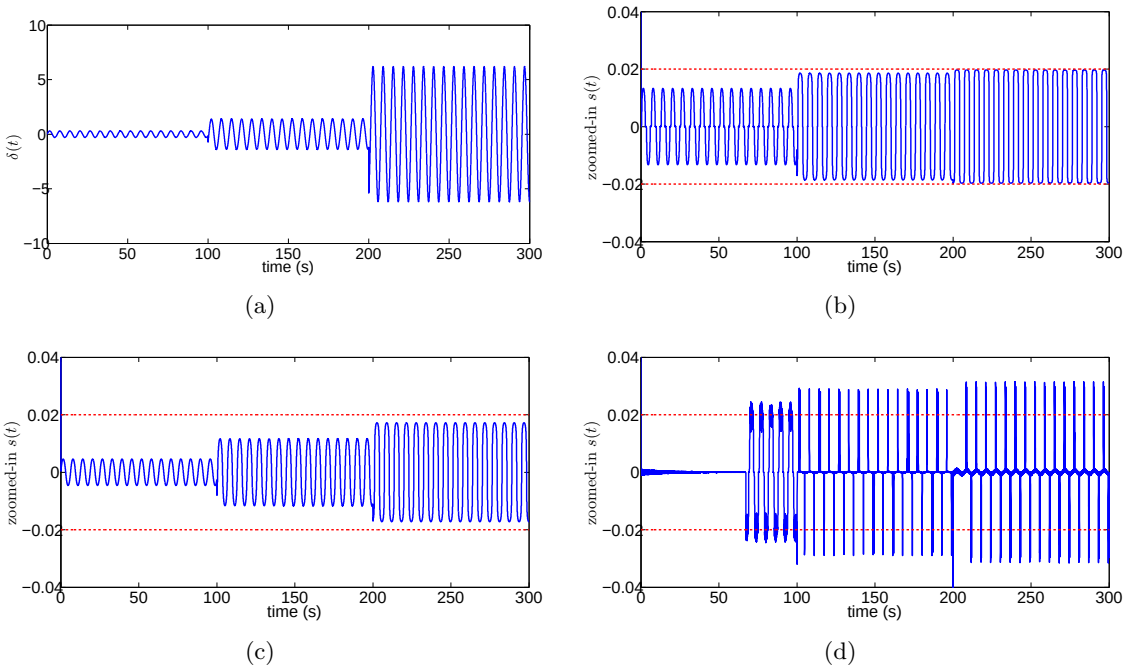

Figure 2.2. *a) Disturbance $\delta(t)$, and the zoomed-in plot of $s(t)$ with: b) PBF, c) PSBF, d) APS*

2.2.4.2 Case of monotonically decreasing disturbance

The following monotonically decreasing disturbance is considered (Fig. 2.3(a))

$$\delta(t) = \frac{8.2}{t+1} + 0.002.$$

Figs. 2.3(b)-2.3(c)-2.3(d) show the behavior of the control signal $u(t)$ with PBF, PSBF and APS. For $t > 83\ s$ the amplitude of the disturbance becomes less than $\bar{F} = \mu = 0.1$ (see Fig. 2.3(a)). That is why starting for this moment, the chattering will appear for both PBF and APS with the amplitude equal to 0.1 (see Figs. 2.3(b)-2.3(d)). On the other hand, the control signal for PSBF is continuous and will go to zero without chattering (see Fig. 2.3(c)).

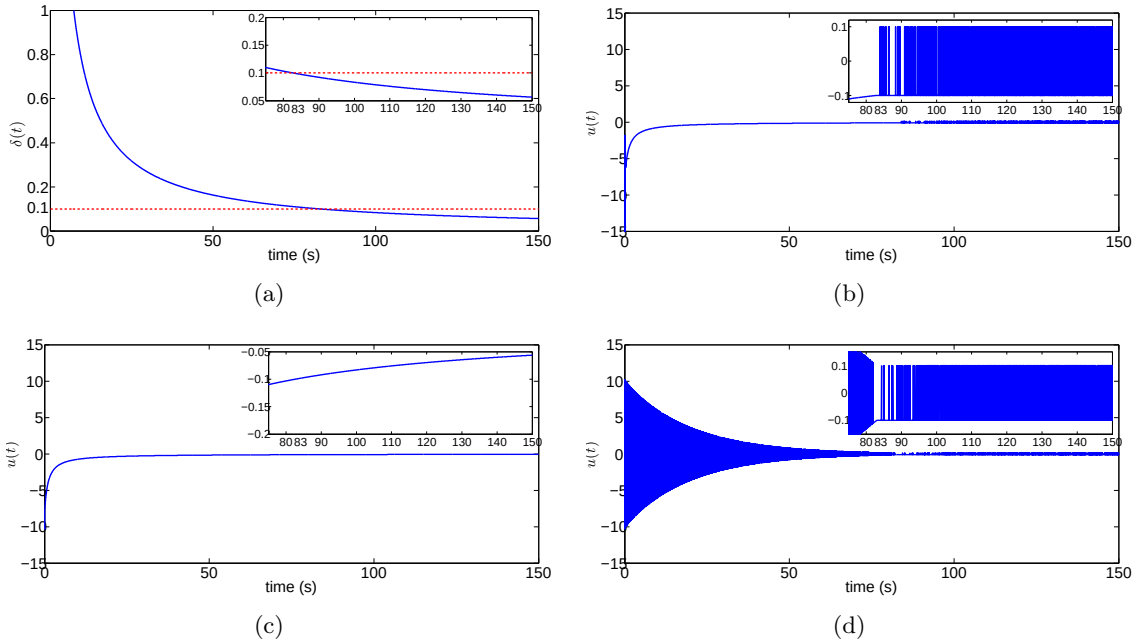

Figure 2.3. *a) Disturbance $\delta(t)$, and the control $u(t)$ with: b) PBF, c) PSBF, d) APS*

2.3 Barrier Function-Based Adaptive DISMC

2.3.1 Preliminaries

Consider the following system

$$\dot{x}(t) = Ax + B(u + \delta(t)), \tag{2.5}$$

where $x \in \mathbb{R}^{n\times 1}$ is the state, $A \in \mathbb{R}^{n\times n}$ is the system matrix, $B \in \mathbb{R}^{n\times 1}$ is the input matrix, $u \in \mathbb{R}$ is the control input and $\delta(t) \in \mathbb{R}$ is the disturbance.

The control input for system (2.5) is a combination of two parts

$$u = u_n + u_{SMC}, \tag{2.6}$$

where u_n is a nominal control and u_{SMC} is an ISMC. The nominal control u_n is designed to ensure a desired performance for system (2.5) assuming $\delta(t) = 0$, and the ISMC u_{SMC} is designed to guarantee the compensation of the disturbance $\delta(t)$, starting from the initial time moment $t = 0$ s.

The auxiliary variable for system (2.5) is defined as

$$s = G\Big[x(t) - x(0) - \int_0^t (Ax + Bu_n)d\tau\Big], \tag{2.7}$$

where $G \in \mathbb{R}^{1\times n}$ is a projection matrix and $x(0)$ is the initial condition. The main specific feature of the following auxiliary variable is that $s(0) = 0$. From (2.7), the dynamic of the auxiliary variable can be expressed as

$$\begin{aligned}\dot{s} &= G\Big[Ax + B(u + \delta(t)) - Ax - Bu_n\Big] \\ &= G\Big[Ax + B(u_n + u_{SMC} + \delta(t)) - Ax - Bu_n\Big] \\ &= GB\Big[u_{SMC} + \delta(t)\Big] \ ,\end{aligned} \tag{2.8}$$

Following [15], it is reasonable to choose $G = B^+$, i.e. $GB = 1$. Then, (2.8) becomes

$$\dot{s} = u_{SMC} + \delta(t) \tag{2.9}$$

In the case of DISMC, and when the disturbance is bounded with unknown upper bound δ_{max}, system (2.9) is exactly equivalent to the first order disturbed system (2.1) described in the problem formulation. It should be noted here that $s(0) = 0$, which was not the case in the initial problem formulation in section 2.2.

In this context, u_{SMC} is to be adapted in accordance with the adaptive strategy defined in section 2.2.3. The objective of this adaptation is to ensure that the auxiliary variable belongs to a prescribed vicinity of zero from the initial time moment, i.e. for all $t \geq 0$, $|s| < \varepsilon$.

In the following subsections, two situations will be considered: in the first one, the adaptive gain is chosen as PBF. In the second situation, the gain is chosen as PSFB.

2.3.2 Adaptation with PBF

Proposition 2.3.1. *Consider system* (2.9) *with the disturbance* $\delta(t)$ *satisfies* $\delta(t) \leq \delta_{max}$ *where* δ_{max} *exists and it is unknown. Then, for any* $\varepsilon > 0$ *and for all* $t \geq 0$*, the inequality* $|s(t)| < \varepsilon$ *holds via the adaptive DISMC* (2.2) *with the adaptive control gain*

$$K(s(t)) = K_{pb}(s(t)) = \frac{\varepsilon \bar{F}}{\varepsilon - |s(t)|} \ . \tag{2.10}$$

Furthermore, an ideal 1-OSM, i.e. $s(t) = 0$ *is achieved if* $\bar{F} > |\delta(t)|$.

*P*roof. The above proposition is a particular case of theorem 2.2.2, where the PBF is used to adapt the gain of DISMC from the initial time moment. That is due to the specific feature of ISMC for which the auxiliary variable satisfies $s(0) = 0$. □

2.3.3 Adaptation with PSBF

Proposition 2.3.2. *Consider system* (2.9) *with the disturbance* $\delta(t)$ *satisfies* $\delta(t) \leq \delta_{max}$ *where* δ_{max} *exists and it is unknown. Then, for any* $\varepsilon > 0$ *and for all* $t \geq 0$*, the inequality* $|s(t)| < \varepsilon$ *holds via the adaptive DISMC* (2.2) *with the adaptive control gain*

$$K(s(t)) = K_{psb}(s(t)) = \frac{|s(t)|}{\varepsilon - |s(t)|} \ . \tag{2.11}$$

Furthermore, the ISMC is continuous for any value of $\delta(t)$*.*

*P*roof. Similar to the proof of Proposition. 2.3.1. □

Remark 2.3.3. *Note that although the discontinuous structure of ISMC in* (2.2)*, it was shown in subsection 2.2.3.2 that in the case of adaptation with PSBF, it provides a continuous control signal. That is due to the reason that the PSBF is equal to zero at the origin.*

Remark 2.3.4. *Remark 2.3.3 motivates the usage of PSBF to adapt the control gain of DISMC instead of PBF. Indeed, the discontinuous control is replaced by continuous one with less control effort, as well as, it maintains the auxiliary variable in a prescribed vicinity of zero from the initial time moment.*

2.3.4 An example

A second order system with matched disturbance is considered as a simple example* to illustrate the performance of the barrier algorithms-based adaptive DISMC and to compare it with the results obtained through APS 2.4.

The second order disturbed system is given by

$$\begin{cases} \dot{x}_1(t) = x_2(t), \\ \dot{x}_2(t) = u(t) + d(t) \ , \end{cases} \tag{2.12}$$

with initial conditions chosen as $x_1(0) = 2$, $x_2(0) = 1$. The disturbance is selected as $\delta(t) = 5sin(2t) + 2cos(5t)$. The nominal control in (2.6) is designed according to [55], in which a continuous controller for the nominal system (i.e. $\delta(t) = 0$) has been proposed. This controller can drive x_1 and x_2 to zero in a finite time. Hence,

$$u_n = -k_1|x_1|^{\frac{1}{3}} sign(x_1) - k_2|x_2|^{\frac{1}{2}} sign(x_2) \tag{2.13}$$

*Indeed, the second order disturbed system is a special case of system (2.5). However, it can be generalized for arbitrary order system.

where $k_1 = 15$ and $k_2 = 7$. The auxiliary variable is defined as $s = x_2(t) - x_2(0) - \int_0^t u_n d\tau$.

The parameter value ε of the three algorithms, PBF, PSBF and APS, is selected as $\varepsilon = 0.01$, the parameter $\bar{F}$ of PBF is taken as $\bar{F} = 0.6$, and finally, the parameter values of APS are set as follows: $\bar{K} = 10000$, $\mu = 0.1$.

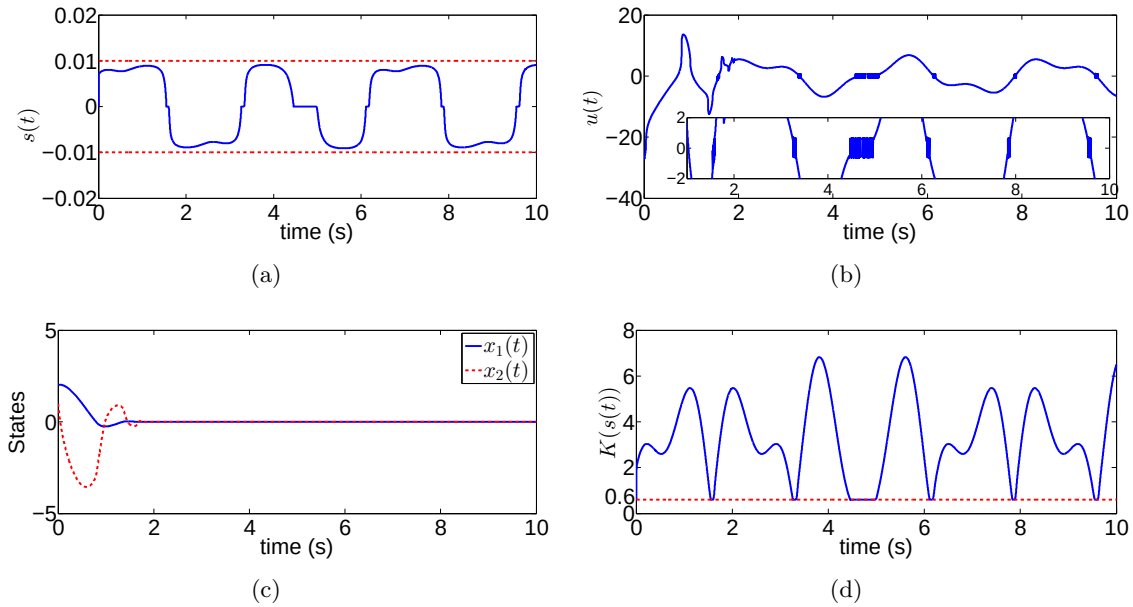

Figure 2.4. *Adaptive DISMC based on PBF*

Fig. 2.4 illustrates the simulation results of the adaptive DISMC based on PBF. Fig. 2.4(a) shows that the auxiliary variable $s(t)$ is maintained in the prescribed vicinity of zero $\varepsilon = 0.01$ from the initial time moment. It can be observed in Fig. 2.4(b) that the overall control is discontinuous when $\bar{F} > |\delta(t)|$, i.e. when $K(s(t)) = \bar{F}$ (see Fig. 2.4(d) and the zoomed-in plots in Fig. 2.4(b)). Moreover, it is seen in Fig. 2.4(d) that the adaptive gain $K(s(t))$ can increase and decrease. The convergence of the state to a vicinity of the origin is depicted in Fig. 2.4(c).

Next, the simulation results of the adaptive DISMC based on PSBF are shown in Fig. 2.5. Fig. 2.5(a) confirms that the auxiliary variable $s(t)$ belongs to the prescribed vicinity of zero $\varepsilon = 0.01$ from the initial time moment. The continuity of the overall control can be observed in Fig. 2.5(b). The convergence of the states to a vicinity of the origin is illustrated in Fig. 2.5(c) and the increasing and decreasing of the adaptive gain can be shown in Fig. 2.5(d).

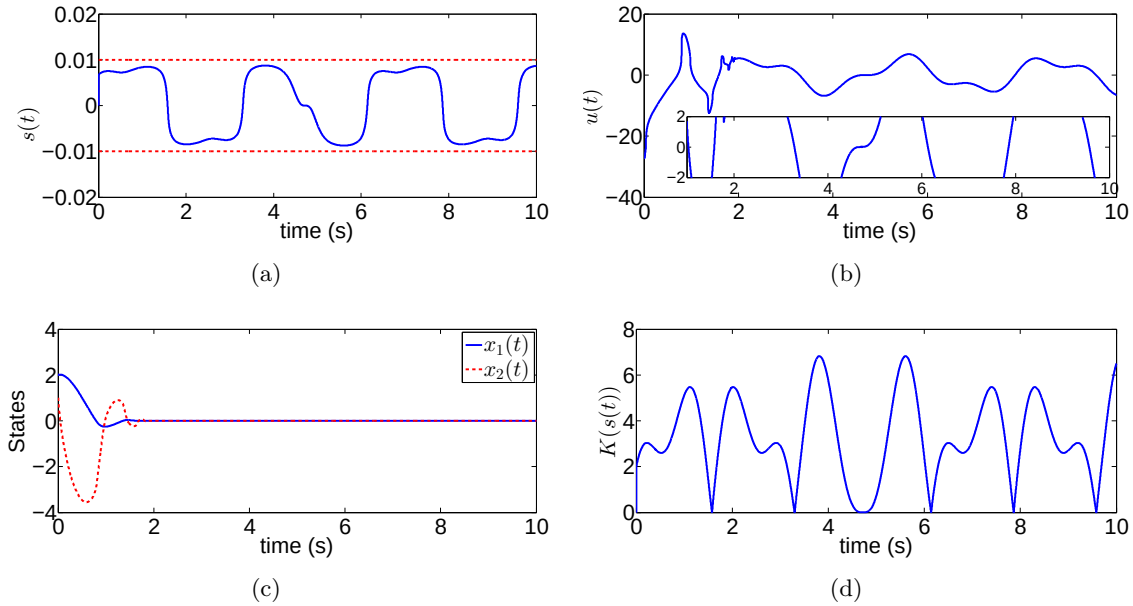

Figure 2.5. *Adaptive DISMC based on PSBF*

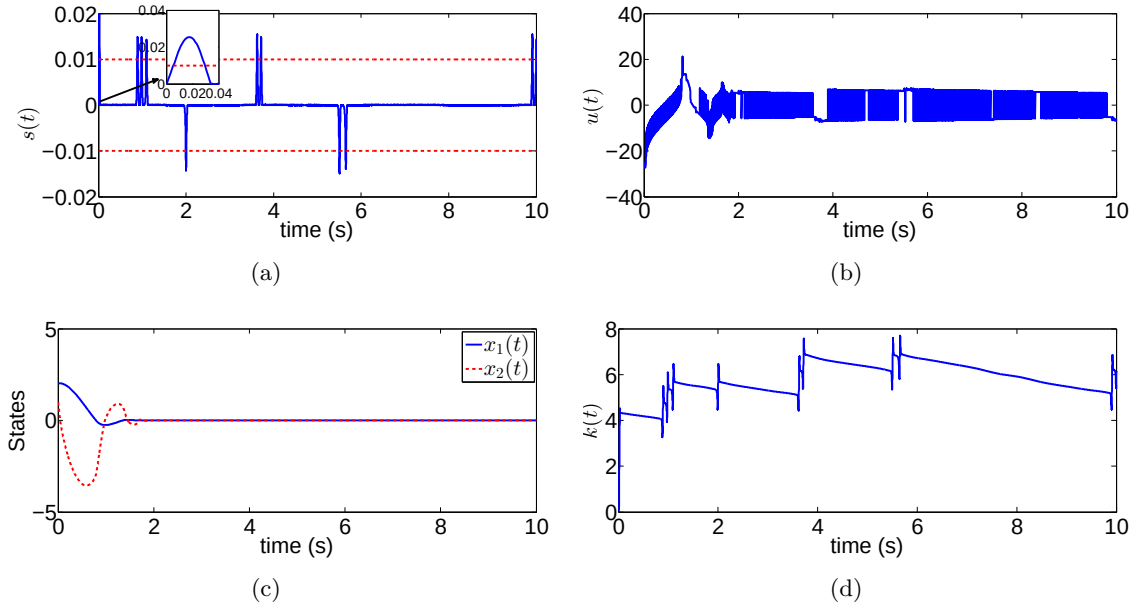

Figure 2.6. *Adaptive DISMC based on APS*

Finally, the simulations results of the adaptive discontinuous ISMC based on APS are depicted in Fig. 2.6. It can be noticed in Fig. 2.6(a) that the auxiliary variable cannot be maintained in the prescribed vicinity of zero. Moreover, it will jump to a big value at

the initial time moment (for $t = 0.01\ s$, $s(t) > 0.025$). Then, the discontinuity of the overall control can be observed in Fig. 2.6(b). And finally, the convergence of the states to some vicinity of origin can be seen in Fig. 2.6(c), while the increasing and decreasing of the adaptive gain can be observed in Fig. 2.6(d).

2.4 Summary

For first order systems affected by bounded disturbance with unknown boundary, a new barrier function-based adaptive FOSMC is presented. The proposed algorithm can ensure the convergence of the sliding variable and maintain it in a predefined neighborhood of zero, independent of the upper bound of the disturbance, and without overestimating the control gain. In order to highlight the properties of this strategy, two different classes of BFs have been studied.

For systems with arbitrary relative degree affected by bounded disturbance, the DISMC was recalled and the barrier adaptive strategy was applied to adapt it. It was shown that the proposed algorithm ensures that the auxiliary variable belongs to a prescribed vicinity of zero starting from the initial time moment despite disturbance with unknown upper bound. Again, the two classes of BFs have been used. It results that this algorithm has two main advantages: it does not require the knowledge of the upper bound of disturbance, and does not overestimate the control gain.

To sum up, in this chapter, adaptive FOSMC and DISMC for first and arbitrary order disturbed systems whose disturbances are bounded with unknown boundary have been introduced. In the next chapter, perturbed systems with Lipschitz disturbances with unknown Lipschitz constants will be considered. For this class of systems, the barrier strategy will be used to design a new adaptive super-twisting controller and a new adaptive continuous integral sliding mode controller.

Chapter 3

Design of Adaptive STC and CISMC

3.1 Introduction

In the previous chapter, an adaptive FOSMC and an adaptive DISMC have been designed for perturbed first order and arbitrary order systems where the disturbances are bounded with unknown boundary. The motivation of current chapter is to design new adaptive SMCs which can deal with Lipschitz disturbances with unknown Lipschitz constants.

For systems with fast actuators, and with relative degree one affected by Lipschitz's disturbance, the Super-Twisting Controller (STC) is one of the most popular strategies to be used [43, 52, 57]. It allows the achievement of second order sliding mode (2-OSM) in finite-time by using a continuous control signal. Moreover, the other benefit of STC compared to FOSMC is that it offers chattering attenuation due to the continuity of the control signal.

In contrast, for systems with arbitrary relative degree affected by Lipschitz's disturbance, the Continuous ISMC (CISMC) has proved its effectiveness [32]. This controller is a combination of STC and a nominal controller. Nevertheless, the weakness of this controller is that the robustness is ensured only after convergence of the STC [17].

To implement the STC, the upper bound of the disturbance's derivative should be known. In practice, this bound is not constant and it is unknown. In this case, the fixed gain of the STC is set to be overestimated, which causes high level of chattering [11]. This problem is an exciting challenge for the CISMC as well, due to the reason that the

STC is a part of the overall control structure. For that reason, it is very important to design an adaptive strategy to adapt the control gains of STC and CISMC guaranteeing the reduction of the chattering effect.

The best known adaptive strategies for STC and their drawbacks have already been presented in chapter 1. In order to overcome the drawback of the strategy proposed in [64], that is the convergence of the sliding variable to an unknown neighborhood of zero, the barrier adaptive strategy proposed in the previous chapter will be used to design a new adaptive STC.
This chapter consists of two main parts: the first part will be devoted to the design of the barrier function based-adaptive STC. We will show that this new controller has the following advantages:

- The sliding variable converges in a finite time to a predefined neighborhood of zero, independently of the bound of the disturbance derivative, and cannot exceed it.
- The gain provided by the proposed strategy is not overestimated, as it can only achieve the convergence of the sliding variable to a predefined neighborhood of zero.
- The proposed strategy does not theoretically require neither the upper bound of the disturbance derivative nor the use of the low-pass filter.

The second part of this chapter will be dedicated to the design of adaptive CISMC based on the concept of the barrier function. Similar to the barrier function based-adaptive DISMC presented in the previous chapter, this strategy ensures that the auxiliary variable belongs to a prescribed vicinity of zero starting from the initial time moment despite disturbance with unknown upper bound of its derivative. Moreover, this strategy allows to avoid the reaching phase, and guarantees that the adaptive gain is not overestimated.

3.2 Barrier Function-Based adaptive STC

3.2.1 Problem formulation

Consider the first order system described by

$$\dot{s}(t) = u_{st}(t) + \delta(t), \tag{3.1}$$

where $s(t) \in \mathbb{R}$ is the sliding variable, $\delta(t)$ is a the disturbance and $u_{st}(t) \in \mathbb{R}$ is the STC. The disturbance $\delta(t)$ is a Lipschitz function with unknown Lipschitz constant so that $|\dot{\delta}(t)| \leq M$. The bound M exists but is not known.

In the presence of Lipschitz disturbance, the standard STC [43] given by

$$\begin{cases} u_{st}(t) = -k_1 |s(t)|^{\frac{1}{2}} sign(s(t)) + u_2(t), \\ \dot{u}_2(t) = -k_2 sign(s(t)), \end{cases} \tag{3.2}$$

drives both $s(t)$ and $\dot{s}(t)$ to zero in a finite time, i.e. it provides a 2-OSM if the control gains k_1 and k_2 are designed as $k_1 = 1.5\sqrt{M}$ and $k_2 = 1.1M$. However, the implementation of this standard STC requires the information of the upper bound M.

In this work, the following adaptive version of the STC is considered [53]

$$\begin{cases} u_{st}(t) = -h_1 L(t,s) |s(t)|^{\frac{1}{2}} sign(s(t)) + u_2(t), \\ \dot{u}_2(t) = -h_2 L^2(t,s) sign(s(t)), \end{cases} \tag{3.3}$$

where the constant gains are set to $h_1 = 1.5$, $h_2 = 1.1$ and the adaptive gain $L(t,s)$ is to be defined based on an adaptive strategy which will be presented latter on. Suppose that $\phi(t) = u_2(t) + \delta(t)$, then the dynamic of the first order system can be expressed as

$$\begin{cases} \dot{s}(t) = -h_1 L(t,s) |s|^{\frac{1}{2}}(t) sign(s(t)) + \phi(t), \\ \dot{\phi}(t) = -h_2 L^2(t,s) sign(s(t)) + \dot{\delta}(t). \end{cases} \tag{3.4}$$

The objective is to adapt the gain $L(t,s)$ ensuring that the sliding variable belongs to a predefined neighborhood of zero $|s(t)| < \varepsilon$, as well as its derivative converges to some neighborhood of zero $|\dot{s}(t)| < \nu$. Note that this objective is fulfilled by choosing the control gain as BF. Hence, due to the reason that the application of BF requires that the sliding variable belongs to some predefined domain, an adaptive strategy based on increasing the gain [53], and an indicator are firstly introduced. The indicator is designed by introducing a time t_1, where t_1 is the smallest root of equation $|s(t)| \leq \frac{\varepsilon}{2}$. The idea is to increase the adaptive gain based on the strategy presented in [53] until the indicator reveals that the sliding variable enters in the predefined neighborhood of zero $|s(t)| \leq \frac{\varepsilon}{2}$. Then, the adaptive gain switches to the BF. Note that from the time instant t_1, the sliding variable belongs to the predefined neighborhood of zero $|s(t)| < \varepsilon$.

3.2.2 Main results

The following theorem is true for both possible STC gains design: using $L_B(s(t)) = L_{pb}(s(t)) = K_{pb}(s(t))$ and $L_B(s(t)) = L_{psb}(s(t)) = K_{psb}(s(t))$.

Theorem 3.2.1. *Consider system* (3.4) *with Lipschitz disturbance* $\delta(t)$ *and with the adaptive control gain* $L(t,s)$

$$L(t,s) = \begin{cases} L_a(t),\ \dot{L}_a(t) = L_1, & \text{if} \quad 0 < t \le t_1 \\ L_B(s(t)) & \text{if} \quad t_1 < t, \end{cases} \tag{3.5}$$

where L_1 *is to be arbitrary positive constant.*

Then for any $s(0)$ *and* $\varepsilon > 0$, *there exist* $\nu(M) > 0$, t_1 *the smallest root of equation* $|s(t)| \le \dfrac{\varepsilon}{2}$, *and* $T \ge t_1$ *such that for all* $t \ge t_1$, *the inequality* $|s(t)| < \varepsilon$ *holds and for all* $t \ge T$, $|\dot{s}(t)| \le \nu(M)$.

The proof of Theorem 3.2.1 is given in appendix B.

3.2.2.1 Adaptation with PBF

Consider the adaptation with PBF. In this case, $L^2_{pb}(s(t))$ has a lower bound $\bar{F}^2$. Suppose that $|\dot{\delta}(t)| < \bar{F}^2$, then the adaptive gain is overestimated, and the adaptive STC provides an ideal 2-OSM. Hence, the parameter $\bar{F}$ needs to be small enough in order to attenuate this overestimation. Although the parameter $\bar{F}$ can be chosen arbitrarily small, the adaptation with PBF will provide an ideal 2-OSM with overestimating gain when $|\dot{\delta}(t)| < \bar{F}^2$.

3.2.2.2 Adaptation with PSBF

Consider now the adaptation with PSBF. Here, $L^2_{psb}(s(t))$ tends to zero when $s(t) \to 0$. This means that if $\dot{\delta}(t)$ and $s(t)$ tend monotonically to zero, consequently the adaptive gain $L^2_{psb}(s(t))$ will go to zero.

Note that there is a benefit in using this adaptation which can ensure that the sliding variable will remain in $|s(t)| < \varepsilon$ with the smallest amplitude of the adaptive gain rather than the adaptation with PBF which does not allow the adaptive gain to decrease below $\bar{F}$.

TABLE 3.1: *Parameter values of the PBF, PSBF and AST for adaptive STCs*

	PBF	PSBF	AST
Parameter values	$L_1 = 12,\ \varepsilon = 0.001,$ $\bar{F} = 0.095$	$L_1 = 12,\ \varepsilon = 0.001,$	$\mu = 1,\ w_1 = 200,\ \gamma_1 = 2,$ $\varepsilon = 0.001,\ \nu = \alpha_m = 0.01$

3.2.3 Simulation results

The performance of the aforementioned barrier strategy is compared with the results obtained through the adaptive STC presented in [64].

In [64], the adaptive ST controller, referred as (AST), is implemented as

$$\begin{cases} u_{st}(t) = -\alpha(t)|s(t)|^{\frac{1}{2}} sign(s(t)) + u_2(t), \\ \dot{u}_2(t) = -\dfrac{\beta(t)}{2} sign(s(t)), \end{cases} \tag{3.6}$$

with $\beta = 2\mu\alpha$, and the adaptive gain α is obtained through

$$\dot{\alpha} = \begin{cases} w_1 \sqrt{\dfrac{\gamma_1}{2}} sign(|s(t)| - \varepsilon), & \text{if } \alpha > \alpha_m \\ \nu, & \text{if } \alpha \leq \alpha_m \end{cases} \tag{3.7}$$

where μ, w_1, γ_1, ε, α_m, and ν are positive constants to be selected.

In the following subsections, two cases are carried out: the first one deals with an increasing disturbance derivative, and the second one considers a monotonically decreasing disturbance derivative. In the simulations, $s(0) = 0.4$ and Table 3.1 contains the parameter values of PBF, PSBF and AST, where the parameter ε is set as $\varepsilon = 0.001$, while all the others are tuned according to [64].

3.2.3.1 Case of increasing disturbance derivative

The disturbance derivative is given by (Fig. 3.1(a))

$$\dot{\delta}(t) = \begin{cases} 0.5sin(3t), & \text{if } t \leq 5\ s, \quad M = 0.5, \\ 10sin(3t), & \text{if } 5\ s < t \leq 10\ s, \quad M = 10, \\ 20sin(3t), & \text{if } t > 10\ s, \quad M = 20. \end{cases} \tag{3.8}$$

The zoomed-in plots of the sliding variable $s(t)$ with PBF, PSBF and AST are compared in Figs. 3.1(b)-3.1(c)-3.1(d). In Figs. 3.1(b)-3.1(c) it can be observed that for both barrier functions PBF and PSBF, the sliding variable does not exceed the predefined neighborhood of zero $\varepsilon = 0.001$. On the other hand, it can be noticed in Fig. 3.1(d) that the size of

the neighborhood of zero to which converges $s(t)$ with AST is changing together with the amplitude of disturbance derivative M (for $t \leq 5$ s, $|s(t)| \leq 0.015$, for $5 < t \leq 10$ s, $|s(t)| < 0.06$, and for $t > 10$ s, $|s(t)| \leq 0.13$). Therefore, it cannot be predefined. Moreover, it can be very large when the amplitude of disturbance derivative is large (for $t > 10$ s, $M = 20$ and $|s(t)| \leq 0.13 = 130\varepsilon$).

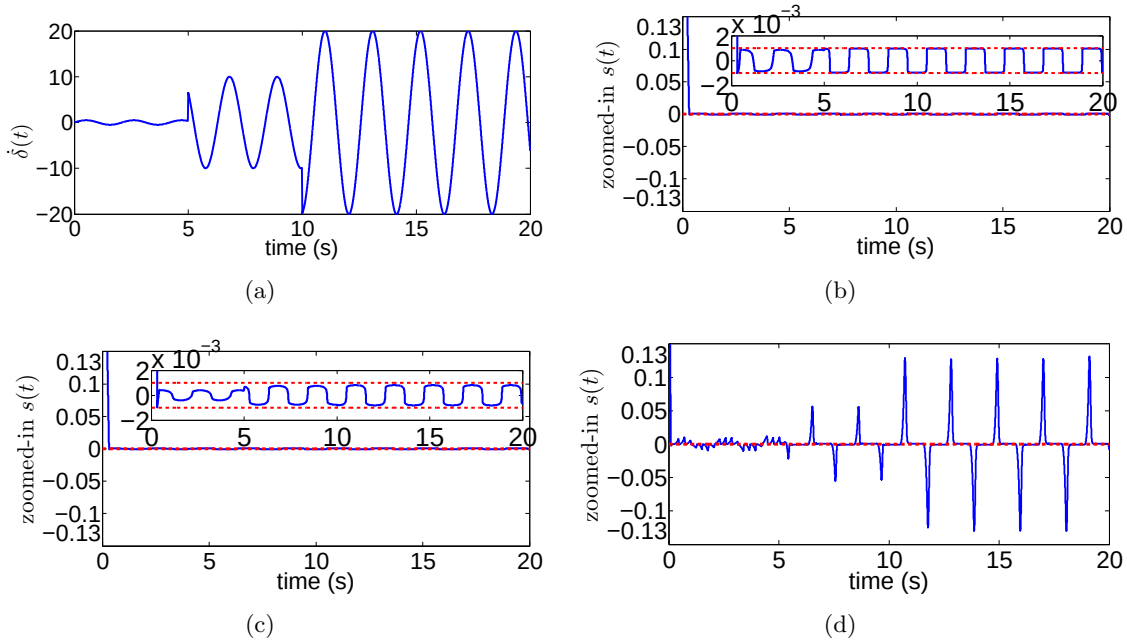

Figure 3.1. *a) Disturbance $\delta(t)$, and the zoomed-in plot of the sliding variable $s(t)$ with: b) PBF, c) PSBF, d) AST*

3.2.3.2 Case of monotonically decreasing disturbance derivative

Consider now the following monotonically decreasing disturbance derivative defined as (Fig. 3.2(a))

$$\dot{\delta}(t) = \frac{0.012}{t+1} + 0.0025.$$

The zoomed-in plots of the adaptive gain with PBF, PSBF and AST are depicted in Figs. 3.2(b)-3.2(c)-3.2(d). For $t > 0.6$ s the amplitude of the disturbance derivative becomes less than 0.01, where $1.1\bar{F}^2 = \alpha_m = 0.01$ (see Fig. 3.2(a)). That is why starting from this moment, the adaptive gains for both PBF and AST will be overestimated and cannot decrease below 0.095 and 0.01, respectively (see Figs. 3.2(b)-3.2(d)). On the other hand, the adaptive gain for PSBF is decreasing and will go to zero (see Fig. 3.2(c)).

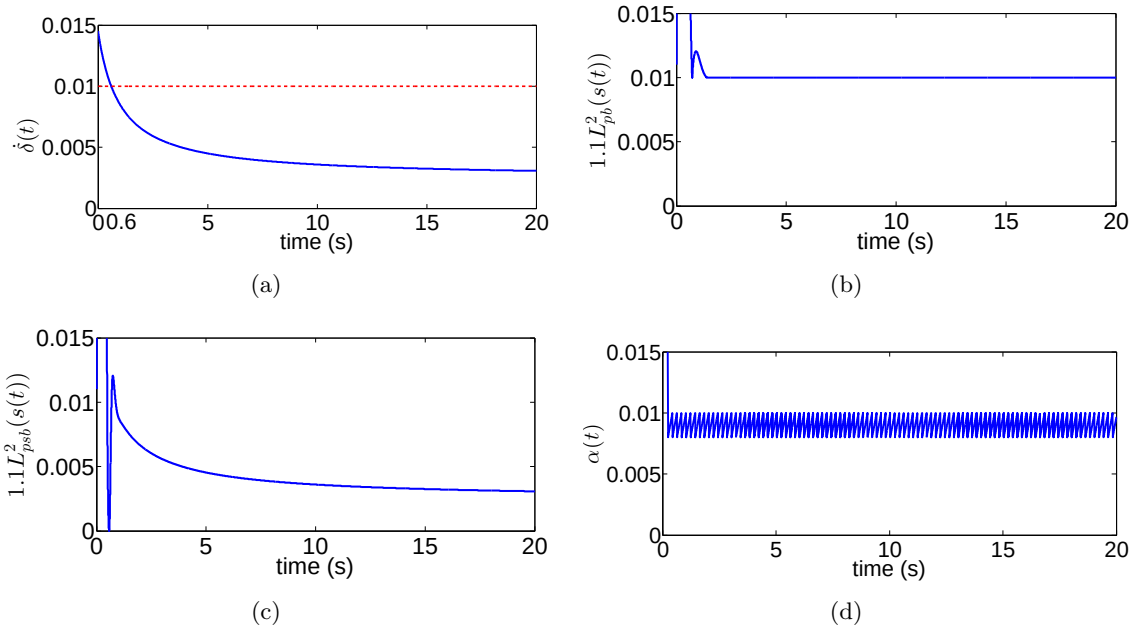

Figure 3.2. *a) Disturbance $\delta(t)$, and the zoomed-in plot of the adaptive gain with: b) PBF, c) PSBF, d) AST*

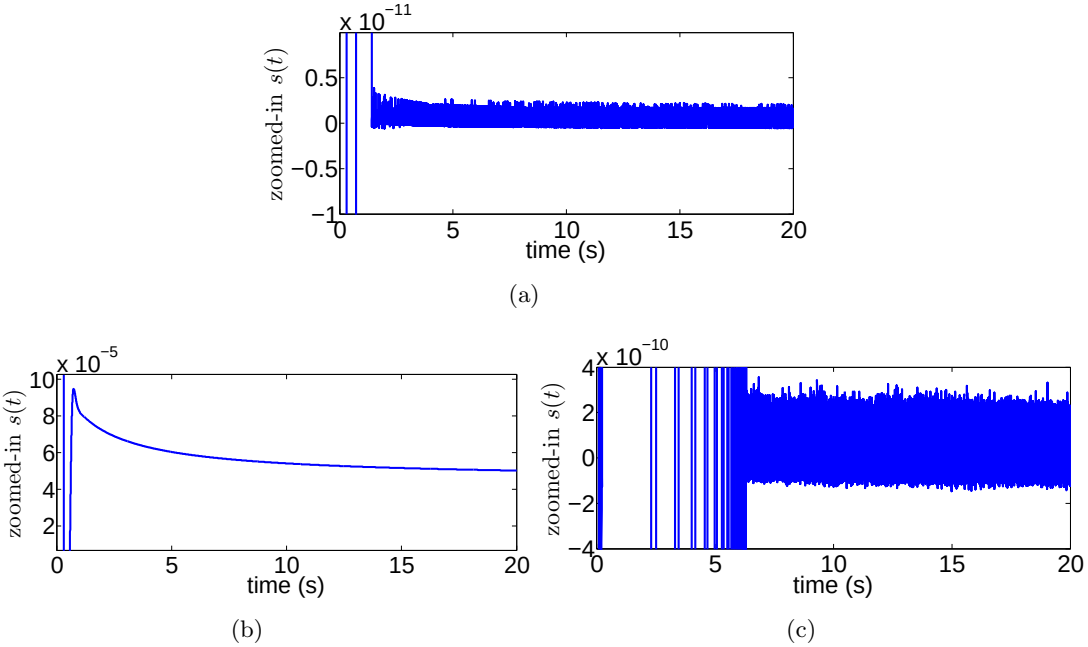

Figure 3.3. *Zoomed-in plot of the sliding variable $s(t)$ with: a) PBF, b) PSBF, c) AST*

The zoomed-in plots of the sliding variable $s(t)$ with PBF, PSBF and AST are illustrated in Figs. 3.3(a)-3.3(b)-3.3(c). The chattering appears for both PBF and AST withs amplitude 0.4×10^{-11} and 3×10^{-10}, respectively (see Figs. 3.3(a)-3.3(c)). On the other hand, it can be noticed that the sliding variable with PSBF will go to zero without chattering (see Fig. 3.3(b)).

3.3 Barrier Function-Based adaptive CISMC

3.3.1 Preliminaries

In the case of CISMC [16], the STC is applied instead of FOSMC in the auxiliary variable dynamic (2.9). This controller has two main limitations: first, the Lipschitz constant M of the disturbance $\delta(t)$ is supposed to be known. Second, the implementation of the standard STC requires a finite time to reach $s(t) = 0$, that is, there exists a $T > 0$ such that for all $t > T$, $s(t) = 0$ [17].

In what will follow, we will propose a new barrier function based-adaptive CISMC which overcomes these two disadvantages. Thus, the proposed approach allows to enforce the sliding variable to a prescribed vicinity of zero starting from the initial time moment under the assumption of Lipschitz disturbance with unknown Lipschitz constant M. As in the previous section two adaptive functions will be considered: first, the case when the adaptive gain is chosen as PBF, and second the case when it is chosen as PSBF.

3.3.2 Adaptation with PBF

Proposition 3.3.1. *Consider system* (2.9) *with Lipschitz disturbance whose Lipschitz constant M is unknown. Then, for any $\varepsilon > 0$ and for all $t \geq 0$, the inequality $|s(t)| < \varepsilon$ holds via the adaptive CISMC* (3.3) *with the adaptive control gain*

$$L(s(t)) = K_{pb}(s(t)) = \frac{\varepsilon \bar{F}}{\varepsilon - |s(t)|} \ . \tag{3.9}$$

Furthermore, an ideal 2-OSM, i.e. $s(t) = \dot{s}(t) = 0$ is guaranteed if $\bar{F}^2 > |\dot{\delta}(t)|$.

Proof. The above proposition is a particular case of theorem 3.2.1, where the PBF is used to adapt the gain of CISMC from the initial time moment. That is due to the specific feature of ISMC for which the auxiliary variable satisfies $s(0) = 0$. □

Remark 3.3.2. *In the case when* $|\dot{\delta}(t)| < \bar{F}^2$*, this adaptation will provide an ideal 2-OSM with overestimated adaptive gain (since the* $L(t(s))$ *cannot decrease below* $\bar{F}$*). Hence, the parameter* $\bar{F}$ *needs to be small enough in order to attenuate this overestimation.*

3.3.3 Adaptation with PSBF

Proposition 3.3.3. *Consider system* (2.9) *with Lipschtiz disturbance whose Lipschitz constant* M *is unknown. Then, for any* $\varepsilon > 0$ *and for all* $t \geq 0$*, the inequality* $|s(t)| < \varepsilon$ *holds via the adaptive CISMC* (3.3) *with the adaptive control gain*

$$L(s(t)) = K_{psb}(s(t)) = \frac{|s(t)|}{\varepsilon - |s(t)|} \ . \tag{3.10}$$

*P*roof. Similar to the proof of Proposition. 3.3.1. □

Remark 3.3.4. *As mentioned in section 3.2.2.2, there is a benefit in using this adaptation which can ensure that the auxiliary variable belongs to* $|s(t)| < \varepsilon$ *with the smallest amplitude of the adaptive gain rather than the adaptation with PBF which does not allow the adaptive gain to decrease below* $\bar{F}$*.*

3.3.4 An example

The second order system given in (2.12) is used again to verify the performance of the barrier algorithms-based adaptive CISMC. Their performances are also compared to those of AST (3.6)-(3.7).

The overall control is designed based on (2.6), where u_n is given in (2.13) and u_{SMC} is the adaptive CISMC. The parameter values of both BFs are the same as in subsection 2.3.4, and for AST the parameter values are set as follows: $w_1 = 200$, $\nu = \alpha_m = 0.1$, $\mu = 1$, $\gamma_1 = 2$, $\varepsilon = 0.01$.

Figs.3.4-3.5-3.6 illustrate the simulation results of the adaptive CISMC based on PBF, PSBF and AST respectively. Figs.3.4(a)-3.5(a) demonstrate that the auxiliary variable $s(t)$ is maintained in the prescribed vicinity of zero $\varepsilon = 0.01$ from the initial time moment. On the other hand, the auxiliary variable for AST cannot be maintained in the prescribed vicinity of zero (see Fig. 3.6(a)). Moreover, it will jump to a big value at the initial time moment (for $t = 0.05$ s, $s(t) > 0.08$). Next, it can be observed in Figs.3.4(b)-3.5(b)-3.6(b) that the overall control is continuous. Then, the convergence of the states to some vicinity of the origin is depicted in Figs.3.4(c)-3.5(c)-3.6(c). And finally, the evolution of the

adaptive gain can be shown in Figs.3.4(d)-3.5(d)-3.6(d). Note that, from Fig. 3.4(d), it can be observed that the adaptive gain cannot decrease below $\bar{F} = 0.6$ (see Remark.3.3.4).

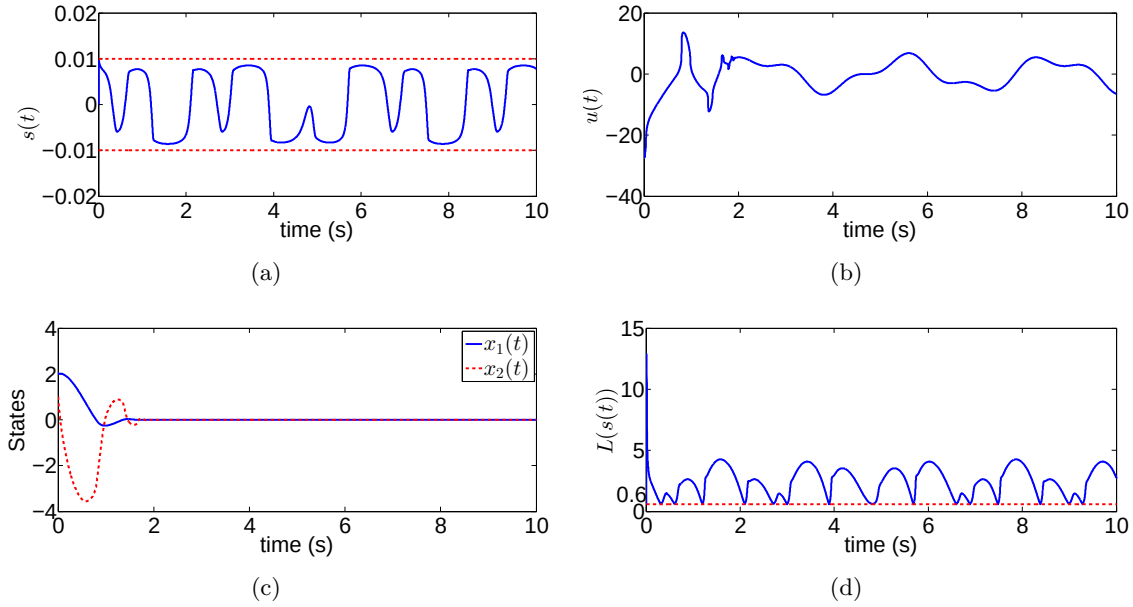

Figure 3.4. *Adaptive CISMC based on PBF*

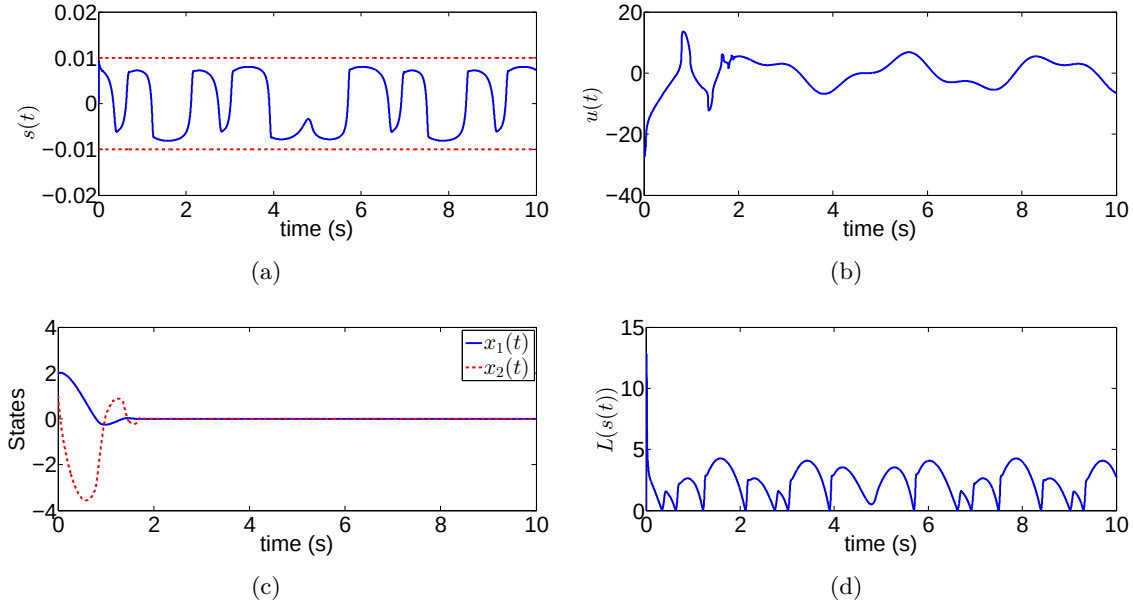

Figure 3.5. *Adaptive CISMC based on PSBF*

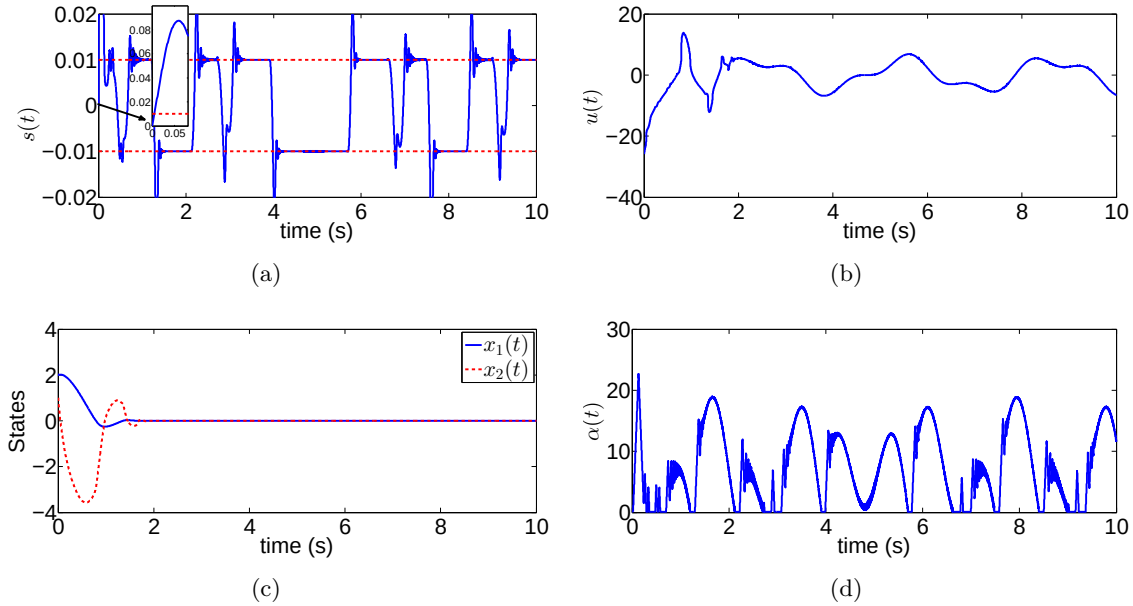

Figure 3.6. *Adaptive CISMC based on AST*

3.4 Summary

In this chapter, a barrier function-based adaptive STC for first order disturbed systems whose disturbance derivative is bounded with unknown boundary was proposed. This strategy ensures the convergence of the sliding variable and prevents its violation outside a predefined neighborhood of zero. Furthermore, the adaptive gain in this strategy is not overestimated.

Then, based on the same adaptive strategy, an adaptation of CISMC was proposed. The barrier strategy allows the CISMC to be implemented to a class of arbitrary order disturbed systems whose disturbance derivative bound is unknown. It was shown that the proposed algorithm ensures that the auxiliary variable belongs to a prescribed vicinity of zero starting from the initial time moment despite disturbance with unknown upper bound of its derivative. Moreover, there is no reaching phase, and the adaptive gain is not overestimated.

In the next chapter, the barrier function adaptation will be used to adapt Levant's differentiator. This adaptation is useful for the case when the upper bound of second derivative of base signal exists but it is unknown.

Chapter 4

Design of Adaptive LD

4.1 Introduction

The Super-Twisting algorithm is a very popular strategy for robust exact differentiation of a signal which has Lipschitz derivative. In this situation, this algorithm is called Levant's robust exact differentiator [44]. It is one of the most popular online differentiators. Recall that differentiators are important and widely incorporated into control design such as PID regulators, the construction of observers [6, 8] and the fault detection problems [27, 21]. Motivated by adaptive STC proposed in the previous chapter, this chapter develops an adaptive version of this Levant's Differentiator (LD) for the case when the upper bound of second derivative of base signal exists but it is unknown.

The LD has been proven that it is efficient theoretically and practically if the constant gains are chosen according to the upper bound of the second derivative of the base signal. Theoretically, this means in the ideal case, i.e. in the absence of noise, this differentiator ensures the finite-time exact estimation of the first derivative of the base signal. Practically, in the presence of noise, this differentiator ensures the finite-time convergence to the vicinity of the first derivative of the base signal whose size depends on the upper bound of the second derivative of the base signal and on the square root of the amplitude of the noise. The overestimation of the aforementioned upper bound causes a big error in the estimation of the first derivative.

In this chapter, the barrier function, used in chapter 2 and chapter 3, is applied to adapt the gains of LD. Such a function has the property to tend to infinity when its arguments come close to some predefined limits. Based on this attractive property, a new strategy to adapt the gains of LD is built up here.

This proposed barrier scheme guarantees that the size of the vicinity of the estimation of the signal belongs to a predefined vicinity of zero starting from the initial condition. Furthermore, it ensures a fast convergence of LD to some vicinity of the derivative of the base signal. However, the size of this vicinity depends on the upper bound of the second derivative of the base signal, which is unknown.

We will also draw in this chapter a comparison between different adaptation strategies of LD [64, 53] to estimate the first derivative. Without noise, it is shown that the proposed adaptive strategy is in competition with the known strategies of adaptation. In the presence of noise, the main advantage of the proposed adaptive strategy is that it could indicate when LD does not converge. However, the other existing strategies for LD adaptation could converge to the sum of the derivatives of the base and noise signals and it is impossible to identify it.

4.2 Problem Formulation

Let the input signal $\sigma_0(t)$ to be differentiated online. This signal has a Lipschitz derivative defined in $[0,\infty[$, i.e. for all t $\in [0,\infty[$ $max(|\ddot{\sigma_0}(t)|) \leq M$, but M is unknown. The standard LD [44] is defined as

$$\begin{cases} \dot{e_1}(t) = -h_1|e_1(t)|^{\frac{1}{2}} sign(e_1(t)) + e_2(t), \\ \dot{e_2}(t) = -h_2 sign(e_1(t)) - \ddot{\sigma_0}(t), \end{cases} \tag{4.1}$$

where $e_1(t) = z_1(t) - \sigma_0(t)$, $e_2(t) = z_2(t) - \dot{\sigma_0}(t)$ are the differentiator errors, $z_1(t), z_2(t) \in \mathbb{R}$ are the states, h_1, h_2 are the constant gains, and $|e_1(t)|$ is the absolute value of $e_1(t)$. The main specific feature of system (4.1) is that $e_1(0)$ can be considered as $e_1(0) = 0$, due to that it is supposed that the signal $\sigma_0(t)$ can be measured exactly. By choosing $h_1 = 1.5\sqrt{M}$ and $h_2 = 1.1M$, this LD can provide theoretically the exact value of the first derivative of the signal in a finite time; that is, there exists a $T > 0$ such that for all $t > T$, $e_1(t) = e_2(t) = 0$ holds, which leads to $z_1(t) = \sigma_0(t)$ and $z_2(t) = \dot{\sigma_0}(t)$ [44]. However, the implementation of this standard LD requires the information of the upper bound M. In this chapter, we assume that M is unknown.

The goal of this chapter is to propose a Barrier Adaptive LD (BALD) ensuring that the estimation error of the signal belongs to a predefined vicinity, as well as LD converges to some vicinity of the first derivative of the base signal.

In this chapter, we will use the following form of the adaptive LD [53]

$$\begin{cases} \dot{e}_1(t) = -k_1 L(e_1(t))|e_1(t)|^{\frac{1}{2}} sign(e_1(t)) + e_2(t), \\ \dot{e}_2(t) = -k_2 L^2(e_1(t)) sign(e_1(t)) - \ddot{\sigma}_0(t), \end{cases} \tag{4.2}$$

where $k_1 = 1.5$, $k_2 = 1.1$ are constants, and $L(e_1(t))$ is the barrier adaptive gain.

4.3 Barrier Function based-adaptive LD

Theorem 4.3.1. *Consider the adaptive form of LD (4.2) with bounded second derivative of the signal and with the adaptive gain $L(e_1(t))$ given by*

$$L(e_1(t)) = L_b(e_1(t)) = \frac{\bar{L}\varepsilon}{\varepsilon - |e_1(t)|}, \tag{4.3}$$

where $\bar{L}$, and ε are positive constants. Then, for any $\varepsilon > 0$ and $M > 0$, there exist $\delta_1 = \delta_1(M) > 0$ and $\bar{t}(M, e_2(0))$ such that for $e_1(0) = 0$ and any $e_2(0)$, for all $t \geq 0$, the inequality $|e_1(t)| = |z_1(t) - \sigma_0(t)| < \varepsilon$ holds and for all $t \geq \bar{t}$, $|e_2(t)| = |z_2(t) - \dot{\sigma}_0(t)| \leq \delta_1(M)$.

Remark 4.3.2. *Fig. 4.1 illustrates the errors $e_1(t)$, $e_2(t)$ and the evolution of the adaptive gain provided by BALD for the case when $\sigma_0(t) = sin(5t)$ and for different values of $e_2(0)$. In Fig. 4.1(a), it is confirmed that the inequality $|e_1(t)| < \varepsilon = 10^{-3}$ holds for $t \geq 0$. Moreover, from the zoomed-in plot of Fig. 4.1(b), it can be noticed that the time period $\bar{t}$ for which the inequality $|e_2(t)| = |z_2(t) - \dot{\sigma}_0(t)| \leq \delta_1$ holds increases when the value of $e_2(0)$ grows. Hence, $\bar{t}$ depends on $e_2(0)$. This specific behavior of $e_1(t)$ and $e_2(t)$ is due to the increase in the barrier adaptive gain depicted in Fig. 4.1(c). Indeed, it is shown in the zoomed-in plot that $L^2(e_1(t))$ increases when the value of $e_2(0)$ grows in order to maintain the error $e_1(t)$ in the predefined vicinity and force $e_2(t)$ toward some unknown vicinity. Note that BALD can ensure fast convergence but at the cost of overestimating the adaptive gain (for $t = 1 \times 10^{-4}$ s and $e_2(0) = 20$, $L^2(e_1(t)) = 6 \times 10^4$). This feature will be dangerous in the case of the presence of noise due to that the error $e_1(t)$ could go outside the predefined vicinity.*

Remark 4.3.3. *In order to demonstrate the statement of Theorem. 4.3.1, we apply BALD to estimate the derivative of the signal $\sigma_0(t) = sin(wt)$ with different values of w, which leads to different values of M. Fig. 4.2 shows the system trajectories in the phase*

plane $(e_1(t), e_2(t))$ *for the different values of* w*. It can be seen that the error* $e_1(t)$ *remains inside the predefined vicinity* $|e_1(t)| < \varepsilon = 10^{-3}$*. We can observe that the size of* $e_2(t)$ *grows when the value of* w *increases. Hence, the error* $e_2(t)$ *depends on* M*.*

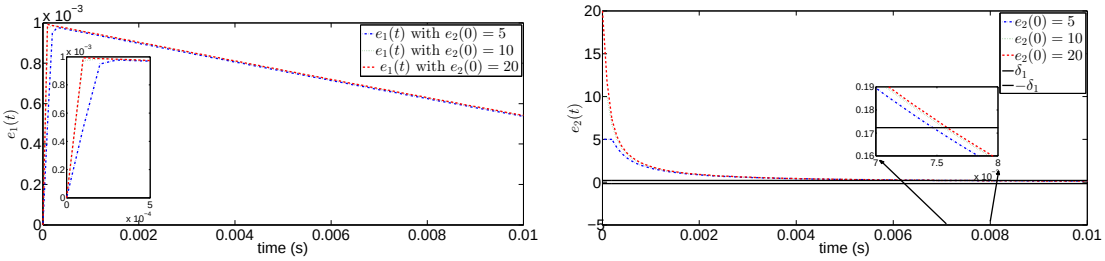

(a) Error $e_1(t)$ (b) Error $e_2(t)$

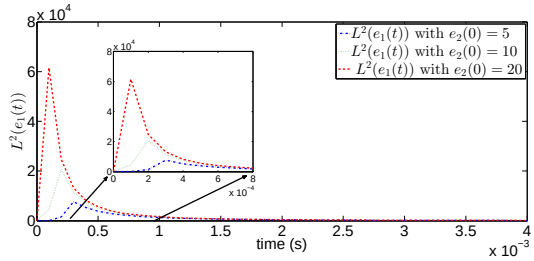

(c) $L^2(e_1(t))$

Figure 4.1. *Errors* $e_1(t)$ *and* $e_2(t)$ *for different values of* $e_2(0)$

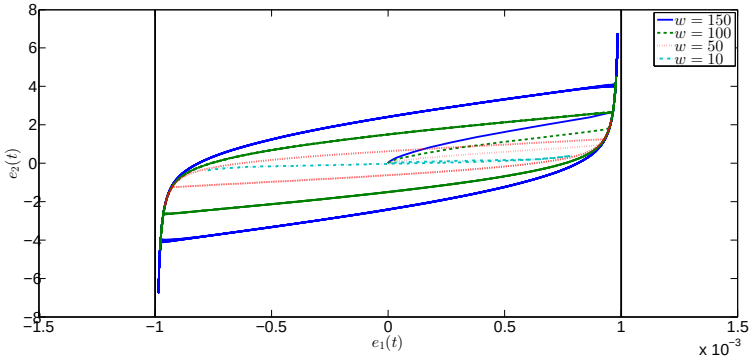

Figure 4.2. *Phase plane* $(e_1(t), e_2(t))$

Remark 4.3.4. *It is noted that the smallest value of the adaptive gain is $\bar{L}$. In a special case, when $M \leq \bar{L}^2$, an exact estimation of the signal and its derivative is achieved, i.e $z_1(t) = \sigma_0(t)$, $z_2(t) = \dot{\sigma_0}(t)$. In this case, the barrier adaptive LD coincides with the standard LD with the fixed gains (see Fig. 2.1).*

4.4 Simulation results

In this section, we will compare the performance of the aforementioned barrier algorithm with the results obtained through the two other adaptive algorithms, which are presented in [64] and [53].

The adaptive algorithm in [64] is proposed to adapt the Super-Twisting controller gains. It can be used to adapt LD parameters. This algorithm can drive LD to some vicinity of the first derivative of the signal. In this case, the Shtessel's Adaptive LD (SALD) is implemented as

$$\begin{cases} \dot{e_1}(t) = -\alpha(t)|e_1(t)|^{\frac{1}{2}} sign(e_1(t)) + e_2(t), \\ \dot{e_2}(t) = -\dfrac{\beta(t)}{2} sign(e_1(t)) - \ddot{\sigma_0}(t), \end{cases} \tag{4.4}$$

with $\beta = 2\varepsilon\alpha$, and the adaptive gain α is obtained through

$$\dot{\alpha} = \begin{cases} w_1 (\dfrac{\gamma_1}{2})^{\frac{1}{2}} sign(|e_1(t)| - \mu), & \text{if } \alpha > \alpha_m \\ \nu, & \text{if } \alpha \leq \alpha_m \end{cases} \tag{4.5}$$

where w_1, γ_1, μ, α_m, and ν are positive constants to be selected.

The second algorithm we will use for comparison is introduced in [53]. This algorithm can ensure theoretically exact finite-time estimation of the first derivative of the signal. In this case, the structure of the Negrete & Moreno's Adaptive LD (NMALD) is proposed as

$$\begin{cases} \dot{e_1}(t) = -k_1\gamma(t)|e_1(t)|^{\frac{1}{2}} sign(e_1(t)) + e_2(t), \\ \dot{e_2}(t) = -k_2\gamma^2(t) sign(e_1(t)) - \ddot{\sigma_0}(t), \end{cases} \tag{4.6}$$

with $k_1 = 1.5$, $k_2 = 1.1$. For some $\upsilon > 0$ and $\varepsilon_0 > 0$, the adaptive gain $\gamma(t)$ is computed through

$$\dot{\gamma}(t) = \begin{cases} \upsilon, & \text{if } |e_1(t)| > \varepsilon_0 \\ 0, & \text{if } |e_1(t)| \leq \varepsilon_0 \end{cases} \tag{4.7}$$

TABLE 4.1: *Parameter values of BALD, SALD and NMALD*

	BALD	SALD	NMALD
Parameter values	$\bar{L} = 2.2$, $\varepsilon = 0.001$	$\varepsilon = 1$, $\mu = 0.001$, $\gamma_1 = 2$, $\nu = 0.01$, $w_1 = 100$, $\alpha_m = 0.01$	$\varepsilon_0 = 0.001$, $\upsilon = 30$

The objective is to estimate the first derivative of the signal $\sigma_0(t)$ with the following second derivative

$$\ddot{\sigma}_0(t) = \begin{cases} 10sin(7t) + 2.3sign(cos(5t)), & \text{if } t \leq 5 \text{ s}, \quad M = 12.3 \\ 120sin(7t) + 2.3sign(cos(5t)), & \text{if } 5 \text{ s} < t \leq 10 \text{ s}, \quad M = 122.3 \\ 2sin(7t) + 2.3sign(cos(5t)), & \text{if } t > 10 \text{ s}, \quad M = 4.3 \end{cases} \tag{4.8}$$

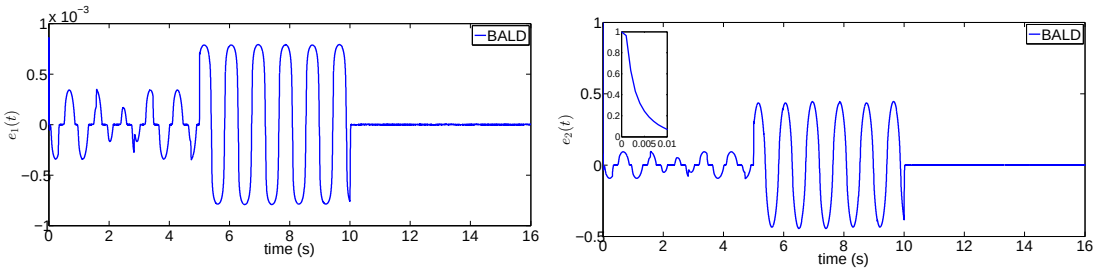

(a) Error $e_1(t)$ (b) Error $e_2(t)$

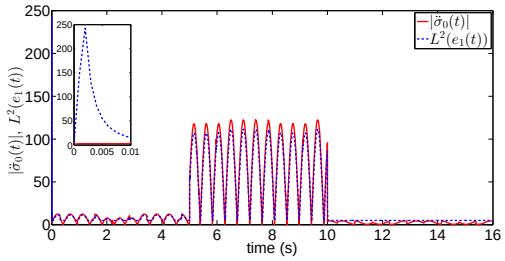

(c) $|\ddot{\sigma}_0(t)|$ and $L^2(e_1(t))$

Figure 4.3. *Simulation results of BALD*

The initial values of the estimation errors for all adaptive LDs are chosen as $e_1(0) = 0$, $e_2(0) = 1$. The parameter values of BALD, SALD, and NMALD are given in Table 4.1.

Fig. 4.3 illustrates the simulation results of BALD. Fig. 4.3(a) shows that the error $e_1(t)$ is maintained in the predefined vicinity of zero $\varepsilon = 10^{-3}$. It can be seen in Fig. 4.3(b) that the error $e_2(t)$ is driven to some vicinity of zero and the size of this vicinity depends

on M. Fig. 4.3(c) confirms that $L^2(e_1(t))$ follows the second derivative of the signal. Moreover, it is indicated that for $t > 10$ s, $L^2(e_1(t)) = \bar{L}^2$ since $M = 4.3$ is smaller than $\bar{L}^2 = 4.4$ (see Remark 4.3.4). Note that the zoomed-in plots in Figs. 4.3(b)-4.3(c) illustrate a fast convergence of the error $e_2(t)$ due to the increase of the adaptive gain (see Remark 4.3.2).

The simulation results of BALD and SALD are depicted in Fig. 4.4. It can be noticed in Fig. 4.4(a) that for both algorithms the error $e_1(t)$ is maintained in some vicinity of zero, but Fig. 4.4(b) shows that the error $e_1(t)$ in BALD does not exceed the predefined vicinity of zero with the size $\varepsilon = 10^{-3}$. On the other hand, it can be seen that the size of vicinity of zero, to which converges $e_1(t)$ in SALD, depends on M. The error $e_2(t)$ is depicted in Fig. 4.4(c). It can be concluded that in both of them, the error $e_2(t)$ is driven to some vicinity of zero depending on M. However, the convergence of the error $e_2(t)$ in BALD is faster than that one in SALD as revealed in the zoomed-in plot in Fig. 4.4(c). It is also shown that the error $e_2(t)$ in BALD is less than that one in SALD. Finally, Fig. 4.4(d) illustrates the adaptive gain evolution. It can be noticed that both adaptive gains can increase and decrease following the second derivative of the signal.

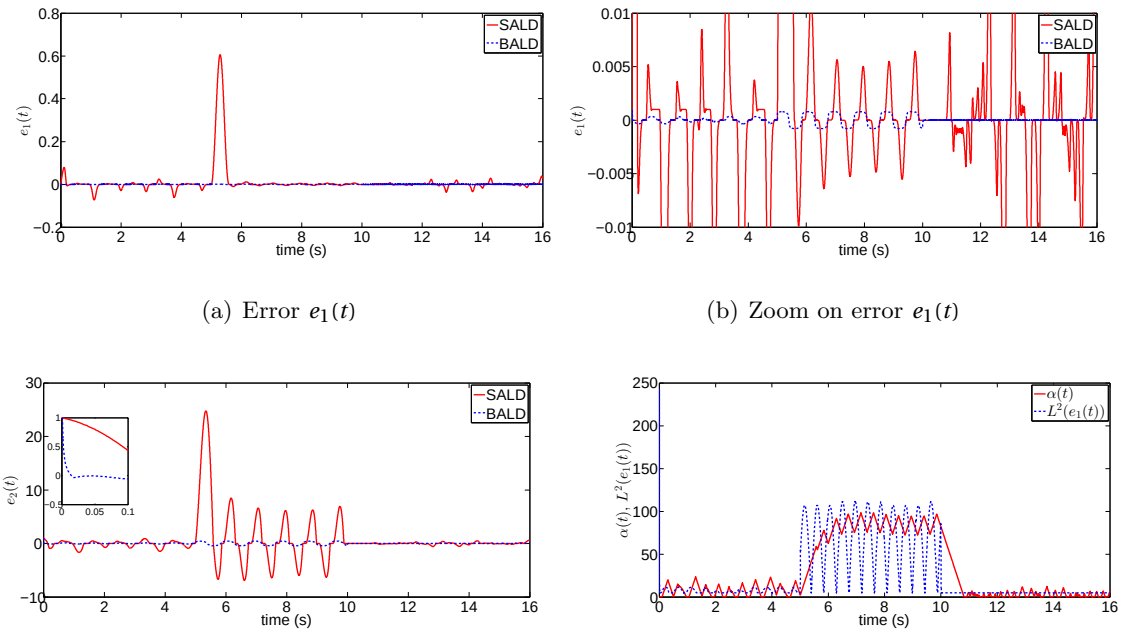

(a) Error $e_1(t)$

(b) Zoom on error $e_1(t)$

(c) Error $e_2(t)$

(d) $\alpha(t)$ and $L^2(e_1(t))$

Figure 4.4. *Simulation results of BALD and SALD*

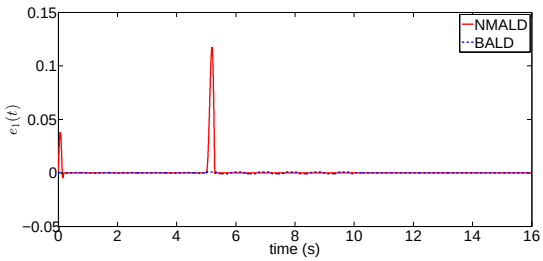

(a) Error $e_1(t)$

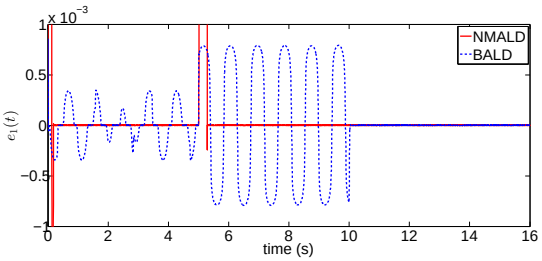

(b) Zoom on error $e_1(t)$

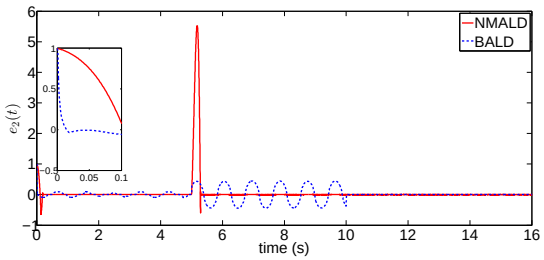

(c) Error $e_2(t)$

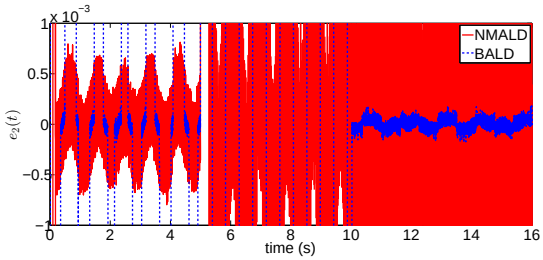

(d) Zoom on error $e_2(t)$

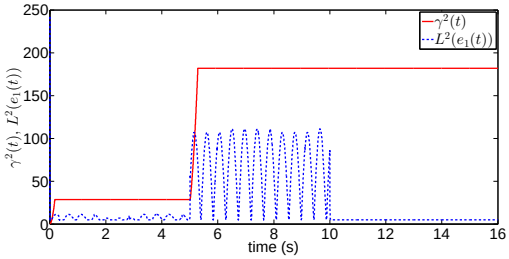

(e) $\gamma^2(t)$ and $L^2(e_1(t))$

Figure 4.5. *Simulation results of BALD and NMALD*

The simulation results of BALD and NMALD are compared in Fig. 4.5. It can be observed in Figs. 4.5(a)-4.5(b) that the error $e_1(t)$ in BALD can never exceed the predefined vicinity of zero, however, in NMALD, the convergence of the error $e_1(t)$ to zero in finite time can be ensured. The error $e_2(t)$ is illustrated in Figs. 4.5(c)-4.5(d). It can be seen in the zoomed-in plot that the error $e_2(t)$ in BALD converges faster than that one in NMALD. Moreover, it can be noticed in Fig. 4.5(d), which is a zoomed-in version of Fig. 4.5(c), that the chattering in BALD is smaller than that one in NMALD for $t > 10$ s. The overestimation of the adaptive gain in NMALD can be observed in Fig. 4.5(e).

In conclusion, the simulation results illustrate the fact that our proposed BALD can compete with other adaptive strategies for LD, such as SALD and NMALD, which implies the effectiveness of our proposed barrier strategy.

4.5 Adaptive LDs in the presence of noise

Consider the case of noisy signal. Suppose we measure the signal $\sigma(t)$ consisting of a base signal $\sigma_0(t)$ and a deterministic non-vanishing noise $\eta(t)$, such that $\forall\, t \geq 0 \quad |\eta(t)| \leq \eta_{max}$, i.e.

$$\sigma(t) = \sigma_0(t) + \eta(t). \tag{4.9}$$

Two cases are considered carrying out simulations in order to show qualitative behavior of the proposed algorithm to estimate $\dot{\sigma_0}(t)$ in the presence of noise.

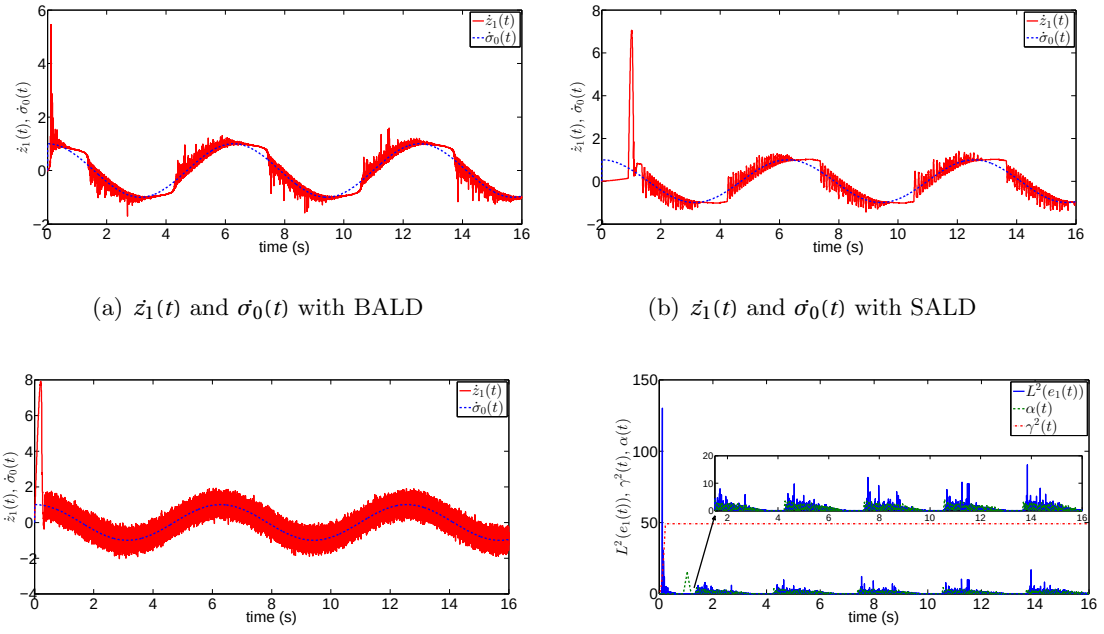

(a) $\dot{z_1}(t)$ and $\dot{\sigma_0}(t)$ with BALD

(b) $\dot{z_1}(t)$ and $\dot{\sigma_0}(t)$ with SALD

(c) $\dot{z_1}(t)$ and $\dot{\sigma_0}(t)$ with NMALD

(d) Adaptive gains

Figure 4.6. *Simulation results for the case when* $\eta_{max} << \varepsilon$

4.5.1 Case when $\eta_{max} << \varepsilon$

Consider the example when the base signal is $\sigma_0(t) = sin(t)$, and the noise $\eta(t)$ is implemented using a normally distributed random signal with maximum amplitude $\eta_{max} = 0.01$.

The parameter ε of BALD is selected as $\varepsilon = 0.1$. In SALD and NMALD, the parameters μ and ε_0 are set based on the amplitude of the noise, i.e. $\mu = \varepsilon_0 = 0.1$. In Figs. 4.6(a)-4.6(b)-4.6(c) it can be observed that $\dot{z}_1(t)$ in the three adaptive LDs comprises essentially the derivative of base signal and some high-frequency noise. Note that $\dot{z}_1(t)$ in NMALD is more affected by the noise than the other ones. Indeed, the adaptive gain in NMALD cannot decrease, while for BALD and SALD the adaptive gains can decrease as shown in Fig. 4.6(d).

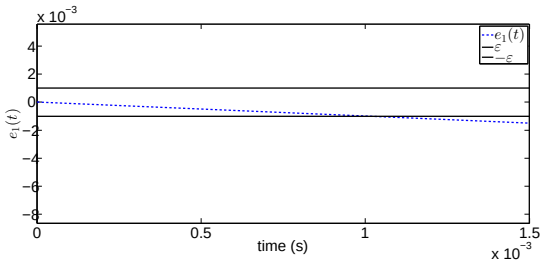

(a) Zoom on error $e_1(t)$ with BALD

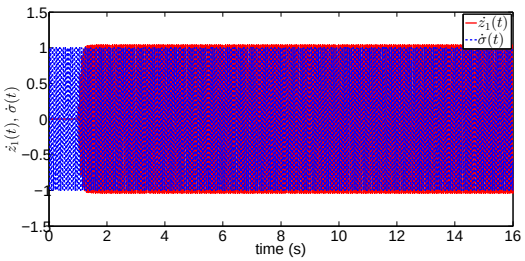

(b) $\dot{z}_1(t)$ and $\dot{\sigma_0}(t)$ with SALD

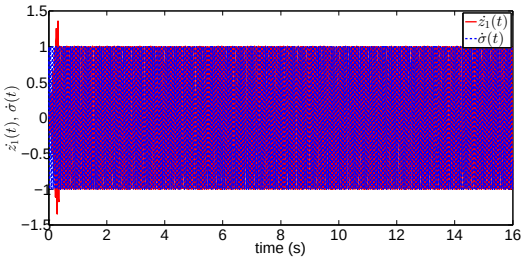

(c) $\dot{z}_1(t)$ and $\dot{\sigma_0}(t)$ with NMALD

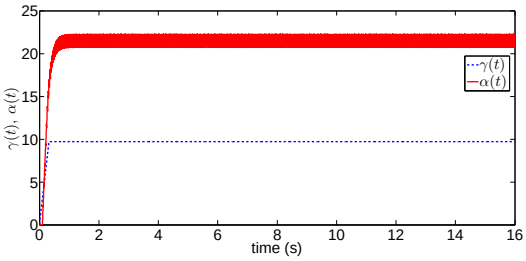

(d) Adaptive gains with SALD and NMALD

Figure 4.7. *Simulation results for the case when* $\eta_{max} > \varepsilon$

4.5.2 Case when $\eta_{max} > \varepsilon$

This section is provided to illustrate a counter-example showing that for $\eta_{max} > \varepsilon$ the proposed barrier strategy indicates that LD does not converge. Moreover, $\dot{z}_1(t)$ in SALD and NMALD converge to the sum of the derivatives of the base signal and the noise. Therefore, we need to consider a noisy signal with known derivative. We consider the simplest example, when the base signal is $\sigma_0(t) = 0$, and the noise is $\eta(t) = 0.01sin(100t)$. Hence,

$$\dot{\sigma}(t) = \dot{\sigma_0}(t) + \dot{\eta}(t) = \dot{\eta}(t) = cos(100t). \tag{4.10}$$

The three adaptive LDs are implemented now with $\varepsilon = \mu = \varepsilon_0 = 0.001 < \eta_{max} = 0.01$. It can be seen in the zoomed-in plot in Fig. 4.7(a) that for $t > 0.001$ s, the error $e_1(t)$ in BALD cannot be maintained in the predefined vicinity of zero. Therefore, it indicates that it does not converge. In Figs. 4.7(b)-4.7(c), it can be observed that $\dot{z}_1(t)$ in SALD and NMALD converge to the derivative of the noise as $\dot{z}_1 = \dot{\sigma}(t) = \dot{\eta}(t)$. It can be noticed in Fig. 4.7(d) that the adaptive gains in SALD and NMALD are growing to the value for which $\dot{z}_1(t)$ converge to the derivative of the noise.

4.5.3 Discussion

The simulation results show that none of the existing strategies of adaptation for LD can ensure its convergence for the case when the upper bound of the second derivative of the base signal exists but it is unknown. This is due to the reason that LD loses its filtration property in this case.

If the noise is small enough and the estimation error of measured variable still belongs to the predefined vicinity, it can be expected that the estimation provided by LD based on barrier strategy belongs to some vicinity of the derivative of the base signal. On the other hand, if the noise is big enough and the estimation error of the measured variable leaves the predefined vicinity of measured signal, the barrier strategy could indicate that BALD does not converge. In the case of SALD and NMALD, it is much more difficult to identify if LD converge to the derivative of the base signal or to the sum of derivatives of the base signal and the noise. Since in both of them, the gains grow to the level in which LD converge to some vicinity of the derivative of the noisy signal.

4.6 Summary

In this chapter, a barrier strategy is proposed to adapt the gain of LD for the case when the upper bound of the second derivative of the base signal exists but it is unknown. The vicinity size of the base signal estimation error does not depend on the upper bound of the second derivative. The proposed strategy ensures a fast convergence of the differentiator to some vicinity of the derivative of the base signal. However, the size of this vicinity depends on the unknown upper bound of the second derivative.

The barrier adaptive LD has two main advantages: it ensures fast convergence and could indicate that LD does not converge in the case of the noisy signal.

Moreover, the discussion made in section 4.5 has shown that none of the existing strategies of adaptation for LD can ensure its convergence for the case when the upper bound of the second derivative of the base signal exists but is unknown.

In the next chapter, two adaptive strategies for discontinuous HOSMC algorithms will be presented. These two strategies allow the discontinuous HOSMC to be implemented in the case of arbitrary chain of integrators system affected by disturbance with unknown upper bound or disturbance with unknown upper bound of its derivative.

Chapter 5

Design of adaptive DHOSMC

5.1 Introduction

In the case of a perturbed chain of integrators system of length n affected by disturbance with unknown upper bound or disturbance with unknown upper bound of its derivative, the adaptive DISMC and the adaptive CISMC presented in chapter 2 and chapter 3 can be applied. They can maintain the auxiliary variable in a predefined vicinity of zero. However, the main drawback of these approaches is that they cannot ensure the convergence of the system states to predefined vicinities of zero. This means that the sizes of vicinities to which converge the states are unknown. To overcome this problem, discontinuous higher order sliding mode controllers can be used. Indeed, it allows the convergence in a finite time of the system states to zero. However, it requires the knowledge of the bound of the disturbance. Therefore, this chapter deals with the adaptation of the discontinuous higher order sliding mode control. It proposes novel algorithms that can ensure the finite time convergence of the states to zero without requiring any information about the disturbances.

Higher Order sliding mode controls (HOSMCs) [63] have been introduced to overcome two main obstacles:

- The restriction that the control needs to appear explicitly in the first derivative of the sliding variable [71].
- The undesired chattering effect [71].

Indeed (HOSMCs) can be designed for systems with arbitrary relative degree n, and can provide the finite time convergence of the sliding variable and its $(n-1)$ derivatives to zero, i.e. achievement of n-th Order Sliding Mode (n-OSM). Unfortunately, the Discontinuous HOSMC (DHOSMC) [42, 22, 19] has the following disadvantages:

(i) Provides discontinuous control signal, i.e. suffers from chattering.

(ii) Requires the disturbance to be bounded with known upper bound.

(iii) Cannot be applied in the case when the disturbance is Lipschitz and not bounded.

Problem (i) can be bypassed by artificially increasing the input-output relative degree, and, consequently, HOSMCs are able to provide continuous control signals [28]. Nevertheless, HOSMC algorithms include all "signum" function frequently multiplied by a gain that depends on bounds of uncertainties or bounds of their derivatives, and thus chattering is not totally deleted even by increasing the relative degree.

On the other hand, to implement existing DHOSMCs, the upper bound of the disturbance is required. However, this upper bound is usually not constant and it is unknown. In this case, the gains of DHOSMC are set to be overestimated. This causes the increase of chattering [11]. Note that adaptive strategies which deal with the problem (ii) still lack. Moreover, the case when the disturbance is Lipschitz and not bounded (iii) remains an open problem for DHOSMC.

The main contribution of this chapter is the proposal of two adaptive DHOSMC strategies that overcome requirements (ii) and (iii) and ensure the achievement in a finite time of n-th OSM. These controllers are based on the adaptation of the homogeneous DHOSMC proposed in [22]. The first strategy deals with the problem (ii), and it consists in growing the gain of DHOSMC until the sliding mode is achieved. Notice that this strategy has been applied to adapt different sliding mode controllers [53, 58, 51]. To implement the DHOSMC in the case when the disturbance is Lipschitz and not bounded (iii), a novel dual layer adaptive strategy which adjusts the gain is proposed. This strategy employs the growing gain-based adaptive DHOSMC in conjunction with barrier function-based adaptive STC presented in chapter 3. Effectiveness of the two adaptive DHOSMC is illustrated through simulations in different disturbances conditions. Moreover, their performance is compared in the case when the disturbance is bounded and Lipschitz.

5.2 Problem Formulation

Consider the following arbitrary order system

$$s^{(n)}(t) = u(t) + \delta(t), \tag{5.1}$$

where n is the relative degree, $s(t)$ is the sliding variable, $u(t)$ is the control input and $\delta(t)$ is the disturbance. Here, $\delta(t)$ can be a bounded function with unknown upper bound δ_{max}, or Lipschitz function with unknown Lipschitz constant M.

The objective in this chapter is to drive in a finite time the sliding variable $s(t)$ and its $(n-1)$ derivatives to zero, i.e. achievement of n-OSM. One of the DHOSMC that can fulfil this objective in the case of bounded disturbance with known upper bound has been recently proposed in [22]. This result is summarized in the following theorem:

Theorem 5.2.1. *[22] Let deg $s = r_0 = \tau n$, with r_0 is a positive weight, and τ is the minus system homogeneity degree. Let deg $s^{(i)} = r_i$, deg $s^{(n)} = 0$,*

$$deg\ s^{(i)} = r_i = r_0 - i\tau = (n-i)\tau, \quad i = 0,\ ...,\ n. \tag{5.2}$$

and consider system (5.1) *with bounded disturbance $\delta(t)$. If the controller $u(t)$ is given by*

$$u = -\alpha sign n \varphi_{n-1}(s,\ \dot{s},\ ...,\ s^{(n-1)}) \tag{5.3}$$

with

$$\begin{aligned} \varphi_{n-1} = \lfloor s^{(n-1)} \rceil^{\frac{a}{r_{n-1}}} + \tilde{\beta}_{n-2} \lfloor s^{(n-2)} \rceil^{\frac{a}{r_{n-2}}} \\ + ... + \tilde{\beta}_1 \lfloor \dot{s} \rceil^{\frac{a}{r_1}} + \tilde{\beta}_0 \lfloor s \rceil^{\frac{a}{r_0}}, \end{aligned} \tag{5.4}$$

where $a > 0$, and the coefficients $\tilde{\beta}_0,\ ...,\ \tilde{\beta}_{n-2}$ satisfy

$$\tilde{\beta}_i = \beta_i\ \beta_{i+1}\ ...\ \beta_{n-2}, \quad i = 0,\ ...,\ n-2 \tag{5.5}$$

with $\beta_0,\ ...,\ \beta_{n-2} > 0$ are chosen sufficiently large in the index order. Then, for any upper bound of disturbance δ_{max}, there exists a sufficiently large α for which the controller in (5.3) *provides finite time achievement of n-OSM.*

In [22], the control gain α depends on the upper bound δ_{max} and it is tuned by simulation. However, in the case when the upper bound δ_{max} is unknown this controller is ineffective. To overcome this limitation, a new growing gain adaptive strategy is proposed in this chapter and will be presented later.

On the other hand, in the case when the disturbance $\delta(t)$ is Lipschitz and not bounded, nor the conventional DHOSMC neither its proposed adaptive version mentioned above can be applied directly. In order to deal with this case, the control $u(t)$ will be designed as a combination of two controls: Adaptive Super Twisting control (ASTC) and DHOSMC, based on a novel dual layer strategy. The idea is to firstly apply a barrier function-based ASTC to reconstruct the disturbance with a bounded reconstruction error. Then, the growing gain adaptation of DHOSMC is designed to compensate this bounded reconstruction error and ensures thus the achievement of the ideal n-OSM. In what follows, the proposed growing gain adaptation of DHOSMC and the dual layer-based adaptive DHOSMC are presented in detail.

5.3 Growing gain based-adaptive DHOSMC

Theorem 5.3.1. *Consider system* (5.1) *with disturbance* $\delta(t)$ *which is bounded with unknown upper bound* δ_{max}. *Using controller* (5.3) *with the constant* a, *the coefficients* $\tilde{\beta}_0, ..., \tilde{\beta}_{n-2}$ *are chosen according to Theorem 5.2.1, and the adaptive control gain satisfies*

$$\dot{\alpha}(t) = \begin{cases} \bar{\alpha}, & \text{if } ||\bar{s}(t)|| > 0 \\ 0, & \text{if } ||\bar{s}(t)|| = 0 \end{cases} \tag{5.6}$$

with $\bar{s} = [s, \dot{s}, ..., s^n]^T$, $\alpha(0)$ *and* $\bar{\alpha}$ *are positive constants to be selected. Then, this adaptive DHOSMC provides in a finite time an ideal* n*-OSM.*

Proof. Let $w_1 = s$, $w_2 = \dot{s}$, ..., $w_n = s^{(n-1)}$. Denote $\vec{w}_i = (w_1, ..., w_i)$, $i = 1, ..., n$. With these variables, system (5.1) is given by

$$\dot{w}_1 = w_2, \quad \dot{w}_2 = w_3, \quad ..., \quad \dot{w}_n = u(t) + \delta(t). \tag{5.7}$$

Consider the following Lyapunov function [22]

$$\begin{aligned} V_i(\vec{w}_i) &= V_{i-1}(\vec{w}_{i-1}) + W_i(\vec{w}_i), \\ W_i(\vec{w}_i) &= \int_{w_i^*}^{z_i} \left\lfloor \lambda \right\rceil^{\frac{a}{r_{i-1}}} - \left\lfloor w_i^* \right\rceil^{\frac{a}{r_{i-1}}} \Big\rceil^{\gamma} d\lambda. \end{aligned} \tag{5.8}$$

with $\rho \geq a$, $w_1^* = 0$, $w_i^* = -\beta_{i-2}^{r_{i-1}/a} \lfloor \xi_i \rceil^{r_{i-1}/a}$, $\xi_i = \lfloor s^{(i-1)} \rceil^{\frac{a}{r_{i-1}}} - \lfloor w_i^* \rceil^{\frac{a}{r_{i-1}}}$, $\gamma = \dfrac{2\rho - r_{i-1} + \tau}{a}$.

The time derivative of $V_n(\vec{w}_n)$ can be derived as

$$\begin{aligned}\dot{V}_n(\vec{w}_n) &= \frac{\partial V_n}{\partial w_1} w_2 + ... + \frac{\partial V_n}{\partial w_n} (u(t) + \delta(t)), \\ &= \underbrace{\frac{\partial V_n}{\partial w_1} w_2 + ... + \frac{\partial V_n}{\partial w_n} u_0}_{\dot{V}_0(\vec{w}_n)} + \frac{\partial V_n}{\partial w_n} (u(t) - u_0 + \delta(t)),\end{aligned} \tag{5.9}$$

with $u_0 = -\alpha_0 sign\varphi_{n-1}$ is the DHOSMC proposed in [22]. From [22], it follows that

$$\dot{V}_0(\vec{w}_n) \leq -cV_n^{\Gamma}, \tag{5.10}$$

where $\Gamma = \dfrac{2\rho}{2\rho+\tau} \in (0,1)$. This implies that

$$\dot{V}_n(\vec{w}_n) \leq -cV_n^{\Gamma} + \frac{\partial V_n}{\partial w_n} (u(t) - u_0 + \delta(t)). \tag{5.11}$$

Next, from (5.8) $\dfrac{\partial V_n}{\partial w_n}$ can be written as

$$\frac{\partial V_n}{\partial w_n} = \left| \lfloor w_n \rceil^{\frac{a}{r_{n-1}}} - \lfloor w_n^* \rceil^{\frac{a}{r_{n-1}}} \right|^{\gamma}. \tag{5.12}$$

In view of (5.4), it can be shown that

$$\varphi_{n-1} = \lfloor w_n \rceil^{\frac{a}{r_{n-1}}} - \lfloor w_n^* \rceil^{\frac{a}{r_{n-1}}}, \tag{5.13}$$

which yields

$$\frac{\partial V_n}{\partial w_n} = \lfloor \varphi_{n-1} \rceil^{\gamma}. \tag{5.14}$$

Then

$$\begin{aligned}\dot{V}_n(\vec{w}_n) &\leq -cV_n^{\Gamma} \\ &\quad + \lfloor \varphi_{n-1} \rceil^{\gamma} \Big((-\alpha(t) + \alpha_0) sign\varphi_{n-1} + \delta(t) \Big) \\ &\leq -cV_n^{\Gamma} - |\varphi_{n-1}|^{\gamma} (\alpha(t) - \alpha_0 - \delta_{max}).\end{aligned} \tag{5.15}$$

The first term on the right-hand side of (5.15) is negative-definite. The second term is also negative when $\alpha(t) > \alpha + \delta_{max}$. Since the adaptive gain $\alpha(t)$ is growing, and the disturbance $\delta(t)$ is bounded, it follows that there exists a constant $\alpha^* = \alpha_0 + \delta_{max}$ such that $\dot{V}(\vec{w}_n)$ is negative-definite for every disturbance if $\alpha(t) > \alpha^*$. Therefore, when $\alpha(t) > \alpha^*$, $\dot{V}_n(\vec{w}_n)$ satisfies

$$\dot{V}_n(\vec{w}_n) \leq -cV_n^{\Gamma}, \tag{5.16}$$

this leads $V_n(\vec{w}_n) = 0$ after a finite time. As a result, the states of the system (5.7) converge to the origin, moreover, $\alpha(t)$ stops growing (see the adaptive law (5.6)). Theorem 5.3.1 is proven.■

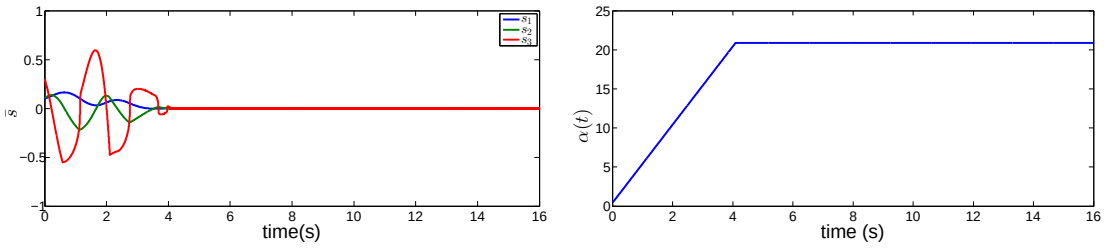

(a) (b)

Figure 5.1. *System* (5.17) *in close loop with growing gain-based adaptive DHOSMC* (5.18) *with disturbance* (5.19).

5.3.1 An example

The system in (5.1) is simulated with relative degree ($n = 3$) with respect to (w.r.t) control input, i.e.

$$\dot{s}_1 = s_2, \quad \dot{s}_2 = s_3, \quad \dot{s}_3 = u + \delta(t), \tag{5.17}$$

Following [22], an adaptive DHOSMC for such system is given by

$$u = -\alpha(t)\text{sign}(s_3^3 + \lfloor s_2 \rceil^{\frac{3}{2}} + s_1), \tag{5.18}$$

where the adaptive gain $\alpha(t)$ is computed through (5.6) with $\alpha(0) = 0.4$, $\bar{\alpha} = 5$. In the simulations, the initial conditions are selected as $\bar{s}(0) = [0.1,\ 0.1,\ 0.3]^T$, and the disturbance is chosen as

$$\delta(t) = 2|t - 5|^{\frac{1}{2}} - 5\cos(2t). \tag{5.19}$$

Fig. 5.1 shows the simulation results of system (5.17) with disturbance (5.19) using the growing gain-based adaptive DHOSMC. It can be seen that the states s_1, s_2, s_3 of system (5.17) converge to the origin in finite-time, the adaptive gain $\alpha(t)$ increases and then remains constant, since it has attained a value that can compensate the disturbance.

According to [22], the adaptive DHOSMC (5.18) provides the following accuracy for the states w.r.t sampling step τ

$$|s_1| \leq \lambda_1 \tau^3, \quad |s_2| \leq \lambda_2 \tau^2, \quad |s_3| \leq \lambda_3 \tau, \tag{5.20}$$

where λ_i are positive constants. By simulations shown in Fig. 5.2 with Euler method and $\tau = 10^{-5}s$, constants λ_i are determined as $\lambda_1 = 4000$, $\lambda_2 = 150$, and $\lambda_3 = 20$. These constants have been confirmed by the simulations with $\tau = 10^{-6}s$ also shown in Fig. 5.2.

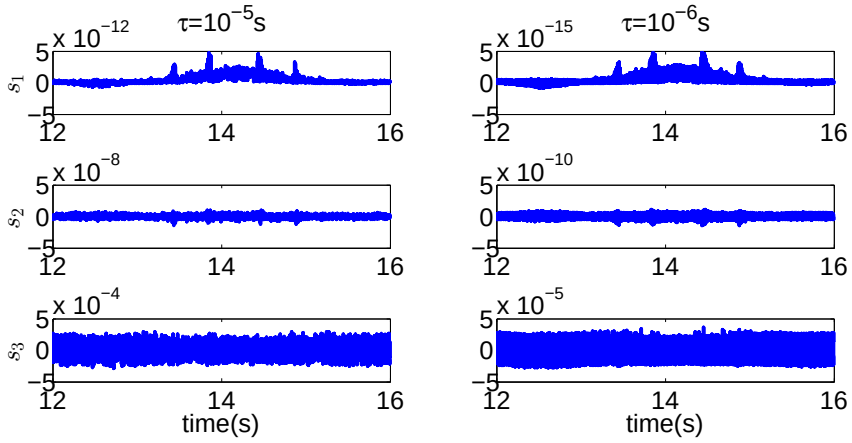

Figure 5.2. *Accuracy provided by growing gain-based adaptive DHOSMC* (5.18) *for system* (5.17) *in close loop with disturbance* (5.19).

5.4 Dual layer-based adaptive DHOSMC

The above controller is not applicable in the case when the disturbance is Lipschitz and not bounded. In order to deal with this case, a Dual layer-based adaptive DHOSMC is proposed in this section.

Consider once again the system in (5.1) where the disturbance $\delta(t)$ is Lipschitz. The controller $u(t)$ is now chosen as a combination of two parts

$$u = u_{ADHOSMC} + u_{ASTC}, \tag{5.21}$$

where $u_{ADHOSMC}$ is the adaptive DHOSMC defined in the previous section and u_{ASTC} is the adaptive STC defined in chapter 3 (3.3).

An auxiliary variable for system (5.1) is defined as

$$\sigma(t) = s^{(n-1)}(t) - s^{(n-1)}(0) - \int_0^t u_{ADHOSMC}(\tau)d\tau, \tag{5.22}$$

where $s^{(n-1)}(0)$ is the initial condition. The main specific feature of the following auxiliary variable is that $\sigma(0) = 0$. From (5.1), the dynamic of the auxiliary variable can be expressed as

$$\begin{aligned} \dot{\sigma} &= s^{(n)}(t) - u_{ADHOSMC} \\ &= u_{ASTC} + \delta(t). \end{aligned} \tag{5.23}$$

Theorem 5.4.1. *Consider system* (5.23) *with disturbance* $\delta(t)$ *which is Lipschitz with unknown Lipschitz constant* M*. Then, for any* $\varepsilon > 0$ *and for all* $t \geq 0$*, the inequality* $|\sigma(t)| < \varepsilon$ *holds. And for all* $t \geq t_1$*, with* t_1 *is the reaching phase, it holds that* $|\dot{\sigma}(t)| < \Delta(\varepsilon, M)$ *via* u_{ASTC} (3.3) *with the adaptive control gain*

$$L(\sigma(t)) = \frac{\varepsilon \bar{F}}{\varepsilon - |\sigma(t)|}, \tag{5.24}$$

where $\bar{F}$ *is positive constant to be selected. Furthermore, an ideal 2-OSM, i.e.* $\sigma(t) = \dot{\sigma}(t) = 0$ *is guaranteed if* $\bar{F}^2 > M$*.*

*P*roof. The above theorem is a particular case of theorem 3.2.1, where the PBF is used to adapt the gain of STC from the initial time moment. □

Remark 5.4.2. *Note that if the initial value of disturbance is equal to zero, the reaching phase* $t_1 = 0$ *[17]. Otherwise, to make this reaching phase small,* ε *should be chosen small enough.*

Remark 5.4.3. *For* $t \geq t_1$*, the ASTC can maintain* $|\dot{\sigma}(t)| \leq \Delta(\varepsilon, M)$*, i.e.*

$$-\Delta(\varepsilon, M) \leq u_{ASTC} + \delta(t) \leq \Delta(\varepsilon, M), \quad \forall t \geq t_1. \tag{5.25}$$

This means that the proposed ASTC cannot exactly reconstruct the disturbance $\delta(t)$*. However, it can provide an upper bound* $\Delta(\varepsilon, M)$ *of its reconstruction error.*

Now, having satisfied (5.25), and from (5.1) and (5.21), $s^{(n)}(t)$ can be derived as

$$\begin{aligned} u_{ADHSOMC} - \Delta(\varepsilon, M) &\leq s^{(n)}(t) \\ &\leq u_{ADHSOMC} + \Delta(\varepsilon, M), \ \forall t \geq t_1. \end{aligned} \tag{5.26}$$

Therefore, the role of the control part $u_{ADHSOMC}$ becomes to compensate the unknown upper bound of the reconstruction error $\Delta(\varepsilon, M)$.

Theorem 5.4.4. *The controller given in* (5.21)*, with* $u_{ADHOSMC}$ *that satisfies Theorem 5.3.1 and* u_{ASTC} *that satisfies Theorem 5.4.1, is a dual layer-based adaptive DHOSMC for system* (5.1)*. It provides the finite time convergence of the states to zero despite the presence of Lipschitz disturbance* $\delta(t)$ *with unknown Lipschitz constant* M*.*

*P*roof. According to Theorem 5.4.1, the barrier function-based ASTC can ensure that $|u_{ASTC} + \delta(t)| \leq \Delta(\varepsilon, M)$ after a finite time t_1. Once t_1 has been attained, the growing gain-based adaptive DHOSMC can drive the states to zero, since the conditions of Theorem 5.3.1, which is the boundaries of the disturbance, is satisfied. □

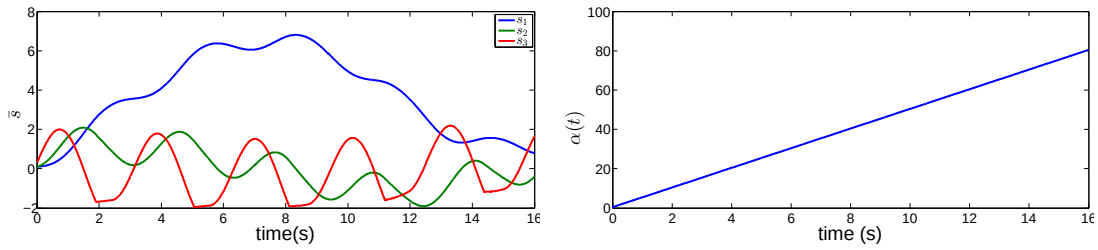

(a) (b)

Figure 5.3. *System* (5.17) *in close loop with growing gain-based adaptive DHOSMC* (5.18) *with disturbance* (5.27).

5.4.1 An example

The third order disturbed system given in (5.17) is used again, but now under the following distubance

$$\delta(t) = 5t + 4cos(2t), \tag{5.27}$$

which is Lipschitz and not bounded. The two proposed strategies to adapt the DHOSMC are tested in this subsection. For the dual layer-based adaptive DHOSMC, the control $u(t)$ is designed based on (5.21), where $u_{ADHOSMC}$ is given in (5.18). The parameter values for the growing gain-based adaptive DHOSMC used in both strategies are the same as in subsection 5.3.1, and for the ASTC the parameter values are set as follows: $\varepsilon = 0.01$, $\bar{F} = 1$.

Fig. 5.3 shows the simulation results of system (5.17) with disturbance (5.27) using the growing gain-based adaptive DHOSMC. It can be noticed that the states s_1, s_2, s_3 of system (5.17) will not converge to the origin, moreover, the adaptive gain $\alpha(t)$ will not stop growing. This is due to the reason that the disturbance (5.27) is not bounded in this case.

The simulation results of the dual layer based-adaptive DHOSMC applied to system (5.17) with disturbance (5.27) are depicted in Fig. 5.4. It can be confirmed that the states s_1, s_2, s_3 of system (5.17) converge to the origin in a finite time. The adaptive gain $\alpha(t)$ grows and reaches a constant value, and the reconstruction error of the disturbance is bounded by an upper bound $\Delta(\varepsilon, M) = 0.05$.

The accuracy provided by the dual layer based-adaptive DHOSMC can be shown in Fig. 5.5. It satisfies (5.20), with the constants λ_i are determined for $\tau = 10^{-5}s$ as $\lambda_1 = 500$, $\lambda_2 = 30$, $\lambda_3 = 20$ and have been verified with $\tau = 10^{-6}s$.

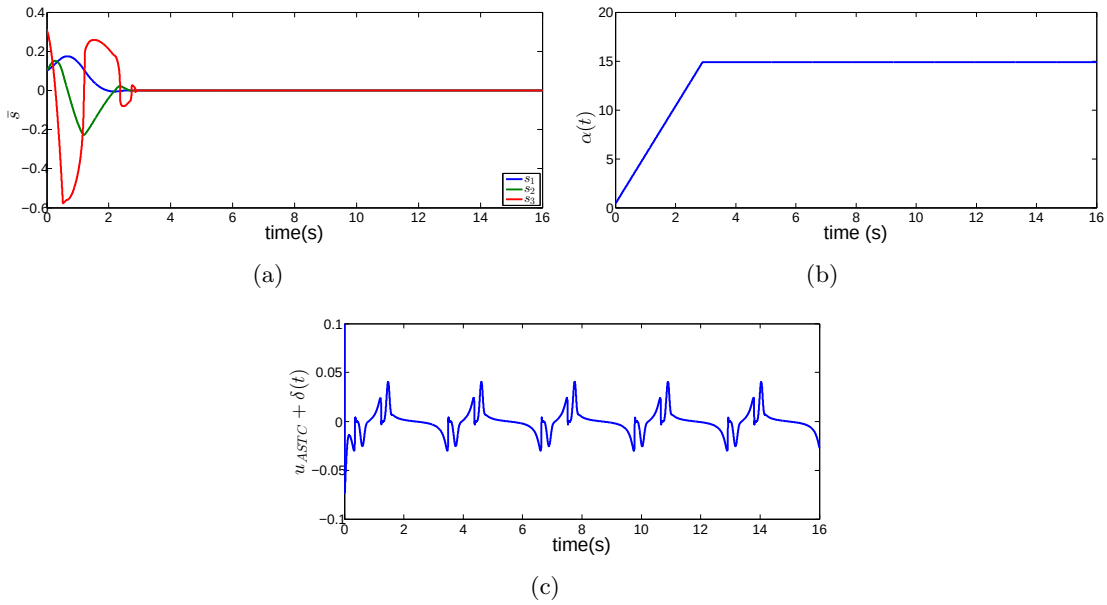

Figure 5.4. *System* (5.17) *in close loop with dual layer-based adaptive DHOSMC* (5.21) *with disturbance* (5.27).

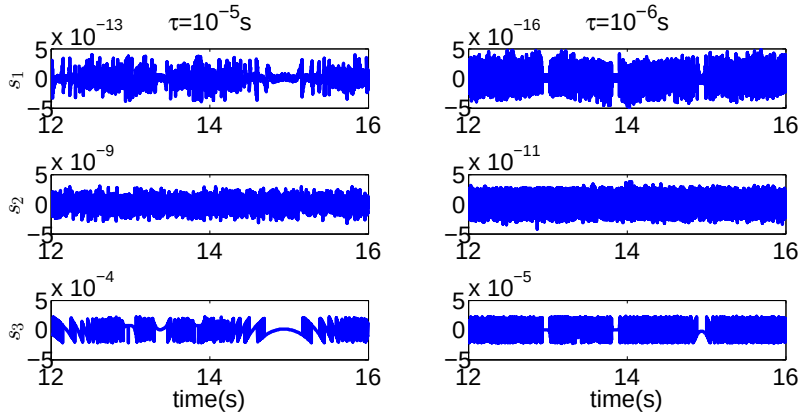

Figure 5.5. *Accuracy provided by dual layer-based adaptive DHOSMC* (5.21) *for system* (5.17) *in close loop with disturbance* (5.27).

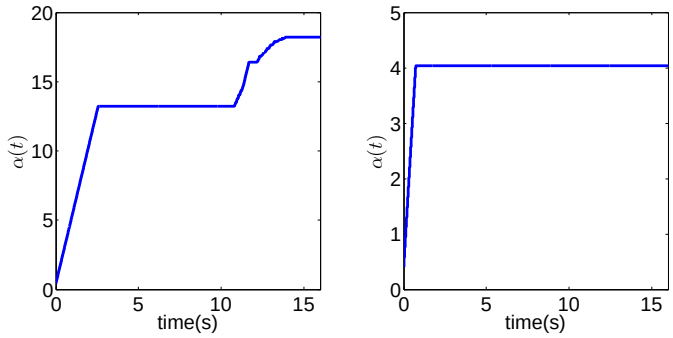

Figure 5.6. *Case of increasing disturbance amplitude: left box:* $\alpha(t)$ *with* (5.18)*, right box:* $\alpha(t)$ *with* (5.21)

5.5 Comparison of both proposed adaptive strategies

Again, consider system in (5.1) with the disturbance $\delta(t)$ is supposed to be Lipschitz and bounded. In order to show which adaptive strategy has a better performance in the sense that it can provide a lower amplitude of the adaptive gain $\alpha(t)$, which means less chattering effect, two cases will be considered.

5.5.1 Case of increasing disturbance amplitude

Consider the example when the disturbance is given by

$$\delta(t) = \begin{cases} 2cos(2t), & \text{if } t \leq 6 \text{ s}, \\ 18cos(\frac{1}{4.5}t), & \text{if } t > 6 \text{ s}. \end{cases} \tag{5.28}$$

It is clear that in this case δ_{max} increases, and M is constant. The initial values are set as $\bar{s}(0) = [0.1,\ 0,\ 0]^T$, and the parameter values for both controllers are the same as in subsection 5.4.1. In Fig. 5.6 it can be observed that $\alpha(t)$ with the growing gain strategy increases along with the increase of δ_{max}. On the other hand, $\alpha(t)$ with the dual layer-strategy remains constant and is not affected by δ_{max}. Indeed, $\alpha(t)$ with this latter strategy depends only on M, which does not change in this case. It can be noted that for this class of disturbance the dual layer strategy provides less amplitude of $\alpha(t)$, which leads to less chattering.

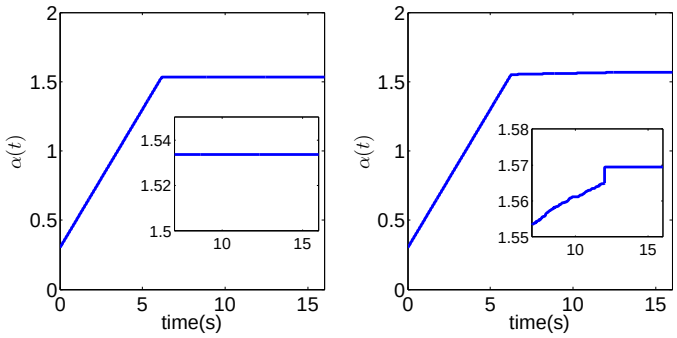

Figure 5.7. *Case of increasing disturbance frequency: left box:* $\alpha(t)$ *with* (5.18)*, right box:* $\alpha(t)$ *with* (5.21)

5.5.2 Case of increasing disturbance frequency

Now, the disturbance is given by

$$\delta(t) = \begin{cases} 1.5cos(80t), & \text{if } t \leq 12 \text{ } s, \\ 1.5cos(300t), & \text{if } t > 12 \text{ } s. \end{cases} \tag{5.29}$$

This means that δ_{max} is constant, and only M increases. In the following simulations, the initial values are selected as $\bar{s}(0) = [0.1,\ 0,\ 0]^T$. The parameter values of ASTC are set as $\varepsilon = 0.02$, $\bar{F} = 1$, and for the growing gain-based adaptive DHOSMC, they are selected as $\bar{\alpha}(t) = 0.2$, $\alpha(0) = 0.3$. It can be seen in the zoomed-in plots in Fig. 5.7 that $\alpha(t)$ with the growing gain strategy is not affected by the change of M. However, $\alpha(t)$ with the dual layer strategy increases along with the increase of M. Moreover, it can be noticed that the amplitude of $\alpha(t)$ with the dual layer strategy is bigger than the one with the growing gain strategy. Therefore, it can be concluded that in this case, the growing gain strategy provides less amplitude of chattering.

5.6 Summary

This chapter proposes two different adaptive strategies for discontinuous higher order sliding mode controllers. These two controllers ensure the finite time convergence of the sliding variable and its $(n-1)$ derivatives to zero without requiring any information about the disturbances. The first strategy consists in growing the gain until the sliding mode is achieved and it can be applied in the case of bounded disturbances with unknown upper

bound. While the second strategy is based on a novel dual layer adaptation and can be applied in the case of Lipschitz disturbance with unknown Lipschitz constant.

In addition, a comparison between these two strategies has been discussed in the case of Lipschitz bounded disturbance. If the disturbance amplitude is increasing, the dual layer strategy has better performance in the sense of less amplitude of chattering. On the other hand, if the disturbance frequency is increasing, the growing gain strategy performs better.

This chapter concludes theoretical and methodological developments of novel adaptive sliding mode controllers and differentiator proposed in this thesis. In the next two chapters, different controllers that have been developed will be tested and their performances illustrated on two types of energy conversion systems. These two systems are nonlinear, uncertain and disturbed. Moreover their output present different relative degrees. The first one has a relative degree equal to one, while the other one has a relative degree equal to two. Hence, in chapter 6, the active and reactive power control of a wind-energy conversion system will be considered. Then, in chapter 7, the control of linear induction motor used in cogeneration system will be addressed.

Chapter 6

Application to Wind Energy Conversion System

Wind energy has been regarded as an environmentally friendly alternative energy source which has attracted much attention [77]. The attention is growing quickly due to different reasons. In the last two decades, wind energy is taking the most important position in the development of renewable energy due to its many benefits, such as cost effectiveness, simple structure and efficiency [14]. With the remarkable growth in the technology of Wind Energy Conversion System (WECS), several works have been focused on improving the performance of the wind turbine, reducing its cost, increasing its lifetime, and investigating the advanced control strategies that improve its efficiency, taking into consideration the characteristics of WECS. However, the WECS is considered as an uncertain and complex system. The complexity comes from the nonlinear system dynamic, parameter uncertainties, external perturbations, and random nature of wind speed. Its electrical dynamic is usually described by two nonlinear systems with relative degree one affected by unknown uncertainties/disturbance.

This chapter discusses the adaptive control of active and reactive power of WECS using the new control strategies developed in this thesis for systems with relative degree equal to one. Recall that, in chapter 2 and chapter 3, two types of adaptive SMCs have been presented for such systems.

6.1 State-of-the-Art and contributions

When WECS is working on the partial load zone of operation (described in section 6.2) the following two main objectives should be fully assured [33],[9],[30]:

- Regulate the active power to track the maximum power point obtained by the Maximum Power Point Tracking (MPPT) controller.
- Control the reactive power to track the reference reactive power.

It has been shown that linear controllers, which are widely used in various control applications, are not robust for uncertain systems [62]. In fact, the main drawback of such type of controllers is that their coefficients should be tuned depending on the generator parameters, which are just partially known, and external disturbances.

For systems with uncertainties, the SMC has proven its high efficiency [71]. Indeed, one of the most famous controllers used to control WECS is the classical FOSMC [38]. However, the main obstacle of FOSMC is chattering. To attenuate this phenomenon, the STC has been introduced. This controller is one of the most popular controls for disturbed systems with relative degree one, and with Lipschitz's disturbances [43]. Hence, many STCs have been used to control WECS [12, 48, 31].

In the above publications, and in order to implement the FOSMC or STC, the upper bound of the disturbance or its derivative were assumed to be known. In practical systems, and specially in WECS, these bounds are unknown. In this case, the control gains of FOSMC and STC are set to be overestimated.

To overcome this difficulty, this chapter proposes the application of the barrier function-based adaptive FOSMC (BAFOSMC) and STC (BASTC), presented in chapter 2 and chapter 3, to control WECS. These two adaptive controllers ensure the convergence in a finite time of the sliding variables to given neighborhoods of zero. The size of these neighborhoods does not depend on the disturbance. Moreover, they do not require neither the upper bound of disturbance nor the upper bound of its derivative. Indeed, they only require information about the sliding variables.

Hence, the main contributions of this chapter are the following:

- BAFOSMC and BASTC are applied to control the WECS in order to extract the maximum power obtained by MPPT controller and to achieve the reference reactive power with predefined errors, independent of the upper bound of the disturbance/uncertainties and their derivatives.

- The proposed controllers are proved to be appropriate choices to control the WECS due to their robustness when applied for nonlinear uncertain systems, where the bounds of the disturbance/uncertainties and their derivatives are unknown.
- The proposed controllers ensure the non overestimation of the adaptive gains.
- Finally, we have compared both proposed adaptive controllers with other adaptive ones [58, 64] to control WECS illustrating the positive features of our proposed barrier strategy.

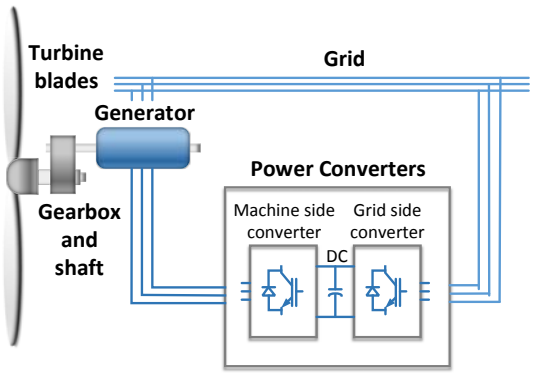

Figure 6.1. *Wind energy conversion system*

6.2 WECS modeling

The famous WECS based Doubly Fed Induction Generator (DFIG) is considered in this chapter. The basic configuration of the WECS is shown in Fig. 6.1. It consists of a wind turbine, a gearbox, a DFIG and a bidirectional converter. In particular, the DFIG converts the power from mechanical into electrical form. Its stator is directly connected to the grid, while the rotor is connected to the same grid through a bidirectional converter. This system can operate at variable speed, but generates electrical power at the frequency and voltage fixed by the grid. The DFIG can work on two different modes, sub- and super-synchronous speed. In the sub-synchronous mode, the grid provides power to the rotor, whereas in the super-synchronous mode the rotor and the stator deliver power to the grid.

Fig. 6.2 illustrates the different zones of operation of the WECS. The partial load zone of operation starts from v_{cut-in} until v_{rated}. Note that, in this chapter our focus is on this

zone, in which one of the control objectives is to extract the maximum active power. On the other hand, the second zone of operation starts above v_{rated} and is not considered in this chapter.

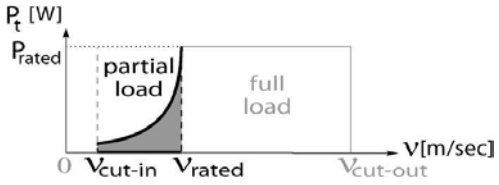

Figure 6.2. *Power in the different wind turbine operation zones*

To model the wind turbine, the mechanical power, which is directly extracted from it, is a multiplication of the available wind power by the power coefficient C_p [13]

$$P_a = 0.5\pi\rho r^2 C_p(\lambda,\beta)V^3, \tag{6.1}$$

where V is the wind speed, r is the turbine radius, and ρ is the air density.

The wind turbine can only convert a percentage of the extracted wind power. This percentage is represented by C_p which can be expressed by the following nonlinear equation [59]

$$C_p(\lambda,\beta) = c_1(\frac{c_2}{\lambda} - c_3\beta - c_4)e^{\frac{-c_3}{\lambda}} + c_6\lambda, \tag{6.2}$$

where β is the pitch angle, c_1 to c_6 are constants parameters, and the tip speed ratio $\lambda = \frac{\omega_{rm} r}{GV}$, in which G is the gearbox ratio and ω_{rm} is the mechanical rotation speed of the generator.

6.2.1 Modeling of the DFIG

The electrical dynamics of the induction machine model is described by the four-set of nonlinear differential equation system consisting of the stator, rotor and flux components in the $d-q$ frame. [56]

$$\begin{cases} \dot{\psi}_{sd} = -R_s i_{rd} + \omega_L \psi_{sq} + v_{sd}, \\ \dot{\psi}_{sq} = -R_s i_{sq} - \omega_L \psi_{sd} + v_{sq}, \\ \dot{\psi}_{rd} = -R_r i_{rd} + (\omega_L - p\omega_{rm})\psi_{rq} + v_{rd}, \\ \dot{\psi}_{rq} = -R_r i_{rq} - (\omega_L - p\omega_{rm})\psi_{rd} + v_{rq}. \end{cases} \tag{6.3}$$

The stator and rotor flux components are given by

$$\begin{cases} \psi_{sd} = L_s i_{sd} + L_m i_{rd}, \\ \psi_{sq} = L_s i_{sq} + L_m i_{rq}, \\ \psi_{rd} = L_r i_{rd} + L_m i_{sd}, \\ \psi_{rq} = L_r i_{rq} + L_m i_{sq}, \end{cases} \tag{6.4}$$

where the subscripts d and q refer to the direct components and quadrature components respectively, and subscripts s and r to the stator and rotor; i_{sd} and i_{sq} are stator currents; i_{rd} and i_{rq} are rotor currents; ψ_{sd} and ψ_{sq} are stator flux linkages; ψ_{rd} and ψ_{rq} are rotor flux linkages; L_s and L_r are the stator and rotor inductance and L_m is the mutual inductance; R_s and R_r are stator and rotor resistances, w_L is the frequency of the grid, and p is the number of the pole pairs.

The mechanical dynamics of the rotating parts can be described by the following differential equation

$$\dot{\omega}_{rm} = \frac{1}{J}(\tau_t - \tau_e), \tag{6.5}$$

where J is the inertia of the whole rotating parts, τ_t is the torque produced by the wind on the blades, and τ_e is the electrical resistant torque of the generator. The different torques in equation (6.5) are given by

$$\tau_e = \frac{3}{2} p L_m \left(i_{sq} i_{rd} - i_{sd} i_{rq}\right), \tag{6.6}$$

$$\tau_t = \frac{1}{G} 0.5 \pi \rho r^3 C_t(\lambda) V^2, \tag{6.7}$$

where $C_t(\lambda)$ is the torque coefficient of the turbine, given by $C_t(\lambda) = \dfrac{C_p(\lambda)}{\lambda}$.

In order to obtain a reduced-order model for the WECS, the d-axis should be aligned with the stator flux vector, which will lead to the achievement of the separation of active and reactive power, the stator flux is to be assumed constant and the stator resistance must be neglected [29].

With these considerations, part of the state variables of the WECS are now chosen to be the rotor currents describing the electrical dynamics, and the other part is chosen to be the motor speed allowing to describe the mechanical dynamics [29], [72]. The state equations of the WECS system is then expressed by

$$\begin{aligned}
\dot{i}_{rd} &= -\frac{L_s R_r}{L_{eq}^2} i_{rd} + (w_L - p\omega_{rm}) i_{rq} + \frac{L_s}{L_{eq}^2} v_{rd}, \\
\dot{i}_{rq} &= -(\frac{L_m V_L}{w_L L_{eq}^2} + i_{rd})(w_L - p\omega_{rm}) - \frac{L_s R_r}{L_{eq}^2} i_{rq} + \frac{L_s}{L_{eq}^2} v_{rq}, \\
\dot{\omega}_{rm} &= \frac{1}{J}(\tau_t(V, \omega_{rm}) - \frac{3 L_m V_L p}{2 L_s w_L} i_{rq}),
\end{aligned} \tag{6.8}$$

where the equivalent inductance $L_{eq}^2 = L_r L_s - L_m^2$, and V_L is the grid line voltage. One can determine the stator currents from the rotor currents based on the following two expressions

$$i_{sq} = -\frac{L_m}{L_s} i_{rq} \quad , \quad i_{sd} = \frac{V_L}{w_L L_s} - \frac{L_m}{L_s} i_{rd}. \tag{6.9}$$

The stator reactive power injected by the system into the grid can be written as [29], [72]

$$Q_s = \frac{3}{2} V_L (-\frac{L_m}{L_s} i_{rd} + \frac{V_L}{L_s w_L}). \tag{6.10}$$

6.2.2 MPPT control objective

The objective of the MPPT is to extract the maximum power from the available wind power [34]. To achieve the MPPT control objective, it is needed to determine the optimal tip-speed ratio λ_{opt} related to the maximum point $C_{p\max}$. Fig. 6.3 illustrates the characteristics $C_p(\lambda, \beta)$. The maximum value of C_p, that is $C_{p\max} = 0.4953$, is achieved for $\lambda_{opt} = 7.5$. The maximum torque can be expressed as

$$\tau_{opt}(\omega_{rm}) = \rho \pi r^5 \frac{C_{p\max} \omega_{rm}^2}{2 \lambda_{opt}^3 G^3} = k_{opt} \omega_{rm}^2, \tag{6.11}$$

with $k_{opt} = \rho \pi r^5 \dfrac{C_{p\max}}{2 G^3 \lambda_{opt}^3}$.

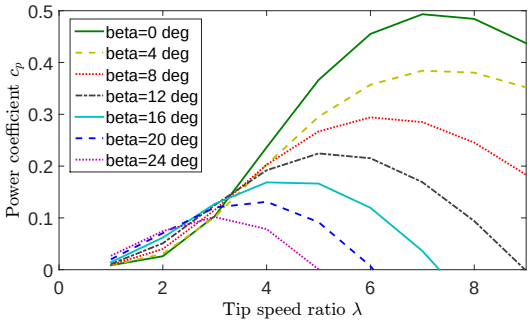

Figure 6.3. *Power coefficient C_p function of the tip-speed ratio λ for various values of the pitch angle β*

6.3 Control objective and SMC design

6.3.1 Control objective

The proposal in this chapter is to focus on presenting two novel strategies to control WECS when it is operating on the partial load zone. In this zone, the first control objective is to extract the maximum power from the wind. And the other aim is to regulate the stator reactive power to track the external reference reactive power, therefore compensate the reactive power needs of the grid.

These objectives are fulfilled by applying the two proposed adaptive SMCs, BAFOSMC and BASTC, which can achieve the following properties for the system:

- Get a predefined error in a finite time in terms of active torque τ_e tracking the desired maximum torque τ_{opt} obtained from the MPPT controller, even if the bounds of disturbance/uncertainties and their derivatives are unknown.

$$|\tau_{opt} - \tau_e| < \varepsilon_\tau, \tag{6.12}$$

  where ε_τ is apriori predefined constant.

- Get a predefined error in a finite time in terms of reactive power Q_s tracking the desired reference reactive power Q_{ref}, even if the bounds of disturbance/uncertainties and their derivatives are unknown.

$$|Q_{ref} - Q_s| < \varepsilon_Q, \tag{6.13}$$

  where ε_Q is apriori predefined constant.

6.3.2 Sliding variable design

The sliding variables for the active torque and the reactive power are designed as [29], [72]

$$s_\tau = \tau_{opt} - \tau_e = \tau_{opt}(\omega_{rm}) - \frac{3}{2}\frac{L_m V_L}{L_s w_L} i_{rq}, \tag{6.14}$$

$$s_Q = Q_{ref} - Q_s = Q_{ref} + \frac{3}{2} V_L \left(\frac{L_m}{L_s} i_{rd} - \frac{V_L}{L_s w_L}\right). \tag{6.15}$$

Note that the variable τ_{opt} is obtained from the MPPT controller through (6.11).

Taking the first order derivative of the sliding variables s_τ and s_Q, we obtain

$$\begin{aligned}\dot{s}_\tau = &\frac{1}{J}(\tau_t - \tau_{opt} + s_\tau)\dot{\tau}_{opt} + \frac{R_r L_s}{L_e}(\tau_{opt} - s_\tau) \\ &+ p(1 - \frac{p}{w_L}\omega_{rm})(s_Q - Q_{ref} + \frac{3L_r V_L^2}{2w_L L_e}) \\ &\underbrace{-\frac{3pL_m V_s}{2L_e w_s} v_{rq}}_{u_1} = G_1(s, w_{rm}, t) + u_1,\end{aligned} \tag{6.16}$$

$$\begin{aligned}\dot{s}_Q = &\frac{w_L^2}{p}(1 - \frac{p}{w_L}\omega_{rm})(\tau_{opt} - s_\tau) - \frac{3R_r V_L^2}{2w_L L_e} - \frac{R_r L_s}{L_e}(s_Q - Q_{ref}) \\ &+ \dot{Q}_{ref} + \underbrace{\frac{3L_m V_L}{2L_e} v_{rd}}_{u_2} = G_2(s, w_{rm}, t) + u_2,\end{aligned} \tag{6.17}$$

$$\dot{w}_{rm} = \frac{1}{J}\Big(\tau_t - \tau_{opt} + s_\tau\Big) = G_3(s, w_{rm}, t), \tag{6.18}$$

where $\dot{\tau}_{opt}$ is the partial derivative of τ_{opt} with respect to ω_{rm}. In view of (6.11), it can be expressed as

$$\dot{\tau}_{opt} = \quad 2k_{opt}\omega_{rm}. \tag{6.19}$$

Then, the system dynamics can be written as follows

$$\dot{s}_\tau = \underbrace{g_1(s_{\tau,Q}, \omega_{rm}, t) + \hat{g}_1(s_{\tau,Q}, \omega_{rm}, t)}_{G_1(s,\omega_{rm},t)} + u_1, \tag{6.20}$$

$$\dot{s}_Q = \underbrace{g_2(s_{\tau,Q}, \omega_{rm}, t) + \hat{g}_2(s_{\tau,Q}, \omega_{rm}, t)}_{G_2(s,\omega_{rm},t)} + u_2, \tag{6.21}$$

$$\dot{\omega}_{rm} = \underbrace{g_3(s, \omega_{rm}, t) + \hat{g}_3(s_{\tau,Q}, \omega_{rm}, t)}_{G_3(s,\omega_{rm},t)}, \tag{6.22}$$

where g are the nominal or unperturbed models and their expressions can be computed from G (6.16)-(6.17)-(6.18) using the nominal values for all the parameters. On the other hand, $\hat{g}$ present the uncertainties in the parameters and external disturbances, and their expressions are computed after calculating the variations of parameters with respect to their nominal values.

6.3.3 Controller design

The control inputs are chosen to be the combination of two parts

$$u_i = u_{eq_i} + \hat{u}_i, \quad i = 1,2 \tag{6.23}$$

with u_{eq_i} are the equivalent control for system (6.20)-(6.21), and $\hat{u}_i$ are designed using the proposed adaptive SMCs. Note that the expressions of u_{eq_i} are computed from the undisturbed system (6.20)-(6.21), i.e. $\hat{g} = 0$. They are obtained by solving u in the algebraic equations $\dot{s} = 0$ with $s = 0$.

The functions $\hat{g}_i$ are supposed to be bounded and Lipshitz. Moreover, the bounds of these functions and their derivatives are unknown. In [29], two different STCs with variable gains have been designed for the two controllers $\hat{u}_1$ and $\hat{u}_2$, where the finite time stablility of system (6.20)-(6.21) and the achievement of the 2-OSM for both sliding variables have been proved using Lyapunov function. Also, following [29], the system's zero dynamics, given in equation (6.22), has been proved to be stable when sliding mode is established in the load zone of operation. In other words, the torque produced by the wind τ_e converges to the optimal maximum torque $\tau_{opt} = k_{opt}\omega_{rm}$, i.e, the rotational speed converges to the optimal point $\omega_{rm} = \dfrac{\lambda_{opt} G}{r} V$.

In this work, it is proposed to use two adaptive SMCs that do not require any information about the bounds of the disturbances and their derivatives, which is not the case in [29], in which a thorough analysis was necessary in order to estimate the upper bound of the disturbances derivatives.

As a result, in order to achieve the control objectives, the problem can be formulated as applying the two adaptive SMCs, BAFOSMC and BASTC, for the two terms $\hat{u}_1$ and $\hat{u}_2$ to control WECS.

In the following section, the application of both barrier adaptive SMCs, along with the comparison with other adaptive strategies are presented through simulations.

6.4 Simulation results

The model of WECS has been designed using MATLAB/Simulink. The parameters of the WECS are detailed in Appendix. C.A. The wind speed model is produced by a test function (see Fig. 6.4(a)) and several references reactive power will be used in the simulations, in order to consider a variety of situations (see Fig. 6.4(b)). Moreover, variation in the rotor resistance R_r, will be taken into account (see Fig. 6.4(c)).

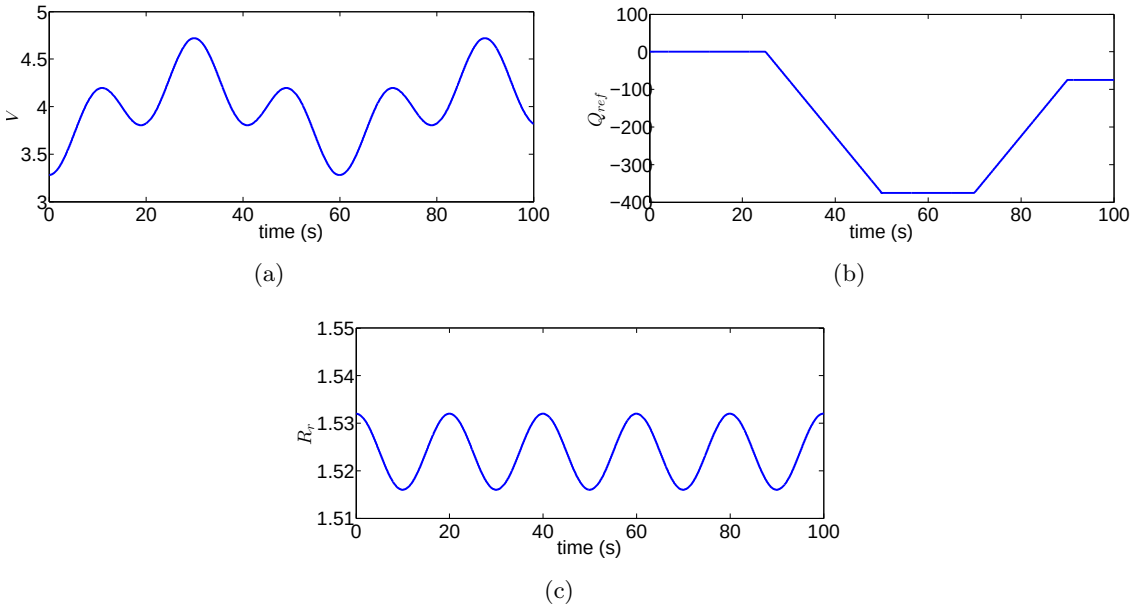

Figure 6.4. *a) Wind speed profile V, b) Reference reative power Q_{ref}, c) Temporal evolution of the rotor resistance R_r*

Now, two situations will be considered: first the situation when the control terms $\hat{u}_1$ and $\hat{u}_2$ are chosen as adaptive FOSMC, and second when they are chosen as adaptive STC.

6.4.1 Adaptive FOSMCs

In order to illustrate the positive features of the proposed BAFOSMC, the two BFs are tested (i.e. PBF and PSBF), and their performances are compared with the results obtained using the adaptive FOSMC presented in [58], referred to as APS.

For the BAFOSMC, the two controls $\hat{u}_1$ and $\hat{u}_2$, related to the active power and the reactive power respectively, are designed according to theorem. 2.2.2. In contrast, for the APS, the two controls are designed according to (2.2)-(2.4). Appendix. C.B contains the parameter values of the two controllers with the two adaptive strategies.

The simulation results of adaptive FOSMCs based on PBF, PSBF and APS are depicted in Figs. 6.5-6.6-6.7. It can be noticed in Figs. 6.5(a)-6.6(a)-6.7(a), that for these three adaptive strategies the tracking of the desired maximum torque τ_{opt} is efficient, which leads the achievement of the first control objective. On the other hand, Figs. 6.5(b)-6.6(b) show that the sliding variable s_τ with PBF and PSBF does not exceed the predefined

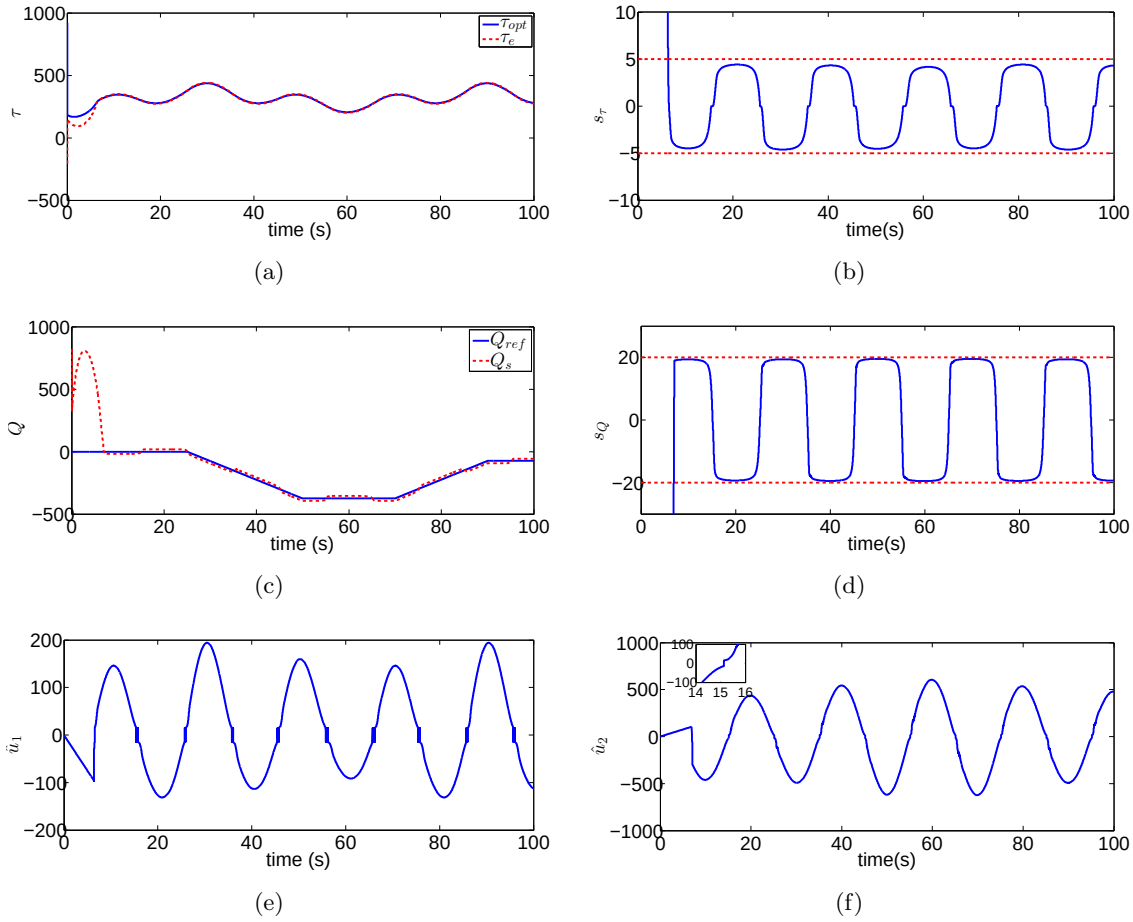

Figure 6.5. *Adaptive FOSMC with PBF a) Active torque and the maximum active torque, b) Sliding variable s_τ, c) Stator reactive power and its reference, d) Sliding variable s_Q, e) Control term $\hat{u}_1$, f) Control term $\hat{u}_2$*

vicinity of zero $\varepsilon_\tau = 5$. But, it can be seen in Fig. 6.7(b) that the size of vicinity to which converges s_τ with APS exceeds $\varepsilon_\tau = 5$. The fulfillment of the second control objective can be shown in Figs. 6.5(c)-6.6(c)-6.7(c), where the stator reactive power and the external reference Q_{ref} are drawn together. Moreover, in Figs. 6.5(d)-6.6(d)-6.7(d), it can be seen that the sliding variable s_Q with PBF and PSBF does not exceed the predefined vicinity of zero $\varepsilon_Q = 20$, which is not the case with APS, in which the sliding variable cannot be maintained in the predefined vicinity of zero. It can be concluded that both PBF and PSBF, are more efficient than the APS regarding the retention of the sliding variables in predefined vicinities of zero. Finally, Figs. 6.5(e)-6.6(e)-6.5(f)-6.6(f)-6.7(e)-6.7(f) present the two control terms $\hat{u}_1$ and $\hat{u}_2$ with the three adaptive strategies. It can be noticed

that only the control signals with PSBF are continuous after the switching time. On the other hand, the control signals obtained with PBF and APS contain a discontinuity. It is important to highlight the continuity of control signals with PSBF after the switching time even in the case of FOSMC (see subsection 2.2.3.2).

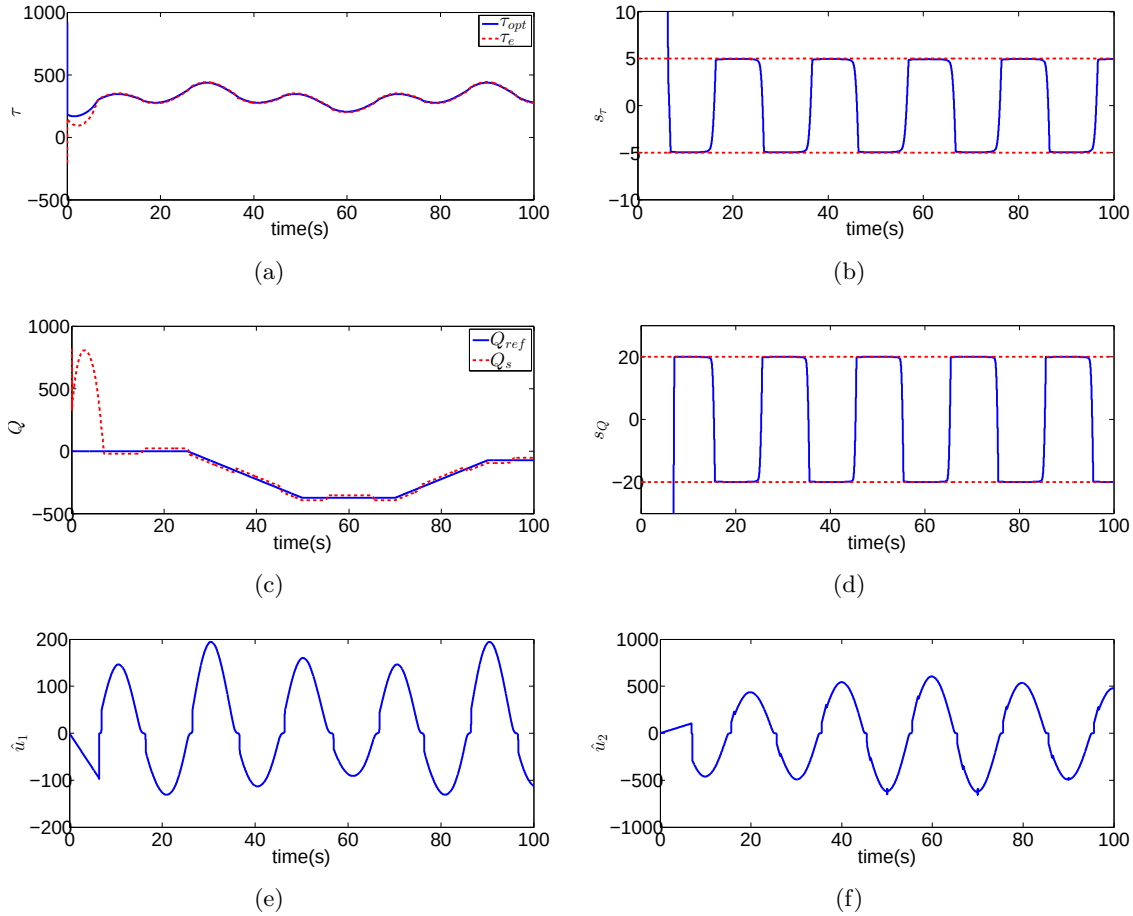

Figure 6.6. *Adaptive FOSMC with PSBF a) Active torque and the maximum active torque, b) Sliding variable s_τ, c) Stator reactive power and its reference, d) Sliding variable s_Q, e) Control term $\hat{u}_1$, f) Control term $\hat{u}_2$*

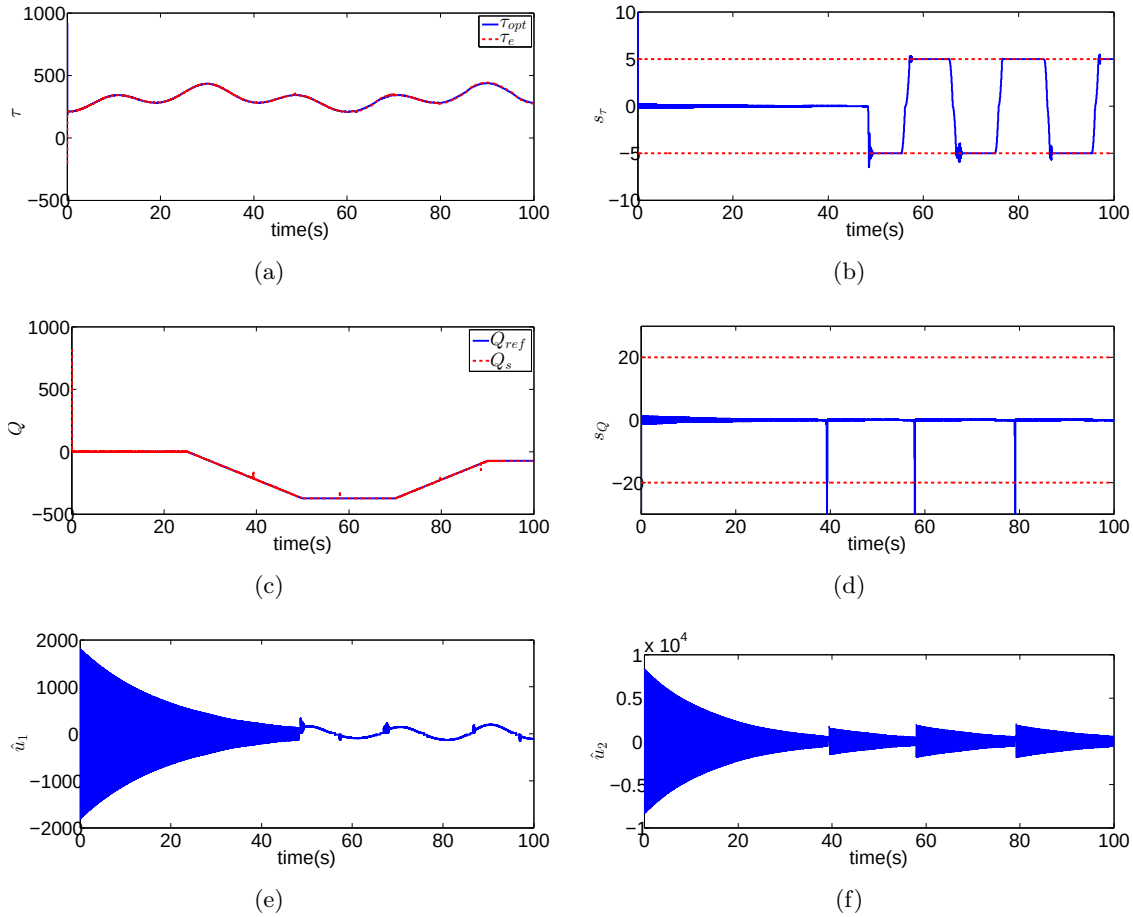

Figure 6.7. *Adaptive FOSMC with APS a) Active torque and the maximum active torque, b) Sliding variable s_τ, c) Stator reactive power and its reference, d) Sliding variable s_Q, e) Control term $\hat{u}_1$, f) Control term $\hat{u}_2$*

6.4.2 Adaptive STCs

This section is provided to illustrate the situation when the two control terms are implemented using BASTC based on BFs with its both variants (PBF and PSBF), and their performances are compared with the results obtained using the adaptive STC presented in [64], referred to as AST.

For the BASTC, the two control terms are designed according to theorem 3.2.1, while for the AST, the two control terms follow (3.6)-(3.7). The parameter values of these two adaptive STC strategies are given in Appendix. C.C

The simulation results of adaptive STCs based on PBF, PSBF and AST are compared in Figs. 6.8-6.9-6.10. It can be observed in Figs. 6.8(a)-6.9(a)-6.10(a)-6.8(c)-6.9(c)-6.10(c),

that both control objectives are fulfilled with efficient tracking performance. One the other hand, it can be seen in Figs. 6.8(b)-6.9(b)-6.8(d)-6.9(d), that the sliding variables s_τ, s_Q with PBF and PSBF do not exceed the predefined vicinities of zero $\varepsilon_\tau = 5$, $\varepsilon_Q = 20$. However, it can be seen in Figs. 6.10(b)-6.10(d) that the sizes of vicinities, to which converge s_τ, s_Q with AST exceed $\varepsilon_\tau = 5$, $\varepsilon_Q = 20$. Again, it can be concluded that PBF and PSBF have a better performance than AST regarding forcing the sliding variables to remain in predefined vicinities of zero. Finally, Figs. 6.8(e)-6.9(e)-6.10(e)-6.8(f)-6.9(f)-6.10(f) present the evolution of the two control terms $\hat{u}_1$ and $\hat{u}_2$ with the three adaptive strategies. It can be noticed that the control signals with these three adaptive strategies are continuous and smooth.

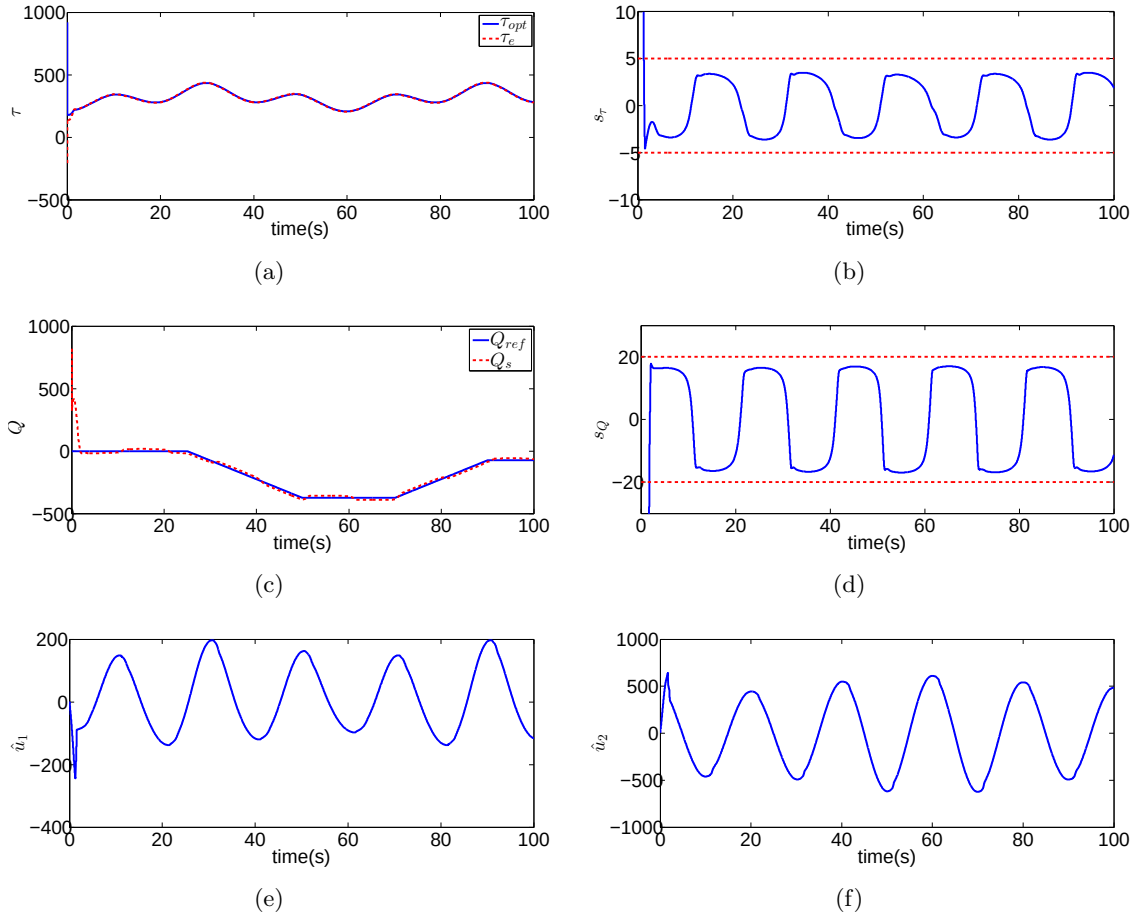

Figure 6.8. *Adaptive STC with PBF a) Active torque and the maximum active torque, b) Sliding variable s_τ, c) Stator reactive power and its reference, d) Sliding variable s_Q, e) Control term $\hat{u}_1$, f) Control term $\hat{u}_2$*

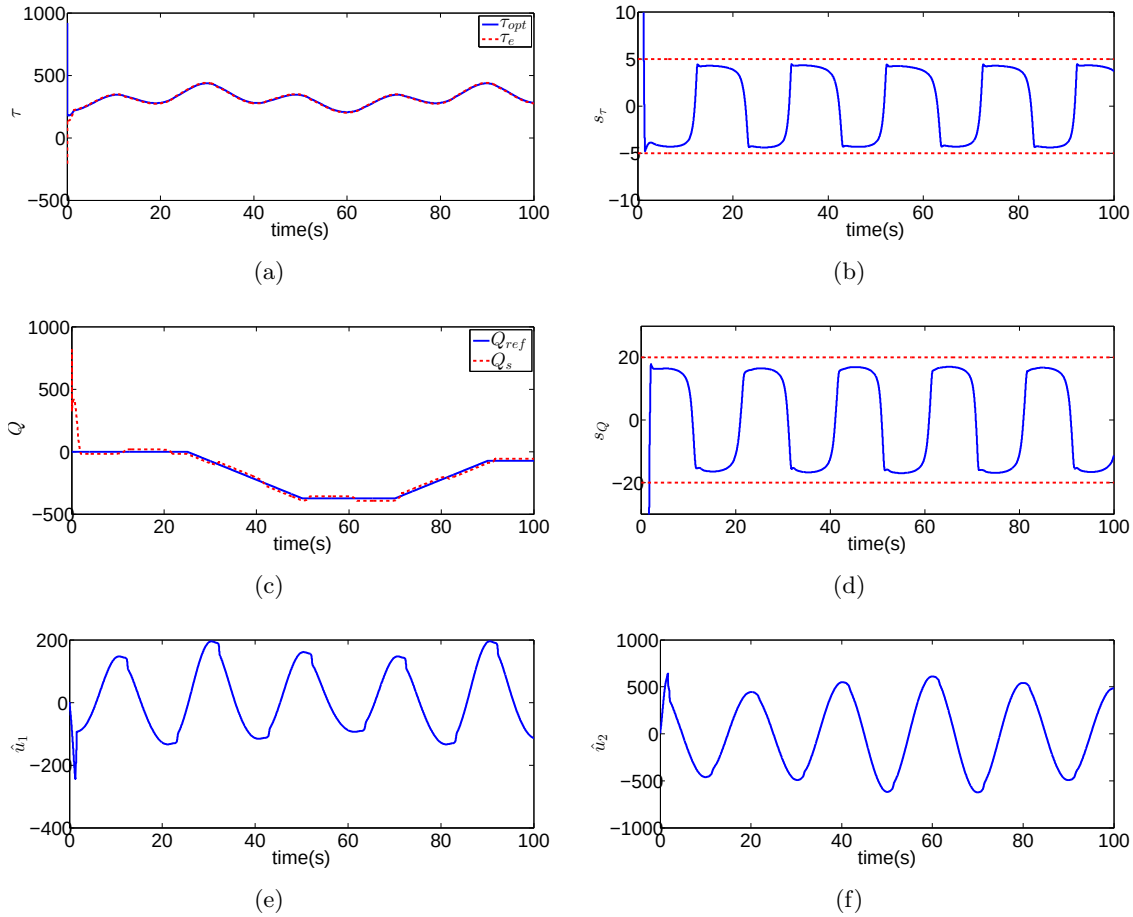

Figure 6.9. *Adaptive STC with PSBF a) Active torque and the maximum active torque, b) Sliding variable s_τ, c) Stator reactive power and its reference, d) Sliding variable s_Q, e) Control term $\hat{u}_1$, f) Control term $\hat{u}_2$*

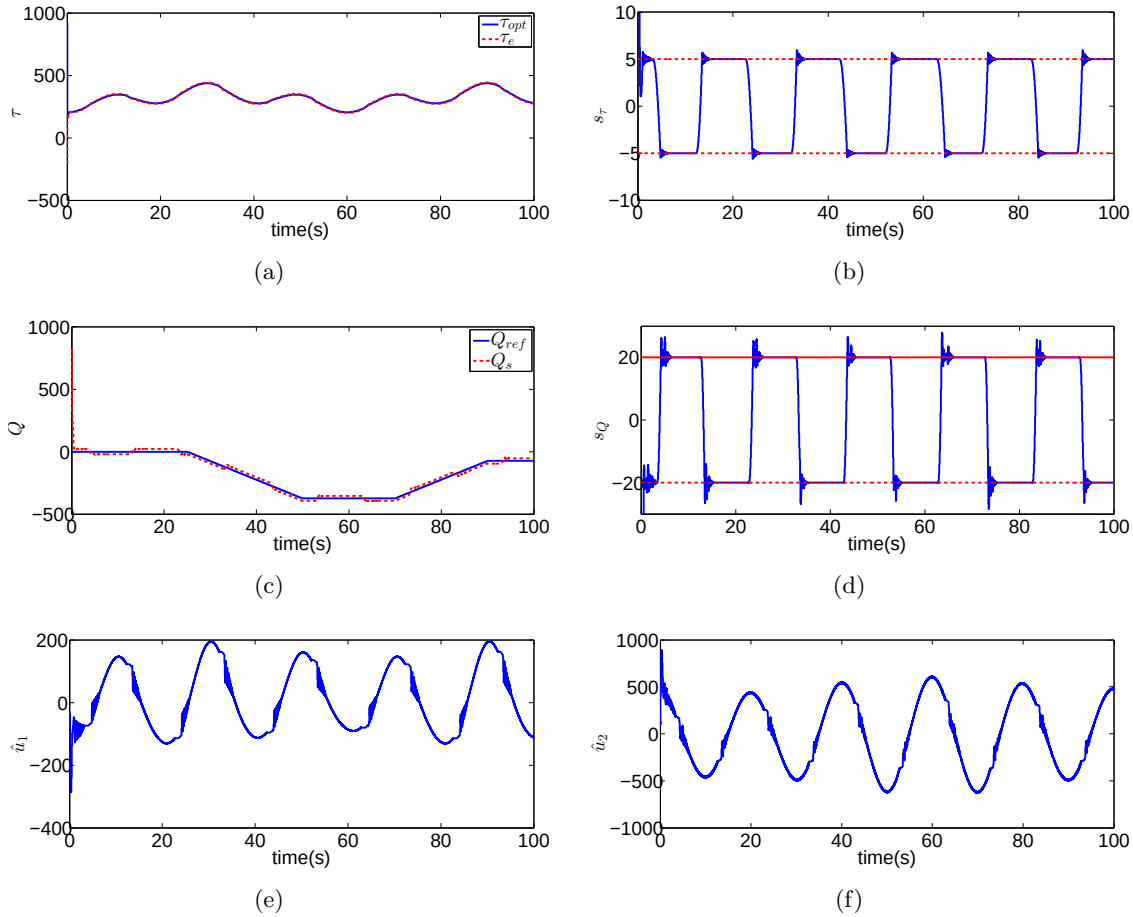

Figure 6.10. *Adaptive STC with AST a) Active torque and the maximum active torque, b) Sliding variable s_τ, c) Stator reactive power and its reference, d) Sliding variable s_Q, e) Control term $\hat{u}_1$, f) Control term $\hat{u}_2$*

6.5 Summary

This chapter proposes the design of the two barrier function-based adaptive SMCs in order to control WECS. The specific feature of WECS is that its electrical model can be described as two first order nonlinear systems with unknown uncertainties. Therefore, such controllers successfully deal with the control of WECS where the upper bounds of the uncertainties and their derivatives are unknown. The proposed controllers are used to extract the maximum power and the achievement of the reference reactive power with predefined errors, regardless of the upper bounds of uncertainties and their derivatives. Simulation results have shown the positive features of the proposed barrier function-based adaptive SMCs, especially compared to other adaptive SMCs.

Chapter 7

Application to Linear induction Motor System

Nowadays energy conversion from mechanical energy to electrical energy is made with rotating machines, particularly with AC induction motors or synchronous generators. However this implies that the mechanical power would be supplied by a torque and an angular speed, which is not always the case for some generation supplies. For example some Stirling motors, which are in essence heat engines operating by cyclic compression and expansion of the working fluid, at different temperature levels produce a net conversion of heat energy to mechanical work with a translational movement. Another example regards some marine energy sources using the wave movement, or finally the so called air-borne kites which supply translational movement of cables from their 8-like wind-based movement at high height. The use of a linear induction motor as a generator appears then to be more natural and convenient than the rotating machine and entails the elimination of gearboxes, with resulting increase of efficiency, decrease of size, better reliability and robustness and reduction of prize. Scientific literature about Linear Induction Motor (LIM) is huge [49, 47, 35]. The feature of LIMs to develop a direct linear motion without any gearbox for the motion transformation (from rotating to linear) has been the key issue for their study [18, 46]. The counterpart of this potential advantage is the increase of complexity of the machine model, which presents the so-called end effects and border effects. These, which are due to the absence of a cylindrical symmetry in the inductor structure with respect to the rotating

machine, both in the longitudinal and in the transversal direction, result in difficulties in obtaining good dynamic performance.

This chapter is dedicated to the control of LIM system, which can be summarized as driving the actual speed and flux to their desired values. Since the flux dynamics and the speed dynamics can be considered as two disturbed double integrator systems, moreover, since the upper bound of the disturbances and their derivatives are unknown, the control strategies proposed in chapter 2, chapter 3 and chapter 5 for such systems can be applied.

7.1 State-of-the-Art and contributions

To describe the phenomenon of end effects in LIM system, Ducan [23] first introduced space-vector equivalent T-model for LIM and gave the flux equation and voltage equation. After that, the state space equation of LIM was proposed in [61]. It is known that if the system's model is more close to the real system, the designed controller and observer will be more efficient. Due to its obvious advantage, the dynamic end effect model of LIM has been widely researched in recent years.

Considering dynamic end effects, several control techniques have been applied into LIM, such as field oriented control [39, 60], combined vector and direct thrust control [40]. However, the dynamic response of these controllers is not very quick. To deal with this problem, Pucci [4] proposed input-output Feedback Linearization (FL) control technique to improve the dynamic response performance. FL method is an extension control technique from Rotary Induction Motor (RIM) to LIM, and it needs a lot of transformations to design the final controllers, which greatly increases the difficulty of calculations. In practice, LIM's parameters will be affected by some physical factors (temperature, humidity, etc ...) and their actual values will sustain little variations [73]. Unfortunately, to guarantee great control performance, all these designed controllers need exact information of LIM parameters and they are not robust when there exist parameter variations or system uncertainty. To solve this problem, an efficient robust and adaptive control is needed.

Sliding mode control theory is one of the most efficient tools for industrial applications when there occur heavy uncertainty conditions [68, 26]. Such controller can theoretically exactly compensate a matched uncertainties by keeping some properly chosen sliding variables at zero. For systems with relative degree greater than one affected by disturbance, different approaches based on SMC can be used. One approach is to use the ISMC, while another one is based on the usage of HOSMC. If the bounds of parametric uncertainties

and disturbance in the system are known, then fixed-gain of ISMC/HOSMC can be designed with relative ease. However, this is usually difficult in practical cases, and specially in LIM, as the estimation of uncertainties bounds requires rigorous experimentation in worst case conditions. In these cases, adaptive-gains or adaptive controllers provide a successful means of controlling the system through dynamically adapting gains.

In this chapter, based on Indirect Rotor Field Oriented Control (IRFOC) strategy [75, 5], the model of the LIM system is written as two disturbed double integrator systems. Then, two adaptive SMCs: barrier function-based adaptive ISMC (BAISMC) and adaptive DHOSMC (ADHOSMC), presented in chapter 2, chapter 3 and chapter 5, are applied to drive the LIM speed and flux to their desired values. Such adaptive SMCs are able to achieve flux tracking and speed tracking, despite of disturbance/uncertainties with unknown upper bound and with unknown upper bound of their derivatives.

Hence, the main contributions of this chapter are the following:

- Novel BAISMC and ADHOSMC are applied to control the LIM system in order to achieve speed tracking and flux tracking.
- The proposed controllers are proved to be appropriate choices to control the LIM system due to their robustness when the bounds of the disturbance/uncertainties and their derivatives are unknown.
- These controls do not require any information about the disturbances/uncertainties.
- Finally, simulation results validated the performance of the proposed adaptive SMCs.

7.2 IRFOC STRATEGY OF LIM

This section is divided into two parts. First, the state space equation of LIM is presented in the well-known $(\alpha,\ \beta)$ stationary reference frame. Secondly, the IRFOC strategy is applied and the new state space equation of LIM is given in the $(d,\ q)$ rotary reference frame.

7.2.1 LIM's State Space Equation

Considering dynamic end effects, the LIM's space-vector dynamic model can be expressed in the inductor part flux reference frame $(\alpha,\ \beta)$ as follows [61, 76]

$$\dot{i}_{s\alpha} = -\gamma i_{s\alpha} + \beta\alpha\psi_{r\alpha} + \beta\frac{p\pi}{h}\upsilon\psi_{r\beta} + \frac{\bar{u}_{s\alpha}}{\delta}, \tag{7.1}$$

$$\dot{i}_{s\beta} = -\gamma i_{s\beta} + \beta\alpha\psi_{r\beta} - \beta\frac{p\pi}{h}v\psi_{r\alpha} + \frac{\bar{u}_{s\beta}}{\delta}, \tag{7.2}$$

$$\dot{\psi}_{r\alpha} = -\eta\psi_{r\alpha} + \varsigma i_{s\alpha} - \frac{p\pi}{h}v\psi_{r\beta}, \tag{7.3}$$

$$\dot{\psi}_{r\beta} = -\eta\psi_{r\beta} + \varsigma i_{s\beta} + \frac{p\pi}{h}v\psi_{r\alpha}, \tag{7.4}$$

$$\dot{v} = \mu(i_{s\beta}\psi_{r\alpha} - i_{s\alpha}\psi_{r\beta}) - \frac{D}{M}v - \frac{T_L}{M}, \tag{7.5}$$

where v is the LIM speed, $\bar{u}_{s\alpha}$ and $\bar{u}_{s\beta}$ are the stator voltages, $i_{s\alpha}$ and $i_{s\beta}$ are the stator currents, $\psi_{r\alpha}$ and $\psi_{r\beta}$ are the rotor fluxes, T_L is the load torque, p is the number of pole pairs, and M is the motor mass. The variables $\gamma,\ \alpha,\ \beta,\ \delta,\ \varsigma,\ \eta,\ \mu$ are expressed as follows

$$\gamma = \frac{1}{\hat{\sigma}\hat{L}_s}\left[R_s + \hat{R}_r(1 - \frac{\hat{L}_m}{\hat{L}_r}) + \frac{\hat{L}_m}{\hat{L}_r}(\frac{\hat{L}_m}{\hat{T}_r} - \hat{R}_r)\right],$$

$$\alpha = (\frac{1}{\hat{T}_r} - \frac{\hat{R}_r}{\hat{L}_m}), \quad \beta = \frac{\hat{L}_m}{\hat{\sigma}\hat{L}_s\hat{L}_r}, \quad \delta = \hat{L}_s\left(1 - \frac{\hat{L}_m^2}{\hat{L}_r\hat{L}_s}\right),$$

$$\varsigma = (\frac{\hat{L}_m}{\hat{T}_r} - \hat{R}_r), \quad \eta = \frac{1}{\hat{T}_r}, \quad \mu = \frac{3p\pi\hat{L}_m}{2Mh\hat{L}_r},$$

with the parameters $Q,\ f(Q),\ \hat{R}_r,\ \hat{L}_m,\ \hat{L}_s,\ \hat{L}_r,\ \hat{T}_r,\ \hat{\sigma}$ are

$$Q = \frac{\tau_m R_r}{(L_m + L_{\sigma r})v}, \quad f(Q) = \frac{1 - e^{-Q}}{Q}, \quad \hat{R}_r = R_r f(Q),$$

$$\hat{L}_m = L_m[1 - f(Q)], \quad \hat{L}_s = L_{\sigma s} + \hat{L}_m, \quad \hat{L}_r = L_{\sigma r} + \hat{L}_m,$$

$$\hat{T}_r = \frac{L_{\sigma r} + L_m(1 - f(Q))}{R_r + R_r f(Q)} = \frac{\hat{L}_r}{R_r + \hat{R}_r}, \quad \hat{\sigma} = 1 - \frac{\hat{L}_m^2}{\hat{L}_s\hat{L}_r},$$

7.2.2 IRFOC Strategy

The relationship between $i_{s\alpha}$, $i_{s\beta}$, $\psi_{r\alpha}$, $\psi_{r\beta}$, $\bar{u}_{s\alpha}$, $\bar{u}_{s\beta}$ and i_{sd}, i_{sq}, ψ_{rd}, ψ_{rq}, $\bar{u}_{sd}$, $\bar{u}_{sq}$ can be expressed by Park's transformation matrix [50] as follows

$$\begin{bmatrix} i_{sd} \\ i_{sq} \end{bmatrix} = \begin{bmatrix} \cos\rho & \sin\rho \\ -\sin\rho & \cos\rho \end{bmatrix} \begin{bmatrix} i_{s\alpha} \\ i_{s\beta} \end{bmatrix} \tag{7.6}$$

$$\begin{bmatrix} \psi_{rd} \\ \psi_{rq} \end{bmatrix} = \begin{bmatrix} \cos\rho & \sin\rho \\ -\sin\rho & \cos\rho \end{bmatrix} \begin{bmatrix} \psi_{r\alpha} \\ \psi_{r\beta} \end{bmatrix} \tag{7.7}$$

$$\begin{bmatrix} \bar{u}_{sd} \\ \bar{u}_{sq} \end{bmatrix} = \begin{bmatrix} \cos\rho & \sin\rho \\ -\sin\rho & \cos\rho \end{bmatrix} \begin{bmatrix} \bar{u}_{s\alpha} \\ \bar{u}_{s\beta} \end{bmatrix} \tag{7.8}$$

where ρ is the induced-part flux angle and $\dot{\rho} = \omega_{mr} = \frac{p\pi}{h}v + (\frac{\hat{L}_m}{\hat{T}_r} - \hat{R}_r)\frac{i_{sq}}{\psi_r}$; ω_{mr} is the induced-part flux vector rotational speed.

By applying the IRFOC strategy proposed in [75, 5] ($\psi_{rq} = 0$ and $\psi_{rd} = \psi_r$), the state space equation of flux can be expressed by

$$\dot{\psi}_r = \varsigma i_{sd} - \eta\psi_r. \tag{7.9}$$

With the Park's transformation, LIM's model can be rewritten in the inductor part flux reference frame (d,q) as follows

$$\dot{i}_{sd} = -\gamma i_{sd} + \frac{p\pi}{h}v i_{sq} + \varsigma\frac{i_{sq}^2}{\psi_r} + \alpha\beta\psi_r + \frac{\bar{u}_{sd}}{\delta}, \tag{7.10}$$

$$\dot{i}_{sq} = -\gamma i_{sq} - \frac{p\pi}{h}v i_{sd} - \varsigma\frac{i_{sd}i_{sq}}{\psi_r} - \beta\frac{p\pi}{h}v\psi_r + \frac{\bar{u}_{sq}}{\delta}, \tag{7.11}$$

$$\dot{\psi}_r = \varsigma i_{sd} - \eta\psi_r, \tag{7.12}$$

$$\dot{\rho} = \frac{p\pi}{h}v + \varsigma\frac{i_{sq}}{\psi_r}, \tag{7.13}$$

$$\dot{v} = \mu\psi_r i_{sq} - \frac{D}{M}v - \frac{1}{M}T_L, \tag{7.14}$$

The related parameters γ, α, β, δ, ς, η, μ are functions that depend on the speed of the LIM, and their waveforms are shown in Fig. 7.1 for speed range between 0 and $10m/s$.

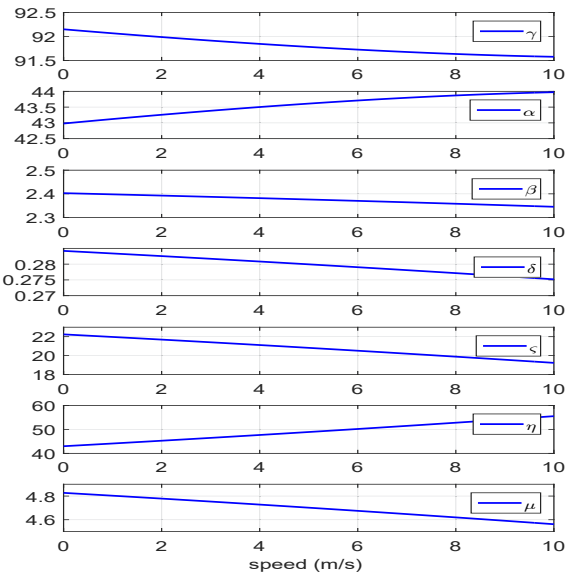

Figure 7.1. *Waveforms of γ, α, β, δ, ς, η, μ when LIM speed v varies*

7.3 Control objective and SMC design

7.3.1 Control Objective

Recall that in LIM system, there exist two control objectives [1]:

- Regulate the actual flux to track the desired flux.
- Drive the actual motor speed to the desired motor speed.

Let us define two new state variables for the flux $e_{\psi 1}$, $e_{\psi 2}$ as follows

$$e_{\psi 1} = \psi_r - \psi_{r,ref}, \tag{7.15}$$

$$e_{\psi 2} = \dot{\psi}_r - \dot{\psi}_{r,ref}, \tag{7.16}$$

where ψ_r and $\psi_{r,ref}$ are the actual flux and desired flux, respectively.
Similarly, two new state variables for the speed e_{v1}, e_{v2} are defined as follows

$$e_{v1} = v - v_{ref}, \tag{7.17}$$

$$e_{v2} = \dot{v} - \dot{v}_{ref}, \tag{7.18}$$

where v and v_{ref} are the actual motor speed and desired motor speed, respectively.

The control objectives can be expressed now as designing the control inputs $\bar{u}_{sd}$, $\bar{u}_{sq}$ that drive $e_{\psi 1}$, $e_{\psi 2}$ and e_{v1}, e_{v2} to zero or to a small domain near to zero, even if in the case when the bounds of the disturbance/uncertainties and their derivatives are unknown.

In the following subsections, the dynamics of the flux model and the speed model are presented.

7.3.2 Flux Loop Control Design

Substitute equation (7.10) and equation (7.12) into equations (7.15-7.16), we obtain [3]

$$\begin{aligned} \dot{e}_{\psi 1} &= e_{\psi 2}, \\ \dot{e}_{\psi 2} &= f_1 + g_1 \bar{u}_{sd}, \end{aligned} \tag{7.19}$$

where g_1 is supposed to be known and is given as follows

$$g_1 = \frac{\varsigma}{\delta} = \frac{(\frac{\hat{L}_m}{\hat{T}_r} - \hat{R}_r)}{\hat{L}_s\left(1 - \frac{\hat{L}_m^2}{\hat{L}_r \hat{L}_s}\right)}, \tag{7.20}$$

and the flux total disturbance f_1 is expressed by

$$\begin{aligned} f_1 = &- q_1\psi_r + \eta^2\psi_r - \varsigma\eta i_{sd} + q_2 i_{sd} - \gamma\varsigma i_{sd} + \varsigma\frac{p\pi}{h}\upsilon i_{sq} \\ &+ \varsigma^2\frac{i_{sq}^2}{\psi_r} + \alpha\beta\varsigma\psi_r - \ddot{\psi}_{r,ref}, \end{aligned} \tag{7.21}$$

where q_1 and q_2 are obtained from [2] as follows

$$\begin{aligned} q_1 =& \frac{R_r\hat{L}_r + R_r L_m\left(1+f(Q)\right)}{\hat{L}_r^2}\frac{T_r a}{\tau_m}\left(1-\left(1+\frac{\tau_m}{T_r\upsilon}\right)e^{-\frac{\tau_m}{T_r\upsilon}}\right), \\ q_2 =& R_r\left(\frac{L_m}{\hat{L}_r^2}\left(1+f^2(Q)\right)+1-2\frac{L_m f(Q)}{\hat{L}_r}\right)\frac{T_r a}{\tau_m}\left(1-\left(1+\frac{\tau_m}{T_r\upsilon}\right)e^{-\frac{\tau_m}{T_r\upsilon}}\right), \end{aligned} \tag{7.22}$$

and $T_r = \dfrac{L_r}{R_r}$. Let us define $\bar{u}_{sd} = \dfrac{1}{g_1}u_{sd}$, then system (7.19) can be written as follows

$$\begin{aligned} \dot{e}_{\psi 1} &= e_{\psi 2}, \\ \dot{e}_{\psi 2} &= f_1 + u_{sd}, \end{aligned} \tag{7.23}$$

System (7.23) is a disturbed double integrators system. Furthermore, the disturbance f_1 is unknown bounded, and its derivative is also unknown bounded. For such system, the interest of our proposed BAISMC and the ADHOSMC appear. Indeed, they do not require any information about the disturbance, moreover, they can guarantee the convergence of $e_{\psi 1}$, $e_{\psi 2}$ to zero or to a small vicinity of zero. This means, they can achieve the flux tracking objective.

7.3.3 Speed Loop Control Design

Similarly, Substitute equation (7.11) and equation (7.13) into equations (7.17-7.18), we get [3]

$$\begin{aligned} \dot{e}_{v1} &= e_{v2}, \\ \dot{e}_{v2} &= f_2 + g_2\bar{u}_{sq}, \end{aligned} \tag{7.24}$$

where g_2 is supposed to be known and is given as follows

$$g_2 = \frac{\mu\psi_r}{\delta} = \frac{3p\pi\hat{L}_m}{2Mh\hat{L}_r}.\frac{\hat{L}_r\psi_r}{\hat{L}_r\hat{L}_s - \hat{L}_m^2}, \tag{7.25}$$

and the speed total disturbance f_2 is described by

$$\begin{aligned} f_2 =& q_3\psi_r i_{sq} + \mu\left(\varsigma i_{sd} - \eta\psi_r\right) i_{sq} - \frac{D}{M}a - \ddot{v}_{ref} \\ &+ \mu\psi_r\left(-\gamma i_{sq} - \frac{p\pi}{h}v i_{sd} - \varsigma\frac{i_{sd}i_{sq}}{\psi_r} - \beta\frac{p\pi}{h}v\psi_r\right), \end{aligned} \tag{7.26}$$

with q_3 is given by

$$q_3 = \frac{3}{2}h\frac{\pi}{p}\frac{1}{M}\left(-\frac{L_{\sigma r}L_m}{\hat{L}_r^2}\frac{T_r a}{\tau_m}\left(1-\left(1+\frac{\tau_m}{T_r v}\right)e^{-\frac{\tau_m}{T_r v}}\right)\right), \tag{7.27}$$

Let us define $\bar{u}_{sq} = \dfrac{1}{g_2}u_{sq}$, then system (7.24) can be written as follows

$$\begin{aligned} \dot{e}_{v1} &= e_{v2}, \\ \dot{e}_{v2} &= f_2 + u_{sq}, \end{aligned} \tag{7.28}$$

Again, following the previous subsection and in order to achieve the speed tracking, the control input u_{sq} can be designed according to BAISMC or ADHOSMC.

Remark 7.3.1. *The parameters q_1, q_2, q_3 are functions of the LIM speed v and speed's derivative $\dot{v} = a$, and are shown in Fig. 7.2.*

7.4 Simulation Results

The LIM system taking into consideration the dynamic end effects, has been developed in Matlab/Simulink software. The solver option type is fixed step, the solver is ode1 (Euler) and the fixed step size is $10^{-5}s$. The nominal parameters of LIM are given in Appendix. D.A. In order to better reflect the performance of the designed adaptive SMCs, we assume that the load torque disturbance is bounded and Lipschitz, and its boundaries are unknown (see Fig. 7.3).

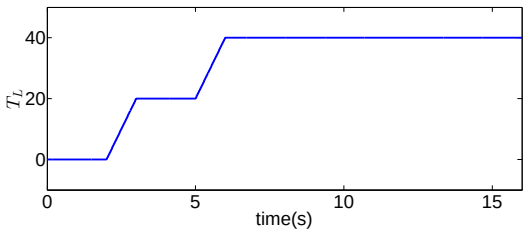

Figure 7.3. *Time history of load torque disturbance*

Now, two situations will be considered: first the situation when the control terms u_{sd} and u_{sq} are chosen as BAISMC, and second when they are chosen as ADHOSMC.

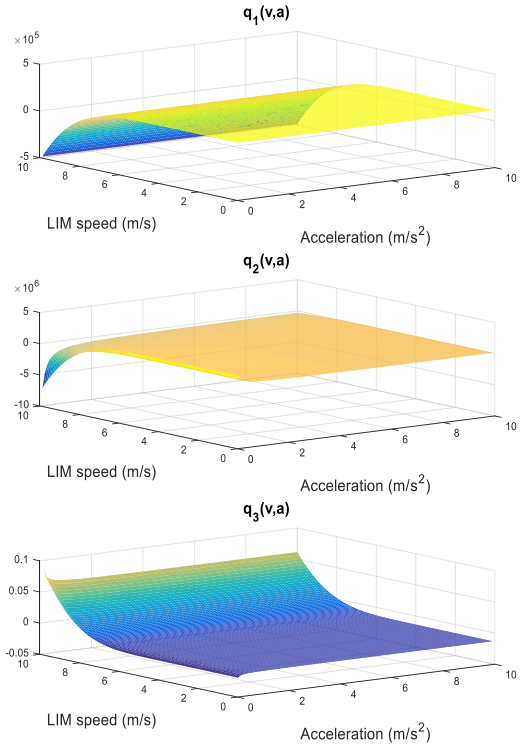

Figure 7.2. *Surfaces of q_1, q_2, q_3 when the LIM speed varies between 0 and 10m/s and the acceleration varies between 0 and 10m/s*

7.4.1 Results with BAISMC

In order to illustrate the positive features of the proposed BAISMC, the two ISMCs are tested (i.e. DISMC and CISMC). Moreover, the BF is chosen as PBF for both cases.

For the proposed BAISMC, the two controls u_{sd}, u_{sq} related to the actual flux and the actual speed respectively, are designed according to (2.6), i.e.

$$u_{sd} = u_{n,sd} + u_{SMC,sd}, \tag{7.29}$$

$$u_{sq} = u_{n,sq} + u_{SMC,sq}, \tag{7.30}$$

where $u_{n,sd}$, $u_{n,sq}$ are given by [55, 19]

$$u_{n,sd} = -15|e_{\psi 1}|^{\frac{1}{3}} sign(e_{\psi 1}) - 7|e_{\psi 2}|^{\frac{1}{2}} sign(e_{\psi 2}), \tag{7.31}$$

$$u_{n,sq} = -15|e_{v1}|^{\frac{1}{3}} sign(e_{v1}) - 7|e_{v2}|^{\frac{1}{2}} sign(e_{v2}), \tag{7.32}$$

and $u_{SMC,sd}$, $u_{SMC,sq}$ follow proposition 2.3.1 in the case of DISMC, while in the case of CISMC, they follow proposition 3.3.1. Appendix. D.B contains the parameter values of the two controllers for both cases.

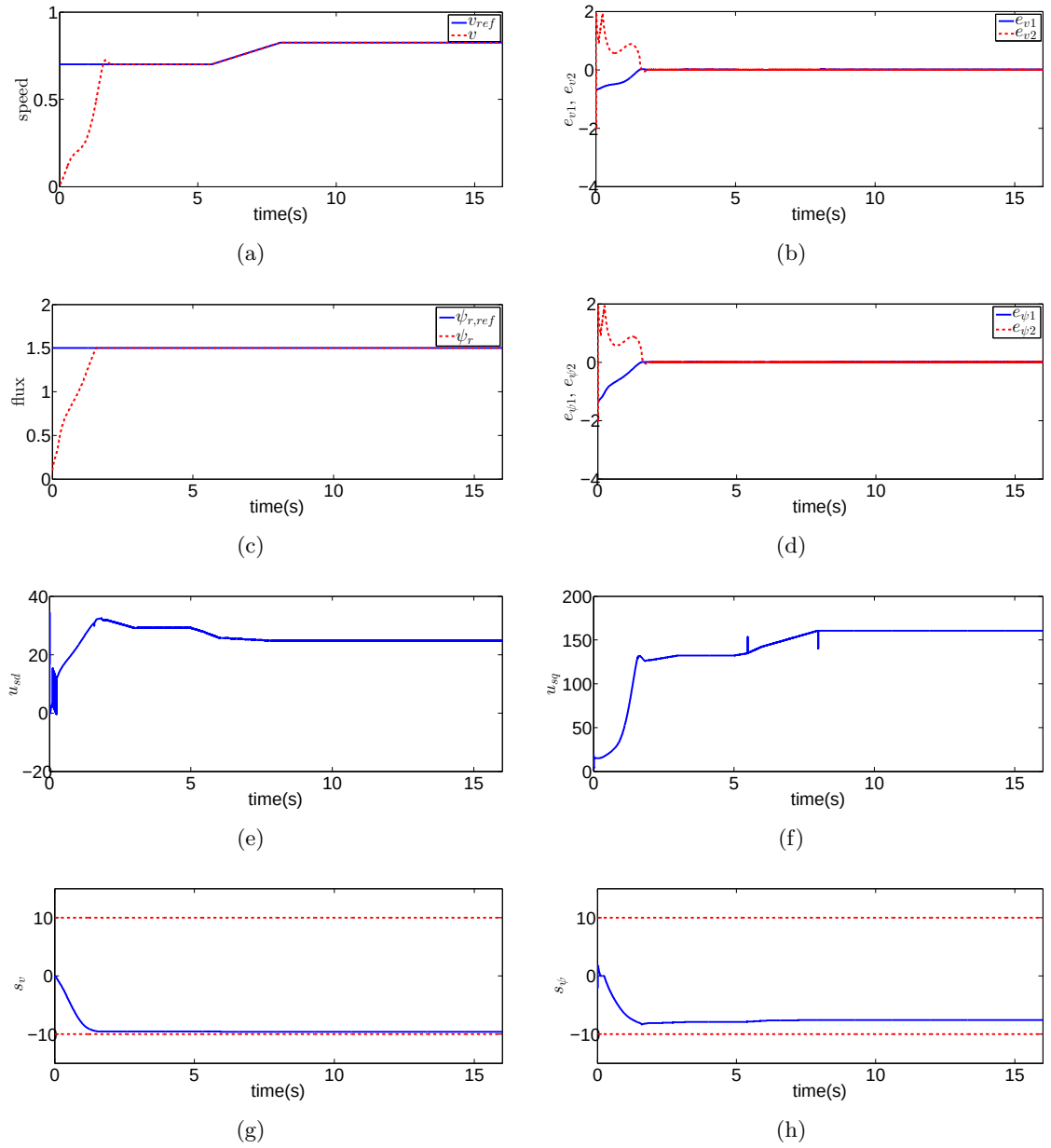

Figure 7.4. *Adaptive DISMC with PBF a) Actual speed and the desired speed, b) State variables* e_{v1}, e_{v2}, *c) Actual flux and the desired flux, d) Sliding variable* $e_{\psi 1}$, $e_{\psi 2}$, *e) Control term* u_{sd}, *f) Control term* u_{sq}, *g) Auxiliary variable* s_v , *h) Auxiliary variable* s_ψ

The simulation results of adaptive DISMC and CISMC with PBF are illustrated in Figs. 7.4-7.5. It can be seen in Figs. 7.4(a)-7.5(a), that these two BAISMCs can ensure efficient tracking of the desired speed. Moreover, it can be shown in Figs. 7.4(b)-7.5(b), that they can guarantee the convergence of the estimated speed error to zero.

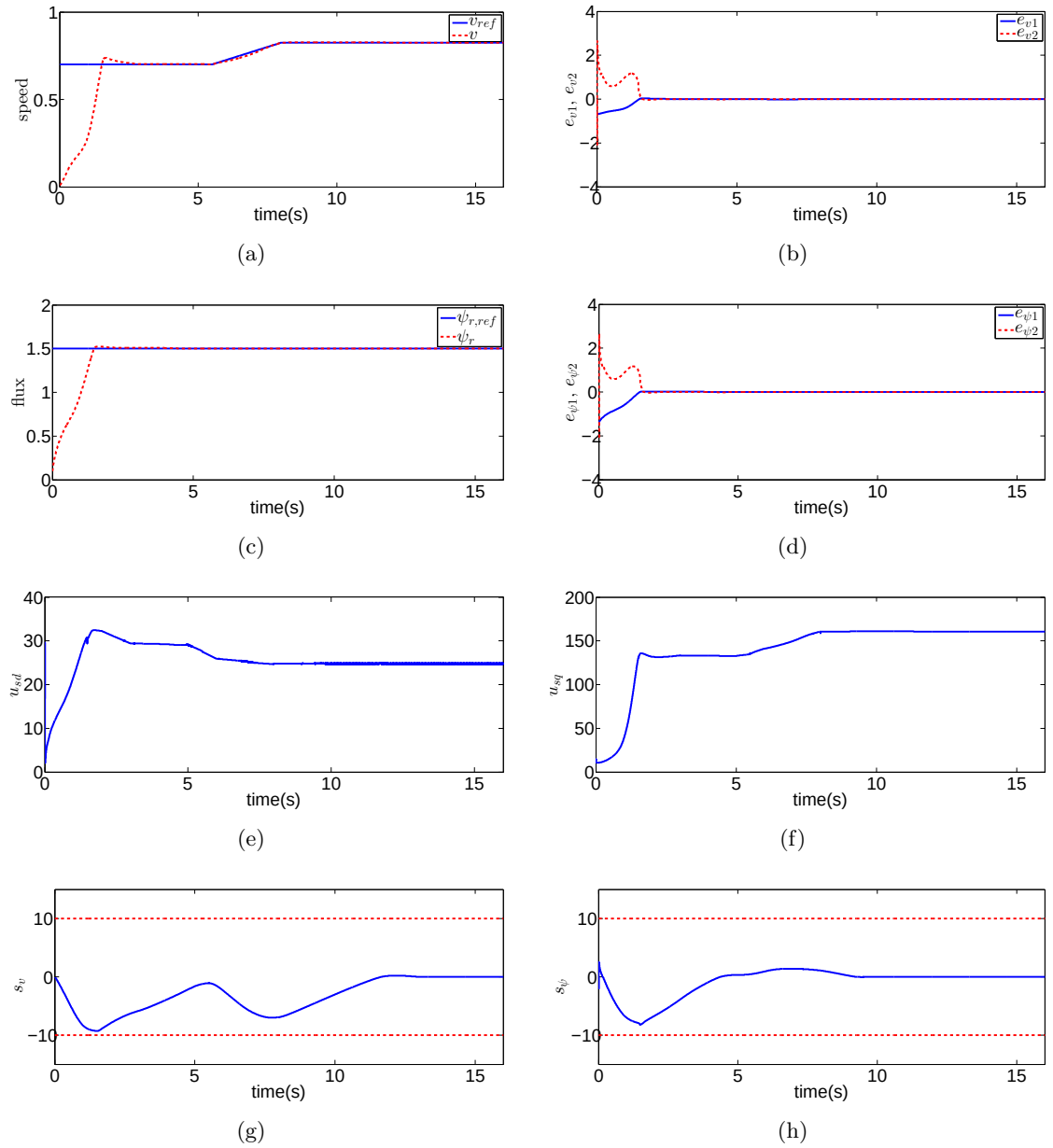

Figure 7.5. *Adaptive CISMC with PBF a) Actual speed and the desired speed, b) State variables* e_{v1}, e_{v2}, *c) Actual flux and the desired flux, d) Sliding variable* $e_{\psi 1}$, $e_{\psi 2}$, *e) Control term* u_{sd}, *f) Control term* u_{sq}, *g) Auxiliary variable* s_v , *h) Auxiliary variable* s_ψ

The tracking of the desired flux using these two BAISMCs can be observed in Figs. 7.4(c)-7.5(c). Furthermore, the accuracy of this tracking can be demonstrated in Figs. 7.4(d)-7.5(d). Figs. 7.4(e)-7.5(e)-7.4(f)-7.5(f) present the two control terms u_{sd} and u_{sq} with these two BAISMCs. It can be noticed that only CISMCs are continuous. On the other

hand, DISMCs contain discontinuity.

It can be concluded that adaptive CISMC, is more efficient than adaptive DISMC regarding continuity of the control signals. It is worth noting that the two auxiliary variables s_υ and s_ψ obtained using these BAISMCs are maintained in the predefined vicinity of zero $\varepsilon_\upsilon = \varepsilon_\psi = 10$ (see. Figs. 7.4(g)-7.5(g)-7.4(h)-7.5(h)).

7.4.2 Results with ADHOSMC

This section is provided to illustrate the situation when the two control terms are implemented using the ADHOSMC. For this, the two strategies proposed in chapter 5, i.e. growing gain-based ADHOSMC and dual layer-based ADHOSMC, are applied.

For the growing gain based-adaptive DHOSMC, the two control terms are designed according to theorem 5.3.1, while for the dual layer-based adaptive DHOSMC, the two control terms follow theorem 5.4.4. Moreover, for both controllers the ideal adaptive gain (5.6) defined in both theorems should be modified to a more practical one [53]

$$\dot{\alpha}(t) = \begin{cases} \bar{\alpha}, & \text{if } ||\bar{\sigma}(t)|| > \varepsilon^* \\ 0, & \text{if } ||\bar{\sigma}(t)|| \leq \varepsilon^* \end{cases} \tag{7.33}$$

where ε^* is small positive constant to be selected. The parameter values of these two ADHOSMCs are given in Appendix. D.C

The simulation results of growing gain-based ADHOSMC and dual layer-based ADHOSMC are presented in Figs. 7.6-7.7. It can be noticed in Figs. 7.6(a)-7.6(b)-7.7(a)-7.7(b), that the accuracy of the speed tracking is better when the dual layer-based ADHOSMC is applied. The accuracy of the flux tracking using these two strategies are comparable (see. Figs. 7.6(c)-7.6(d)-7.7(c)-7.7(d)). It is clear that the control signals provided by these two strategies are discontinuous (see. Figs. 7.6(e)-7.7(e)-7.6(f)-7.7(f)). Finally, it can be shown that the adaptive gain α_υ obtained from dual layer-based ADHOSMC is less than that one obtained from growing gain-based ADHOSMC. While, the adaptive gain α_ψ obtained from these two strategies is almost the same. It can be concluded that dual layer-based ADHOSMC is more efficient than growing gain-based ADHOSMC regarding accuracy in the speed tracking and less amplitude of the adaptive gain α_υ.

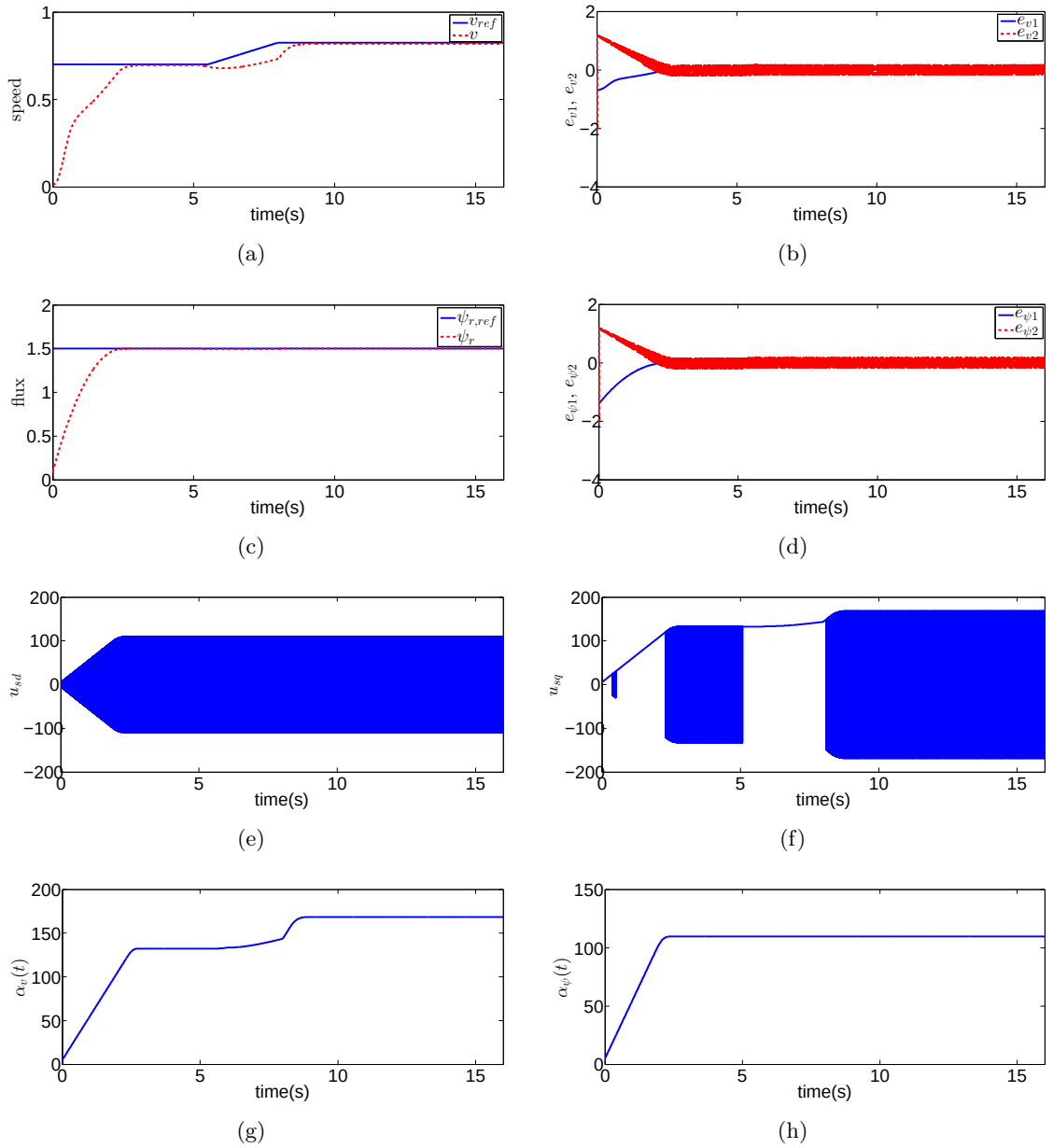

Figure 7.6. *Growing gain-based ADHOSMC a) Actual speed and the desired speed, b) State variables e_{v1}, e_{v2}, c) Actual flux and the desired flux, d) Sliding variable $e_{\psi 1}$, $e_{\psi 2}$, e) Control term u_{sd}, f) Control term u_{sq}, g) Adaptive gain α_v, h) Adaptive gain α_ψ*

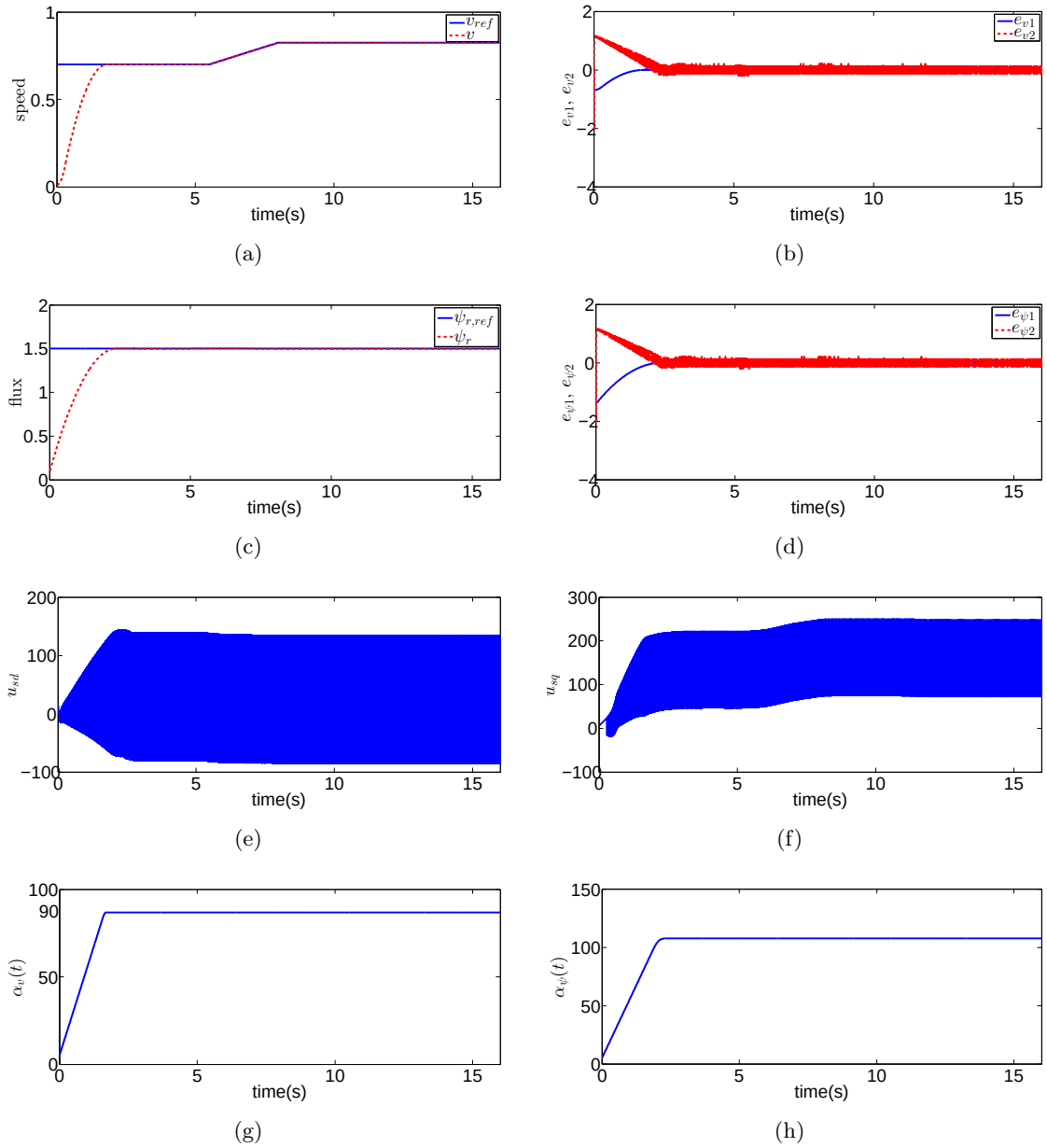

Figure 7.7. *Dual layer-based ADHOSMC a) Actual speed and the desired speed, b) State variables e_{v1}, e_{v2}, c) Actual flux and the desired flux, d) Sliding variable $e_{\psi 1}$, $e_{\psi 2}$, e) Control term u_{sd}, f) Control term u_{sq}, g) Adaptive gain α_v, h) Adaptive gain α_ψ*

7.5 Summary

This chapter deals with the speed and flux tracking control of LIM system. Combined with indirect field oriented control strategy, the LIM's dynamics model are expressed as two subsystems: flux model and speed model. These two models can be viewed as two disturbed double integrator systems. Moreover, the bounds of the disturbances are unknown and the bounds of their derivatives are also unknown. Therefore, the novel BAISMC and ADHOSMC are appropriate choices to control such system. Indeed, they can ensure the convergence of the speed and the flux to their desired values. The simulation results show the performance of these two SMCs, moreover, they demonstrate that BAISMC is better than ADHOSMC regarding the continuity of the control signal.

Conclusion and Perspectives

Overview

In this thesis, several adaptive sliding mode and higher order sliding mode algorithms have been developed for disturbed systems whose disturbances and/or their derivatives are bounded with unknown boundaries. These algorithms are based on a new concept of adaptation that we called here Barrier Function. They ensure the following features:

- The sliding variable in case of ASMC/AHOSMC converges in a finite time to zero or to a predefined neighborhood of zero, independently of upper bounds of disturbances and their derivatives, and cannot exceed it.
- The sliding variable derivatives in the case of AHOSMC converge in a finite time to zero or to some neighborhoods of zero.
- The gains are not overestimated.
- The knowledge of the upper bounds of disturbances and their derivatives is not necessary.

In chapter 1, a descriptive, non-exhaustive overview of adaptive ASMCs/AHOSMCs proposed in the scientific literature is presented and their advantages and disadvantages are discussed.

In chapter 2, the concept of barrier adaptive strategy has been presented. The idea of this strategy is to apply a monotonically increasing gain in order to ensure the convergence of the sliding variable to some predefined neighborhood of zero. Once the sliding variable attains this value, the adaptive gain switches to the barrier function. This strategy does not require any information of the disturbance and avoids the overestimation

of the adaptive gain. Based on this strategy, adaptive FOSMC and DISMC have been developed. For the adaptive FOSMC, it can be applied in the case of first order disturbed systems. Moreover, it can ensure the convergence of the sliding variable and maintain it in a predefined neighborhood of zero independent of the upper bound of the disturbance. For the adaptive DISMC, it can be applied for systems with arbitrary relative degree, and can maintain the auxiliary variable in a predefined neighborhood of zero starting from the initial time moment.

In chapter 3, the design of adaptive barriers functions for first and arbitrary order systems affected by Lipschitz disturbances with unknown Lipschitz constants has been studied. For first order systems, an adaptive STC which can ensure the convergence of the sliding variable and prevents its violation outside a predefined neighborhood of zero has been presented. On the other hand, for arbitrary order systems, an adaptive CISMC has been proposed. The important feature of this adaptive CISMC is that it maintains the auxiliary variable in a predefined neighborhood of zero starting from the initial time moment.

In chapter 4 the adaptation of LD using the barrier strategy has been presented. The discussion made in section 4.5 has shown that none of the existing strategies of adaptation for LD can ensure its convergence in the case when the upper bound of the second derivative of the base signal exists but is unknown. This is due to the reason that LD loses its filtration property in this case.

In chapter 5, the design of adaptive DHOSMCs for perturbed chain of integrators with different classes of disturbances has been studied. For the case of bounded disturbances with unknown upper bounds, the growing gain based-adaptive DHOSMC has been proposed. On the other hand, for the case of Lipschitz disturbances with Lipschitz constants, the dual layer-based adaptive DHOSMC has been designed. In addition, the comparison made in section 5.5 for the case of Lipschitz bounded disturbance has shown that if the disturbance amplitude is increasing, the dual layer strategy has better performance regarding amplitude of chattering. On the other hand, if the disturbance frequency is increasing, the growing gain strategy performs better.

chapter 6 and chapter 7 presented the applications of these new adaptive SMC/HOSMC algorithms for the control of two types of energy conversion systems. In chapter 6 the control of the active and the reactive power for the wind energy conversion system have been considered. One important feature of this system is that it has a relative degree equal to one. The adaptive FOSMC controller and STC controller have been designed to reach

the control objective. Moreover, their performances have been illustrated and compared through simulations.

In chapter 7, the speed and flux tracking for a linear induction motor have been considered. Combined with indirect field oriented control strategy, the linear induction motor dynamic model is expressed as two second order subsystems: flux subsystem and speed subsystem. These two dynamics have been considered as two disturbed double integrators. Then, the adaptive ISMCs and DHOSMCs have been applied in order to ensure the desired tracking. Moreover, their performances have been shown through simulations.

Future Research

There are many remained directions in which the research can be explored and improved. These include:

- The results of chapter 6 and chapter 7 have been validated only by simulation. The experimental validation phase on two test benches for the WECS and the LIM will be the subject of a future work to validate our techniques on real systems.
- An important direction is to study the design of adaptive continuous twisting algorithm for second order perturbed systems using barrier strategy. It should be noted that a first work on the adaptation of this algorithm has been proposed recently in [51]. However, this adaptive strategy allows only the gain to increase in order to achieve the convergence.
- It will be interesting to develop an adaptive version for the higher order super-twisting controller proposed in [41]. Note that adaptive strategies to deal with such controllers still lack.
- In future works it may be interesting to study the barrier function-based adaptive SMCs/HOSMCs in the context of discrete systems. This would allow a better quantification of the predefined area of the convergence as well as the accuracy which are related to the sampling step.

List of Figures

List of Tables

Bibliography

[1] Angelo Accetta, Francesco Alonge, Maurizio Cirrincione, Marcello Pucci, and Antonino Sferlazza. Feedback linearizing control of induction motor considering magnetic saturation effects. *IEEE Transactions on Industry Applications*, 52(6):4843–4854, 2016. [cited at p. 100]

[2] Francesco Alonge, Maurizio Cirrincione, Filippo D'Ippolito, Marcello Pucci, and Antonino Sferlazza. Active disturbance rejection control of linear induction motor. *IEEE Transactions on Industry Applications*, 53(5):4460–4471, 2017. [cited at p. 101]

[3] Francesco Alonge, Maurizio Cirrincione, Filippo D'Ippolito, Marcello Pucci, and Antonino Sferlazza. Robust active disturbance rejection control of induction motor systems based on additional sliding-mode component. *IEEE Transactions on Industrial Electronics*, 64(7):5608–5621, 2017. [cited at p. 100, 101]

[4] Francesco Alonge, Maurizio Cirrincione, Marcello Pucci, and Antonino Sferlazza. Input-output feedback linearizing control of linear induction motor taking into consideration the end-effects. part i: Theoretical analysis. *Control Engineering Practice*, 36:133–141, 2015. [cited at p. 96]

[5] Hechmi Ben Azza, Noureddaher Zaidi, Mohamed Jemli, and Mohamed Boussak. Development and experimental evaluation of a sensorless speed control of spim using adaptive sliding mode-mras strategy. *IEEE Journal of emerging and selected topics in power electronics*, 2(2):319–328, 2014. [cited at p. 97, 99]

[6] Jean-Pierre Barbot, Driss Boutat, and Thierry Floquet. An observation algorithm for nonlinear systems with unknown inputs. *Automatica*, 45(8):1970–1974, 2009. [cited at p. 53]

[7] Giorgio Bartolini, Arie Levant, Franck Plestan, Mohammed Taleb, and Elisabetta Punta. Adaptation of sliding modes. *IMA Journal of Mathematical Control and Information*, 30(3):285–300, 2013. [cited at p. 2, 3, 19]

[8] FJ Bejarano, A Pisano, and E Usai. Finite-time converging jump observer for switched linear systems with unknown inputs. *Nonlinear Analysis: Hybrid Systems*, 5(2):174–188, 2011. [cited at p. 53]

[9] B. Beltran, M. E. H. Benbouzid, and T. Ahmed-Ali. Second-order sliding mode control of a doubly fed induction generator driven wind turbine. *IEEE Transactions on Energy Conversion*, 27(2):261–269, June 2012. [cited at p. 80]

[10] S.P. Bhat and D.S. Bernstein. Geometric homogeneity with applications to finite-time stability. *Mathematics of Control, Signals and Systems*, 17(2):101–127, 2005. [cited at p. 17]

[11] Igor Boiko. *Discontinuous control systems: frequency-domain analysis and design*. Springer Science & Business Media, 2008. [cited at p. 27, 28, 41, 66]

[12] Navid Bolouki, Sam Roozbehani, and Karim Abbaszadeh. Second order sliding mode control of permanent-magnet synchronous wind generator for direct active and reactive power control. In *Power Electronics, Drive Systems and Technologies Conference (PEDSTC), 2014 5th*, pages 434–439. IEEE, 2014. [cited at p. 80]

[13] Tony Burton, Nick Jenkins, David Sharpe, and Ervin Bossanyi. *Wind energy handbook*. John Wiley & Sons, 2011. [cited at p. 82]

[14] J. M. Carrasco, L. G. Franquelo, J. T. Bialasiewicz, E. Galvan, R. C. PortilloGuisado, M. A. M. Prats, J. I. Leon, and N. Moreno-Alfonso. Power-electronic systems for the grid integration of renewable energy sources: A survey. *IEEE Transactions on Industrial Electronics*, 53(4):1002–1016, June 2006. [cited at p. 79]

[15] Fernando Castaños and Leonid Fridman. Analysis and design of integral sliding manifolds for systems with unmatched perturbations. *IEEE Transactions on Automatic Control*, 51(5):853–858, 2006. [cited at p. 35]

[16] Asif Chalanga, Shyam Kamal, and B Bandyopadhyay. Continuous integral sliding mode control: A chattering free approach. In *Industrial Electronics (ISIE), 2013 IEEE International Symposium on*, pages 1–6. IEEE, 2013. [cited at p. 48]

[17] Asif Chalanga and Franck Plestan. Finite time stabilization of an uncertain chain of integrators by integral sliding mode approach. *IFAC-PapersOnLine*, 50(1):9613–9618, 2017. [cited at p. 41, 48, 72]

[18] Jung-Hyun Choi, Jung-Su Kim, and Kyeong-Hwa Kim. Robust tracking performance of linear induction motor-based automatic picking system using a high-gain disturbance observer. *IET Electric Power Applications*, 10(1):45–53, 2016. [cited at p. 95]

[19] Emmanuel Cruz-Zavala and Jaime A Moreno. Homogeneous high order sliding mode design: a lyapunov approach. *Automatica*, 80:232–238, 2017. [cited at p. 66, 103]

[20] Emmanuel Cruz-Zavala, Jaime A Moreno, and Leonid M Fridman. Uniform robust exact differentiator. *IEEE Transactions on Automatic Control*, 56(11):2727–2733, 2011. [cited at p. 135]

[21] Jorge Davila, Alessandro Pisano, and Elio Usai. Continuous and discrete state reconstruction for nonlinear switched systems via high-order sliding-mode observers. *International Journal of Systems Science*, 42(5):725–735, 2011. [cited at p. 53]

[22] Shihong Ding, Arie Levant, and Shihua Li. Simple homogeneous sliding-mode controller. *Automatica*, 67:22–32, 2016. [cited at p. 6, 66, 67, 68, 69, 70]

[23] J Duncan. Linear induction motor-equivalent-circuit model. In *IEE Proceedings B-Electric Power Applications*, volume 130, pages 51–57. IET, 1983. [cited at p. 96]

[24] Christopher Edwards and Yuri Shtessel. Adaptive dual-layer super-twisting control and observation. *International Journal of Control*, 89(9):1759–1766, 2016. [cited at p. 2, 13]

[25] Christopher Edwards and Yuri B Shtessel. Adaptive continuous higher order sliding mode control. *Automatica*, 65:183–190, 2016. [cited at p. 2, 13]

[26] Christopher Edwards and Sarah Spurgeon. *Sliding Mode Control: Theory and Applications*. London: Taylor and Francis, 1998. [cited at p. 96]

[27] Denis Efimov, Ali Zolghadri, and Tarek Raïssi. Actuator fault detection and compensation under feedback control. *Automatica*, 47(8):1699–1705, 2011. [cited at p. 53]

[28] S.V. Emel'yanov, S.K. Korovin, and A. Levant. High-order sliding modes in control systems. *Computational Mathematics and Modeling*, 7(3):294–318, 1996. [cited at p. 1, 9, 66]

[29] C. Evangelista, F. Valenciaga, and P. Puleston. Active and reactive power control for wind turbine based on a mimo 2-sliding mode algorithm with variable gains. *IEEE Transactions on Energy Conversion*, 28(3):682–689, Sept 2013. [cited at p. 83, 84, 85, 87]

[30] CA Evangelista, F Valenciaga, and P Puleston. Multivariable 2-sliding mode control for a wind energy system based on a double fed induction generator. *international journal of hydrogen energy*, 37(13):10070–10075, 2012. [cited at p. 80]

[31] Carolina Evangelista, P Puleston, Fernando Valenciaga, and Leonid M Fridman. Lyapunov-designed super-twisting sliding mode control for wind energy conversion optimization. *IEEE Transactions on Industrial Electronics*, 60(2):538–545, 2013. [cited at p. 80]

[32] R Galván-Guerra, L Fridman, JE Velazquez-Velazquez, S Kamal, and B Bandyopadhyay. Continuous output integral sliding mode control for switched linear systems. *Nonlinear Analysis: Hybrid Systems*, 22:284–305, 2016. [cited at p. 41]

[33] Jiabing Hu, Heng Nian, Bin Hu, Yikang He, and ZQ Zhu. Direct active and reactive power regulation of dfig using sliding-mode control approach. *IEEE Transactions on energy conversion*, 25(4):1028–1039, 2010. [cited at p. 80]

[34] Can Huang, Fangxing Li, and Zhiqiang Jin. Maximum power point tracking strategy for large-scale wind generation systems considering wind turbine dynamics. *IEEE Transactions on Industrial Electronics*, 62(4):2530–2539, 2015. [cited at p. 84]

[35] Chin-I Huang and Li-Chen Fu. Adaptive approach to motion controller of linear induction motor with friction compensation. *IEEE/ASME transactions on mechatronics*, 12(4):480–490, 2007. [cited at p. 95]

[36] Y.J. Huang, T.C. Kuo, and S.H. Chang. Adaptive sliding-mode control for nonlinear systems with uncertain parameters. *IEEE Transactions on Automatic Control*, 38(2):534–539, 2008. [cited at p. 21]

[37] Alberto Isidori. *Nonlinear control systems*. Springer Science & Business Media, 2013. [cited at p. 10]

[38] D Kairous, R Wamkeue, and B Belmadani. Sliding mode control of dfig based variable speed wecs with flywheel energy storage. In *Electrical Machines (ICEM), 2010 XIX International Conference on*, pages 1–6. IEEE, 2010. [cited at p. 80]

[39] G Kang and K Nam. Field-oriented control scheme for linear induction motor with the end effect. *IEE Proceedings-Electric Power Applications*, 152(6):1565–1572, 2005. [cited at p. 96]

[40] Hossein Karimi, Sadgeh Vaez-Zadeh, and Farzad Rajaei Salmasi. Combined vector and direct thrust control of linear induction motors with end effect compensation. *IEEE Transactions on Energy Conversion*, 31(1):196–205, 2016. [cited at p. 96]

[41] Salah Laghrouche, Mohamed Harmouche, and Yacine Chitour. Higher order super-twisting for perturbed chains of integrators. *IEEE Transactions on Automatic Control*, 62(7):3588–3593, 2017. [cited at p. 113]

[42] Salah Laghrouche, Franck Plestan, and Alain Glumineau. Higher order sliding mode control based on integral sliding mode. *Automatica*, 43(3):531–537, 2007. [cited at p. 27, 66]

[43] Arie Levant. Sliding order and sliding accuracy in sliding mode control. *International journal of control*, 58(6):1247–1263, 1993. [cited at p. 41, 43, 80]

[44] Arie Levant. Robust exact differentiation via sliding mode technique. *automatica*, 34(3):379–384, 1998. [cited at p. 53, 54]

[45] Arie Levant. Higher-order sliding modes, differentiation and output-feedback control. *International journal of Control*, 76(9-10):924–941, 2003. [cited at p. 10, 11]

[46] Faa-Jeng Lin, Rong-Jong Wai, Wen-Der Chou, and Shu-Peng Hsu. Adaptive backstepping control using recurrent neural network for linear induction motor drive. *IEEE Transactions on Industrial Electronics*, 49(1):134–146, 2002. [cited at p. 95]

[47] P Liu, C-Y Hung, C-S Chiu, and K-Y Lian. Sensorless linear induction motor speed tracking using fuzzy observers. *IET electric power applications*, 5(4):325–334, 2011. [cited at p. 95]

[48] Xinyi Liu, S. Laghrouche, M. Harmouche, R. Fellag, and M. Wack. Super twisting sliding mode mppt control of an im based wind energy conversion system. In *2015*

4th International Conference on Electrical Engineering (ICEE), pages 1–5, Dec 2015. [cited at p. 80]

[49] Gang Lv, Dihui Zeng, Tong Zhou, and Zhiming Liu. Investigation of forces and secondary losses in linear induction motor with the solid and laminated back iron secondary for metro. *IEEE Transactions on Industrial Electronics*, 64(6):4382–4390, 2017. [cited at p. 95]

[50] Riccardo Marino, Patrizio Tomei, and Cristiano M Verrelli. *Induction motor control design*. Springer Science & Business Media, 2010. [cited at p. 98]

[51] Jaime A Moreno, Daniel Y Negrete, Victor Torres-González, and Leonid Fridman. Adaptive continuous twisting algorithm. *International Journal of Control*, 89(9):1798–1806, 2016. [cited at p. 66, 113]

[52] Jaime A Moreno and Marisol Osorio. Strict lyapunov functions for the super-twisting algorithm. *IEEE transactions on automatic control*, 57(4):1035–1040, 2012. [cited at p. 41]

[53] Daniel Y Negrete-Chávez and Jaime A Moreno. Second-order sliding mode output feedback controller with adaptation. *International Journal of Adaptive Control and Signal Processing*, 2016. [cited at p. 2, 3, 5, 21, 43, 54, 55, 57, 66, 106, 132, 133]

[54] Tiago Roux Oliveira, José Paulo VS Cunha, and Liu Hsu. Adaptive sliding mode control for disturbances with unknown bounds. In *Variable Structure Systems (VSS), 2016 14th International Workshop on*, pages 59–64. IEEE, 2016. [cited at p. 2, 3, 18]

[55] Harshal B Oza, Yury V Orlov, and Sarah K Spurgeon. Continuous uniform finite time stabilization of planar controllable systems. *SIAM Journal on Control and Optimization*, 53(3):1154–1181, 2015. [cited at p. 36, 103]

[56] R Pena, JC Clare, and GM Asher. Doubly fed induction generator using back-to-back pwm converters and its application to variable-speed wind-energy generation. *IEE Proceedings-Electric Power Applications*, 143(3):231–241, 1996. [cited at p. 82]

[57] U. Perez Ventura and Leonid Fridman. When it is reasonable to implement the discontinuous sliding-mode controllers instead of the continuous ones: Frequency domain criteria. *Journal of Robust and Nonlinear Control*, DOI:10.1002/rnc.4347. [cited at p. 27, 41]

[58] Franck Plestan, Yuri Shtessel, Vincent Bregeault, and Alexander Poznyak. New methodologies for adaptive sliding mode control. *International journal of control*, 83(9):1907–1919, 2010. [cited at p. 2, 3, 22, 28, 29, 32, 66, 81, 88, 129]

[59] M. Pucci and M. Cirrincione. Neural mppt control of wind generators with induction machines without speed sensors. *IEEE Transactions on Industrial Electronics*, 58(1):37–47, Jan 2011. [cited at p. 82]

[60] Marcello Pucci. Direct field oriented control of linear induction motors. *Electric Power Systems Research*, 89:11–22, 2012. [cited at p. 96]

[61] Marcello Pucci. State space-vector model of linear induction motors. *IEEE Transactions on Industry Applications*, 50(1):195–207, 2014. [cited at p. 96, 97]

[62] S. Sharma, J. P. Mishra, and S. Datta. Sliding mode power control of a dfig based variable speed wind energy conversion system. In *2015 Annual IEEE India Conference (INDICON)*, pages 1–6, Dec 2015. [cited at p. 80]

[63] Yuri Shtessel, Christopher Edwards, Leonid Fridman, and Arie Levant. Sliding mode control and observation. Springer, 2014. [cited at p. 9, 11, 65]

[64] Yuri Shtessel, Mohammed Taleb, and Franck Plestan. A novel adaptive-gain supertwisting sliding mode controller: methodology and application. *Automatica*, 48(5):759–769, 2012. [cited at p. 2, 3, 5, 22, 42, 45, 54, 57, 81, 91]

[65] Yuri B Shtessel, Jaime A Moreno, and Leonid M Fridman. Twisting sliding mode control with adaptation: Lyapunov design, methodology and application. *Automatica*, 75:229–235, 2017. [cited at p. 2, 3, 22]

[66] J.J. Slotine. Sliding controller design for non-linear systems. *International Journal of Control*, 40(2):421 – 434, 1984. [cited at p. 1]

[67] Mohammed Taleb, Arie Levant, and Franck Plestan. Pneumatic actuator control: Solution based on adaptive twisting and experimentation. *Control Engineering Practice*, 21(5):727–736, 2013. [cited at p. 2, 3, 19]

[68] V I Utkin, J Guldner, and J Shi. *Sliding mode in control in electromechanical systems*. London: Taylor and Francis, 1999. [cited at p. 1, 9, 96]

[69] Vadim Utkin and Jingxin Shi. Integral sliding mode in systems operating under uncertainty conditions. In *Decision and Control, 1996., Proceedings of the 35th IEEE Conference on*, volume 4, pages 4591–4596. IEEE, 1996. [cited at p. 27]

[70] Vadim I Utkin and Alex S Poznyak. Adaptive sliding mode control with application to super-twist algorithm: Equivalent control method. *Automatica*, 49(1):39–47, 2013. [cited at p. 2, 11]

[71] VI Utkin. *Sliding modes in optimization and control problems*. Springer Verlag, New York, 1992. [cited at p. 1, 2, 3, 9, 11, 18, 27, 65, 80]

[72] F. Valenciaga and C. A. Evangelista. 2-sliding active and reactive power control of a wind energy conversion system. *IET Control Theory Applications*, 4(11):2479–2490, November 2010. [cited at p. 83, 84, 85]

[73] Sakae Yamamura. Theory of linear induction motors. *New York, Halsted Press, 1979. 246 p.*, 1979. [cited at p. 96]

[74] K.D. Young, V.I. Utkin, and U. Ozguner. A control engineer's guide to sliding mode control. *IEEE Transactions on Control System Technology*, 7(3):328–342, 1999. [cited at p. 1, 9]

[75] Noureddaher Zaidi, Hechmi Ben Azza, Mohamed Jemli, and Abdelkader Chaari. Dsp full implementation of second order sliding mode control to drive a spim. In *Electrical Engineering and Software Applications (ICEESA), 2013 International Conference on*, pages 1–6. IEEE, 2013. [cited at p. 97, 99]

[76] Lei Zhang, Salah Laghrouche, Mohamed Harmouche, and Maurizio Cirrincione. Super twisting control of linear induction motor considering end effects with unknown load torque. In *American Control Conference (ACC), 2017*, pages 911–916. IEEE, 2017. [cited at p. 97]

[77] Qing-Chang Zhong and Tomas Hornik. *Control of power inverters in renewable energy and smart grid integration*, volume 97. John Wiley & Sons, 2012. [cited at p. 79]

Appendices

Appendices

A Proof of theorem 2.2.2.

*P*roof.

According to [58] the system solution will reach $\frac{\varepsilon}{2}$ in finite time.

Denote $t = \bar{t}$ the smallest root of equation $|s(t)| \leq \frac{\varepsilon}{2}$, and consider the Lyapunov candidate function containing both the sliding variable and the adaptive gain dynamics

$$V\Big(s(t), K_B(s(t))\Big) = \frac{1}{2}s^2(t) + \frac{1}{2}\Big(K_B(s(t)) - K_B(0)\Big)^2.$$

A.A Adaptation with PBF

Consider the case when $K_B(s(t)) = K_{pb}(s(t))$. It is shown that if $|s(\bar{t})| > s_1$ where

$$s_1 = \begin{cases} \varepsilon(1 - \dfrac{\bar{F}}{\delta_{max}}), & \text{if } \bar{F} < \delta_{max} \\ 0, & \text{if } \bar{F} \geq \delta_{max} \end{cases} \tag{34}$$

then PBF ensures that $|s(t)| \leq s_1$ in a finite time period τ_1. Furthermore, it is proven that for all $t \geq \bar{t} + \tau_1$, the sliding variable will remain inside $|s(t)| \leq s_1 < \varepsilon$. Note that $\tau_1 = 0$ if $|s(\bar{t})| \leq s_1$.

Lemma A.1. *Given the sliding variable dynamics (2.1) controlled by (2.2) and (2.3) with $K_B(s(t)) = K_{pb}(s(t))$. Then, for all $t \geq \bar{t}$, and for all $|s(t)| > s_1$, the time derivative of the Lyapunov function satisfies the following inequality*

$$\dot{V}\Big(s(t), K_{pb}(s(t))\Big) \leq -\beta_1 V^{\frac{1}{2}}\Big(s(t), K_{pb}(s(t))\Big), \text{ with } \beta_1 > 0.$$

Which yields a finite time convergence to the domain $|s(t)| \leq s_1$.

Proof. The time derivative of $V\Big(s(t), K_B(s(t))\Big)$ is given as follows

$$\begin{aligned}\dot{V} &= s\delta - sK_B(s)sign(s) + (K_B(s) - K_B(0))\dot{K}_B(s) \\ &\leq \delta_{max}|s| - K_B(s)|s| + (K_B(s) - K_B(0))\dot{K}_B(s),\end{aligned} \tag{35}$$

since $K_B(s(t)) = K_{pb}(s(t))$, one gets

$$\begin{aligned}\dot{V} \leq & -\underbrace{(-\delta_{max} + K_{pb}(s))}_{\beta_s}|s| \\ & -\underbrace{\frac{\varepsilon\bar{F}}{(\varepsilon - |s(t)|)^2}}_{\zeta>0}\underbrace{(-\delta_{max} + K_{pb}(s))}_{\beta_s}|K_{pb}(s) - \bar{F}| \\ & = -\beta_s|s| - \zeta\beta_s|K_{pb}(s) - \bar{F}|.\end{aligned} \tag{36}$$

- Suppose that $\bar{F} < \delta_{max}$, and consider the case when $|s(t)| > s_1$. Then, taking into account that $K_{pb}(s(t))$ is an increasing function on $[0, \varepsilon[$, it yields $K_{pb}(s(t)) > K_{pb}(s_1) = \delta_{max}$. This leads to $\beta_s > 0$. Therefore

$$\begin{aligned}\dot{V} &\leq -\beta_s|s| - \zeta\beta_s|K_{pb}(s) - \bar{F}| \\ &= -\beta_s\sqrt{2}\Big(\frac{|s|}{\sqrt{2}} + \zeta\frac{|K_{pb}(s) - \bar{F}|}{\sqrt{2}}\Big) \\ &\leq -\beta_s\sqrt{2}\min\{1,\zeta\}\Big(\frac{|s|}{\sqrt{2}} + \frac{|K_{pb}(s) - \bar{F}|}{\sqrt{2}}\Big) \\ &\leq -\beta_1 V^{\frac{1}{2}}, \quad \text{with} \quad \beta_1 = \beta_s\sqrt{2}\min\{1,\zeta\}.\end{aligned} \tag{37}$$

- Suppose that $\bar{F} \geq \delta_{max}$ and $|s(t)| > s_1 = 0$. Thus, $\beta_s > 0$ since $K_{pb}(s(t)) > K_{pb}(0) = \bar{F} \geq \delta_{max}$ (see Eq. 36). It yields that $\dot{V} \leq -\beta_1 V^{\frac{1}{2}}$.

Therefore, finite time convergence to the domain $|s(t)| \leq s_1$ is ensured, and the reaching time τ_1 can be estimated as

$$\tau_1 \leq \frac{2\Big(-V\Big(s_1, K_{pb}(s_1)\Big)^{\frac{1}{2}} + V\Big(s(\bar{t}), K_{pb}(s(\bar{t}))\Big)^{\frac{1}{2}}\Big)}{\beta_1}.$$

□

Now, the case when $t \geq \bar{t} + \tau_1$, and $|s(t)| < s_1$ is studied. In this case, $\dot{V}$ would be sign indefinite (see Eq. 36), and $s(t)$ can go toward s_1. Please note that at the time instant when $|s(t)|$ reaches s_1, $\dot{V} \leq 0$ since $\beta_s = 0$, and V would be constant or decreasing. This means that for all $t \geq \bar{t} + \tau_1$, $|s(t)| \leq s_1$.

Finally, as $|s(\bar{t})| \leq \dfrac{\varepsilon}{2}$, it becomes evident that for all $t \geq \bar{t}$ the inequality $|s(t)| < \varepsilon$ holds.

A.B Adaptation with PSBF

Consider now the case when $K_B(s(t)) = K_{psb}(s(t))$. Following the same proof and replacing Lemma. A.1 by the following Lemma. A.2, it is easy to demonstrate that if $|s(\bar{t})| > s_2$ where

$$s_2 = \varepsilon\left(\frac{\delta_{max}}{\delta_{max}+1}\right). \tag{38}$$

then PSBF ensures that $|s(t)| \leq s_2$ in a finite time period τ_2. Moreover, for all $t \geq \bar{t} + \tau_2$ the sliding variable will remain inside $|s(t)| \leq s_2 < \varepsilon$. Note that $\tau_2 = 0$ if $|s(\bar{t})| \leq s_2$.

Lemma A.2. *Given the sliding variable dynamics (2.1) controlled by (2.2) and (2.3) with $K_B(s(t)) = K_{psb}(s(t))$. Then, for all $t \geq \bar{t}$, and for all $|s(t)| > s_2$, the time derivative of the Lyapunov function satisfies the following inequality*

$$\dot{V}\Big(s(t), K_{psb}(s(t))\Big) \leq -\beta_2 V^{\frac{1}{2}}\Big(s(t), K_{psb}(s(t))\Big), \text{ with } \beta_2 > 0.$$

Which yields a finite time convergence to the domain $|s(t)| \leq s_2$.

*P*roof.

Taking into account that $K_B(s(t)) = K_{psb}(s(t))$, the upper bound of Eq. 35 can be derived as

$$\begin{aligned}
\dot{V} \leq & -\underbrace{(-\delta_{max} + K_{psb}(s))}_{\beta_s}|s| \\
& - \underbrace{\frac{\varepsilon}{(\varepsilon - |s(t)|)^2}}_{\zeta>0}\underbrace{(-\delta_{max} + K_{psb}(s))}_{\beta_s}|K_{psb}(s)| \\
& = -\beta_s|s| - \zeta\beta_s|K_{psb}(s)|.
\end{aligned} \tag{39}$$

Consider the case when $|s(t)| > s_2$. Then, $K_{psb}(s(t)) > K_{psb}(s_2) = \delta_{max}$. This leads to $\beta_s > 0$. Therefore

$$\begin{aligned}
\dot{V} &\leq -\beta_s|s| - \zeta\beta_s|K_{psb}(s)| \\
&= -\beta_s\sqrt{2}\Big(\frac{|s|}{\sqrt{2}} + \zeta\frac{|K_{psb}(s)|}{\sqrt{2}}\Big) \\
&\leq -\beta_s\sqrt{2}\min\{1,\zeta\}\Big(\frac{|s|}{\sqrt{2}} + \frac{|K_{psb}(s)|}{\sqrt{2}}\Big) \\
&\leq -\beta_2 V^{\frac{1}{2}}, \quad \text{with} \quad \beta_2 = \beta_s\sqrt{2}\min\{1,\zeta\}.
\end{aligned} \tag{40}$$

Therefore, finite time convergence to the domain $|s(t)| \leq s_2$ is ensured, and the reaching time τ_2 can be estimated as

$$\tau_2 \leq \frac{2\Big(-V\Big(s_2, K_{psb}(s_2)\Big)^{\frac{1}{2}} + V\Big(s(\bar{t}), K_{psb}(s(\bar{t}))\Big)^{\frac{1}{2}}\Big)}{\beta_2}.$$

□

Theorem. 2.2.2 is proven.

B Proof of Theorem 3.2.1.

Proof. The proof will be done in two steps.

First step: In this step, it is shown that the equation $|s(t)| \leq \frac{\varepsilon}{2}$ has at least one root. Suppose that $|s(0)| > \frac{\varepsilon}{2}$, then from (3.5), the adaptive gain is given by $\dot{L}_a(t) = L_1$.
Consider the following change of variables

$$\xi_1 = \frac{s(t)}{L_a^2(t)} \quad , \quad \xi_2 = \frac{\phi(t)}{L_a^2(t)}. \tag{41}$$

In theses variables, system (3.4) can be described as follows

$$\begin{cases} \dot{\xi_1} = -h_1 |\xi_1|^{\frac{1}{2}} sign(\xi_1) + \xi_2 - 2\dfrac{\dot{L}_a(t)}{L_a(t)}\xi_1, \\ \dot{\xi_2} = -h_2 sign(\xi_1) + \dfrac{\dot{\delta}(t)}{L_a^2(t)} - 2\dfrac{\dot{L}_a}{L_a(t)}\xi_2. \end{cases} \tag{42}$$

Consider the quadratic Lyapunov function candidate proposed in [53]

$$V_0(\zeta) = \zeta^\top P \zeta \quad , \quad \zeta^\top = [|\xi_1|^{\frac{1}{2}} sign(\xi_1), \xi_2], \tag{43}$$

where P is a constant symmetric and positive-definite matrix.
The time derivative of $\zeta(t)$ can be given as follows

$$\dot{\zeta}(t) = \frac{1}{2|\xi_1|^{\frac{1}{2}}} H\zeta + \frac{\dot{L}_a(t)}{L_a(t)} N\zeta + \frac{W(t)}{L_a^2(t)}, \tag{44}$$

where

$$H = \begin{bmatrix} -h_1 & 1 \\ -2h_2 & 0 \end{bmatrix}, \; N = \begin{bmatrix} -1 & 0 \\ 0 & -2 \end{bmatrix}, \; W(t) = \begin{bmatrix} 0 \\ \dot{\delta}(t) \end{bmatrix}. \tag{45}$$

Thus, the time derivative of V_0 along the trajectories of (42) can be written as

$$\dot{V}_0 = -\frac{1}{2|\xi_1|^{\frac{1}{2}}}\zeta^\top Q\zeta - \frac{\dot{L}_a(t)}{L_a(t)}\zeta^\top R\zeta + \frac{2}{L_a^2(t)}W(t)P\zeta, \tag{46}$$

where

$$H^\top P + PH = -Q, \tag{47}$$

$$N^\top P + PN = -R. \tag{48}$$

According to [53], there exist a symmetric and positive-definite matrix P in the Lyapunov function (43) such that Q and R are positive definite.
Finally, similar to [53], the following upper bound of $\dot{V}_0$ can be obtained

$$\dot{V}_0 \leq -\alpha_1 V_0^{\frac{1}{2}} + 2\alpha_3\frac{M}{L_a^2(t)}V_0^{\frac{1}{2}} - \frac{\dot{L}_a(t)}{L_a(t)}\alpha_2 V_0, \tag{49}$$

where

$$\alpha_1 = \frac{\lambda_{\min}(Q)}{2\sqrt{p_{11}}\lambda_{\max}(P)},\ \alpha_2 = \frac{\lambda_{\min}(R)}{\lambda_{\max}(P)},\ \alpha_3 = \frac{\lambda_{\max}(P)}{\sqrt{\lambda_{\min}(P)}}, \tag{50}$$

with $\lambda_{\min}(.)$, $\lambda_{\max}(.)$ the minimal and maximal eigenvalue of the corresponding matrix respectively, and p_{11} is the first component of matrix P.

The first term on the right-hand side of (49) is negative-definite. Then, taking into account that the adaptive gain $L_a(t)$ is growing, it follows that the second term will decrease and become smaller than the first one in finite time. In addition, the third term will also decrease.

In conclusion, it is clear that V_0 will decrease as soon as the adaptive gain $L_a(t)$ is big enough to compensate the disturbance derivative. When $\dot{V}_0$ becomes negative-definite, V_0 will converge to zero in finite time. Therefore, the equation $|s(t)| \leq \frac{\varepsilon}{2}$ has at least one root. Denote $t = t_1$ the smallest root of this equation.

Second step: In this step, the proof of the adaptation with BFs is given. In order to do it, the following quadratic Lyapunov candidate function is considered

$$V\Big(z, L_B(s(t))\Big) = V_1(z) + \frac{1}{2}(L_B(s(t)) - L_B(0))^2, \tag{51}$$

where

$$V_1(z) = z^\top P_1 z, \tag{52}$$

with P_1 is a symmetric and positive definite matrix and

$$z = \begin{bmatrix} z_1 & z_2 \end{bmatrix}^\top = \begin{bmatrix} |s|^{\frac{1}{2}} sign(s) & \phi \end{bmatrix}^\top. \tag{53}$$

B.A Adaptation with PBF

Proposition B.1. *If* $|s(t_1)| > \bar{s}_1$ *with* $\bar{s}_1 = \max\{s_1, s_2\}$, *where*

$$s_1 = \begin{cases} \varepsilon(1 - \dfrac{\bar{F}}{\Theta}),\ \Theta = \Big(\dfrac{4M^2}{h_1^2(2h_2 - \frac{1}{4}h_1^2)}\Big)^{(\frac{1}{4})}, & \text{if } \bar{F} < \Theta \\ 0, & \text{if } \bar{F} \geq \Theta, \end{cases} \tag{54}$$

and

$$s_2 = \Big(\frac{-h_1\varepsilon\bar{F} + \Big((h_1\varepsilon\bar{F})^2 + 4\varepsilon|\phi|^2\Big)^{\frac{1}{2}}}{2|\phi|}\Big)^2, \tag{55}$$

then PBF ensures that $|s(t)| \leq \bar{s}_1$ *in a finite time period* τ_1. *Moreover, it is proven that for all* $t \geq T$ *with* $T = t_1 + \tau_1$, *the inequalities* $|s(t)| \leq \mu_1$ *and* $|\dot{s}(t)| \leq \nu(M)$ *hold with* $\bar{s}_1 < \mu_1 < \varepsilon$. *Note that* $\tau_1 = 0$ *is* $|s(t_1)| \leq \bar{s}_1$.

Remark B.2. *In order to prove the existence of a value* μ_1 *such that* $\bar{s}_1 < \mu_1 < \varepsilon$, *it is necessary to show that* $\bar{s}_1 < \varepsilon$. *From* (54), *it is clear that* $s_1 < \varepsilon$. *Moreover, based in the inequality* $a^2 + b^2 < (a+b)^2$ *for* $a > 0$ *and* $b > 0$, *it follows that*

$$(h_1\varepsilon\bar{F})^2 + (2\varepsilon^{\frac{1}{2}}|\phi|)^2 < (h_1\varepsilon\bar{F} + 2\varepsilon^{\frac{1}{2}}|\phi|)^2. \tag{56}$$

Using the previous inequality, the upper bound of (55) *becomes*

$$\begin{aligned} s_2 &< \Big(\frac{-h_1\varepsilon\bar{F} + \Big((h_1\varepsilon\bar{F} + 2\varepsilon^{\frac{1}{2}}|\phi|)^2\Big)^{\frac{1}{2}}}{2}\Big)^2 \\ &= \Big(\frac{-h_1\varepsilon\bar{F} + (h_1\varepsilon\bar{F} + 2\varepsilon^{\frac{1}{2}}|\phi|)}{2|\phi|}\Big)^2 = (\frac{2\varepsilon^{\frac{1}{2}}|\phi|}{2|\phi|})^2 = \varepsilon. \end{aligned} \tag{57}$$

Therefore, the existence of μ_1 *is proved.*

Proof. Firstly, the time derivative of $V_1(z)$ is studied. In order to do this, system (3.4) is described with the new state vector z

$$\begin{cases} \dot{z}_1 = \dfrac{1}{2|z_1|}\Big(-h_1 L_B z_1 + z_2\Big) \\ \dot{z}_2 = \dfrac{1}{2|z_1|}\Big(-2h_2 L_B^2 z_1\Big) + \dot{\delta}(t). \end{cases} \tag{58}$$

It is possible to write (58) as

$$\begin{aligned} \begin{bmatrix} \dot{z}_1 \\ \dot{z}_2 \end{bmatrix} &= \frac{1}{2|z_1|}\left[\begin{bmatrix} -h_1 L_B & 1 \\ -2h_2 L_B^2 & 0 \end{bmatrix} z + \begin{bmatrix} 0 \\ 1 \end{bmatrix}\xi\right] \Longrightarrow \\ \dot{z} &= \frac{1}{2|z_1|}(Az + B\xi), \end{aligned} \tag{59}$$

where

$$A=\begin{bmatrix}-h_1L_B & 1\\ -2h_2L_B^2 & 0\end{bmatrix},\quad B=\begin{bmatrix}0\\1\end{bmatrix},\quad \xi=2|z_1|\dot{\delta}(t). \tag{60}$$

Taking into account that $|z_1|\leq||z||$, we can write $|\xi|\leq 2M||z||$. According to [20], the selection of the adaptive gain that can provide the negative definiteness of $\dot{V}_1(z)$ is to be determined from the following Linear Matrix Inequality (LMI)

$$\begin{bmatrix}A^\top P_1+P_1A+4M^2C^\top C+\varrho I & P_1B\\ B^\top P_1 & -1\end{bmatrix}\leq 0, \tag{61}$$

where $C=\begin{bmatrix}1 & 0\end{bmatrix}$, $P_1=P_1^\top>0$ is the solution of this LMI and for some $\varrho>0$. Using the classical circle criterium the LMI (61) will be satisfied if and only if the Nyquist diagram of the transfer function $G(s)=C(sI-A)^{-1}B$ is contained in the circle centered in the origin and with radius $\frac{1}{2M}$, that is, if and only if

$$\max_w|G(jw)|<\frac{1}{2M}. \tag{62}$$

Note that

$$\begin{aligned}G(s)&=\frac{1}{s^2+h_1L_Bs+2h_2L_B^2},\\ |G(jw)|^2&=\frac{1}{(2h_2L_B^2-w^2)^2+(h_1L_Bw)^2}.\end{aligned} \tag{63}$$

From the derivative, and the second derivative of $|G(jw)|^2$ it can be deduced that

$$\max_w|G(jw)|^2=\begin{cases}\frac{1}{(2h_2L_B^2)^2} & \text{if } 2h_2L_B^2<\frac{1}{2}(h_1L_B)^2\\ \frac{1}{(h_1L_B)^2(2h_2L_B^2-\frac{1}{4}(h_1L_B)^2)} & \text{if } 2h_2L_B^2>\frac{1}{2}(h_1L_B)^2.\end{cases}$$

The second set of the adaptive gain is only important due to the reason that $2h_2L_B^2>\frac{1}{2}(h_1L_B)^2$. Then, based on that, if

$$(h_1L_B)^2\left(2h_2L_B^2-\frac{1}{4}(h_1L_B)^2\right)>4M^2, \tag{64}$$

it leads to

$$\begin{aligned}\dot{V}_1&\leq\frac{1}{2|z_1|}\begin{bmatrix}z\\ \xi\end{bmatrix}^\top\begin{bmatrix}A^\top P_1+P_1A+4M^2C^\top C & P_1B\\ B^\top P_1 & -1\end{bmatrix}\begin{bmatrix}z\\ \xi\end{bmatrix}\\ &\leq-\frac{1}{2|z_1|}\varrho||z||^2\\ &\leq-rV_1^{\frac{1}{2}},\ \text{with } r=\frac{\varrho\lambda_{min}^{\frac{1}{2}}\{P_1\}}{2\lambda_{max}\{P_1\}}.\end{aligned} \tag{65}$$

Next, the time derivative of the Lyapunov function $V\Big(z, L_B(s)\Big)$ in (51) is computed:

$$\dot{V} = \dot{V}_1 + \Big(L_B(s) - L_B(0)\Big)\dot{L}_B(s). \tag{66}$$

Since $L_B(s) = L_{pb}(s)$, it implies that

$$\dot{V} \leq \dot{V}_1 - \underbrace{\frac{\varepsilon\bar{F}}{(\varepsilon - |s|)^2}}_{\zeta_1 > 0}\beta_{s1}|L_{pb}(s) - \bar{F}|. \tag{67}$$

with

$$\begin{aligned}\beta_{s1} &= \Big(-|\phi| + h_1 L_{pb}(s)|s|^{\frac{1}{2}}\Big) \\ &= \underbrace{\frac{1}{\varepsilon - |s|}}_{\eta}\Big(h_1\varepsilon\bar{F}|s|^{\frac{1}{2}} - |\phi|\varepsilon + |s||\phi|\Big).\end{aligned} \tag{68}$$

Case 1 Suppose that $t \geq t_1$ and $|s(t)| > \bar{s}_1$. Then from (54)-(55), it follows that

$$L_{pb}(s) > \Theta, \tag{69}$$

and

$$|s(t)| > s_2. \tag{70}$$

Inequality (69) ensures that (64) holds. Moreover, taking into account that $\eta > 0$ (since $|s(t_1)| < \varepsilon$), and s_2 is the positive root of (68), thus, (70) ensures that $\beta_{s1} > 0$. Finally, the upper bound of $\dot{V}$ can be written as

$$\begin{aligned}\dot{V} &\leq -rV_1^{\frac{1}{2}} - \zeta_1\beta_{s1}|L_{pb}(s) - \bar{F}| \\ &= -rV_1^{\frac{1}{2}} - \sqrt{2}\zeta_1\beta_{s1}\frac{|L_{pb}(s) - \bar{F}|}{\sqrt{2}} \\ &\leq -\beta_1 V^{\frac{1}{2}}, \quad \text{with } \beta_1 = \min\{r, \sqrt{2}\zeta_1\beta_{s1}\}.\end{aligned} \tag{71}$$

Therefore, the finite time convergence to the domain $|s(t)| \leq \bar{s}_1$ is guaranteed, and the reaching time τ_1 can be estimated by $\tau_1 \leq \tau_{r1} \leq \dfrac{2V(t_1)^{\frac{1}{2}}}{\beta_1}$ (τ_{r1} is obtained by assuming that $\bar{s}_1 = 0$).

Case 2 Suppose that $t \geq T$ and $|s(t)| < \bar{s}_1$. In this case, $\dot{V}$ would be sign indefinite, and $|s(t)|$ may become larger than $\bar{s}_1$. Note that at the time instant when $|s(t)|$ reaches μ_1, $\dot{V} \leq -\beta_1 V^{\frac{1}{2}}$ (**C**ase 1 holds) so that $|s(t)|$ reaches the domain $|s(t)| \leq \bar{s}_1$ in finite time, and so on.

This means that PBF ensures the convergence of the sliding variable to $|s(t)| \leq \bar{s}_1$ in finite time, then the sliding variable can leave this domain for a finite time, moreover, the specific property of this adaptation is that the sliding variable cannot leave the larger domain $|s(t)| \leq \mu_1$, with $\bar{s}_1 < \mu_1 < \varepsilon$.

Inside the domain $|s(t)| \leq \bar{s}_1$, the upper bound of $|\dot{s}(t)|$ can be estimated as follows

$$\begin{aligned} |\dot{s}(t)| &\leq h_1 L_{pb}(\bar{s}_1)|\bar{s}_1|^{\frac{1}{2}} \\ &+ \Big(h_2 L_{pb}^2(\bar{s}_1) + M\Big)\Big(t_2 - T\Big) + |\phi(t_2)| = \bar{v}_1, \end{aligned} \tag{72}$$

where t_2 is the time instant when $s(t)$ leaves the domain $|s(t)| \leq \bar{s}_1$. When $|s(t)|$ becomes $\bar{s}_1 < |s(t)| \leq \mu_1$ then

$$\begin{aligned} |\dot{s}(t)| &\leq h_1 L_{pb}(\mu_1)|\mu_1|^{\frac{1}{2}} \\ &+ \Big(h_2 L_{pb}^2(\mu_1) + M\Big)(t_3 - t_2) + |\phi(t_3)| = \check{v}_1, \end{aligned} \tag{73}$$

where t_3 is the time instant when $s(t)$ enters the domain $|s(t)| \leq \bar{s}_1$. Combining the conditions (72)-(73), it follows that

$$|\dot{s}(t)| \leq \max\{\bar{v}_1, \check{v}_1\} = v. \tag{74}$$

Finally, PBF can ensure the convergence of the sliding variable and its derivative to the following domain

$$W_1 = \{s(t), \dot{s}(t) : |s(t)| \leq \mu_1, |\dot{s}(t)| \leq v(M), \bar{s}_1 < \mu_1 < \varepsilon\} \tag{75}$$

and since $\mu_1 < \varepsilon$, this means that the domain to which converges $|s(t)|$ is predefined. Adaptation with PBF is proven. □

B.B Adaptation with PSBF

Proposition B.3. *If $|s(t_1)| > \bar{s}_2$ with $\bar{s}_2 = \max\{s_3, s_4\}$, where*

$$s_3 = \varepsilon\left(\frac{\Theta}{1+\Theta}\right),\ \Theta = \left(\frac{4M^2}{h_1^2(2h_2 - \frac{1}{4}h_1^2)}\right)^{\left(\frac{1}{4}\right)}, \tag{76}$$

and

$$s_4 = \left(\frac{-1 + \left(1 + 4\varepsilon|\phi|^2\right)^{\frac{1}{2}}}{2|\phi|}\right)^2, \tag{77}$$

then PSBF ensures that $|s(t)| \leq \bar{s}_2$ in a finite time period τ_2. Moreover, it is proven that for all $t \geq T$ with $T = t_1 + \tau_2$, the inequalities $|s(t)| \leq \mu_2$ and $|\dot{s}(t)| \leq v(M)$ hold with $\bar{s}_2 < \mu_2 < \varepsilon$. Note that $\tau_2 = 0$ is $|s(t_1)| \leq \bar{s}_2$.

Remark B.4. *Similar to Remark. B.2, it can be proved that there exist* μ_2 *such that* $\bar{s}_2 < \mu_2 < \varepsilon$.

*P*roof. Taking into account that $L_B(s) = L_{psb}(s)$, the upper bound of (67) can be derived as

$$\dot{V} \leq \dot{V}_1 - \underbrace{\frac{\varepsilon}{(\varepsilon - |s|)^2}}_{\zeta_2 > 0} \beta_{s2} |L_{psb}(s)|. \tag{78}$$

with

$$\begin{aligned} \beta_{s2} &= \left(- |\phi| + h_1 L_{psb}(s) |s|^{\frac{1}{2}} \right) \\ &= \underbrace{\frac{1}{\varepsilon - |s(t)|}}_{\eta} (h_1 |s(t)|^{\frac{3}{2}} - |\phi(t)|\varepsilon + |\phi(t)||s(t)|). \end{aligned} \tag{79}$$

Case 1 Suppose that $t \geq t_1$ and $|s(t)| > s_2$. Then in accordance with (76)-(77) the following two inequalities hold

$$L_{psb}(s) > \Theta, \tag{80}$$

and

$$|s(t)| > s_4. \tag{81}$$

Inequality (80) ensures that (64) holds, and taking into account that $\eta > 0$ (since $|s(t_1)| < \varepsilon$), β_{s2} can be rewritten as

$$\beta_{s2} \geq \frac{1}{\varepsilon - |s(t)|} (-|s(t)|^{\frac{1}{2}} - |\phi(t)|\varepsilon + |\phi(t)||s(t)|). \tag{82}$$

Please note that s_4 is the positive root of (82). Thus, from inequality (81), it follows that $\beta_{s2} > 0$. Finally, the upper bound of (78) can be expressed as

$$\begin{aligned} \dot{V} &\leq -r V_1^{\frac{1}{2}} - \zeta_2 \beta_{s2} |L_{psb}(s)| \\ &= -r V_1^{\frac{1}{2}} - \sqrt{2} \zeta_2 \beta_{s2} \frac{|L_{psb}(s)|}{\sqrt{2}} \\ &\leq -\beta_2 V^{\frac{1}{2}}, \quad \text{with } \beta_2 = \min\{r, \sqrt{2}\zeta_2 \beta_{s2}\}. \end{aligned} \tag{83}$$

Therefore, the finite time convergence to the domain $|s(t)| \leq \bar{s}_1$ is ensured, and the reaching time τ_2 can be estimated by $\tau_2 \leq \tau_{r2} \leq \dfrac{2V(t_1)^{\frac{1}{2}}}{\beta_2}$ (τ_{r2} is obtained by assuming that $\bar{s}_2 = 0$).

Case 2 Similar to the proof of B.A (Case 2), it can be shown that the sliding variable can

leave the domain $|s(t)| \leq \bar{s}_2$, to the larger domain $|s(t)| \leq \mu_2 < \varepsilon$.
Then, for $|s(t)| \leq \bar{s}_2$, the value of $|\dot{s}(t)|$ can be estimated as

$$\bar{\nu}_2 = h_1 L_{psb}(\bar{s}_2)|\bar{s}_2|^{\frac{1}{2}} + \Big(h_2 L_{psb}^2(\bar{s}_2) + M\Big)\Big(t_2 - T\Big) + |\phi(t_2)|. \tag{84}$$

where t_2 is the time instant when $s(t)$ leaves the domain $|s(t)| \leq \bar{s}_2$. When $|s(t)|$ becomes $\bar{s}_2 < |s(t)| \leq \mu_2$ then

$$\check{\nu}_2 = h_1 L_{psb}(\mu_2)|\mu_2|^{\frac{1}{2}} + \Big(h_2 L_{psb}^2(\mu_1) + M\Big)(t_3 - t_2) + |\phi(t_3)|. \tag{85}$$

where t_3 is the time instant when $s(t)$ enters the domain $|s(t)| \leq \bar{s}_2$. Hence,

$$|\dot{s}(t)| \leq \max\{\bar{\nu}_2, \check{\nu}_2\} = \nu. \tag{86}$$

In conclusion, PSBF can ensure the convergence of the trajectories to the following domain

$$W_2 = \{s(t), \dot{s}(t) : |s(t)| \leq \mu_1, |\dot{s}(t)| \leq \nu(M), \bar{s}_2 < \mu_2 < \varepsilon\} \tag{87}$$

and since $\mu_2 < \varepsilon$, the domain to which converges $|s(t)|$ is predefined. Adaptation with PSBF is proven. □

Theorem. 3.2.1 is proven.

C Parameter values considered in chapter 6

C.A Nominal parameters of WECS

$P_{rated} = 60KW$; $w_L = 2\pi 60 rad/s$; $V_L = 220V$;
$L_s = 223.1mH$; $L_r = 229.3mH$; $L_m = 216.9mH$;
$R_s = 2990m\Omega$; $R_r = 1524m\Omega$; $p = 2$;
$\lambda_{opt} = 7.5$; $r = 5.3m$; $G = 25$;
$J = 3.662Kgm^2$; $\rho = 1.22422Kg/m^3$; $c_1 = 9.5946$;
$c_2 = 12$; $c_3 = c_6 = 0$; $c_4 = 1$;
$c_5 = 20$; $C_{pmax} = 0.4$.

C.B Parameter values of the two adaptive FOSMCs based on PBF, PSBF and APS

Parameters values of the two adaptive FOSMCs based on:

- PBF: $\varepsilon_\tau = 5,\ \varepsilon_Q = 20,\ \bar{K}_\tau = \bar{K}_Q = 15,\ \bar{F}_\tau = \bar{F}_Q = 15$.
- PSBF: $\varepsilon_\tau = 5,\ \varepsilon_Q = 20,\ \bar{K}_\tau = \bar{K}_Q = 15.$
- APS: $\varepsilon_\tau = 5,\ \varepsilon_Q = 20,\ \bar{K}_\tau = \bar{K}_Q = 1000,\ \mu_\tau = \mu_Q = 15.$

C.C Parameter values of the two adaptive STCs based on PBF, PSBF and APS

Parameters values of the two adaptive STCs based on:

- PBF: $\varepsilon_\tau = 5,\ \varepsilon_Q = 20,\ \bar{L}_{1,\tau} = \bar{L}_{1,Q} = 15,\ \bar{F}_\tau = \bar{F}_Q = 2$.
- PSBF: $\varepsilon_\tau = 5,\ \varepsilon_Q = 20,\ \bar{L}_{1,\tau} = \bar{L}_{1,Q} = 15.$
- AST: $\varepsilon_\tau = 5,\ \varepsilon_Q = 20,\ \mu_\tau = \mu_Q = 1,\ w_{1,\tau} = w_{1,Q} = 200,\ \gamma_{1,\tau} = \gamma_{1,Q} = 2,\ \nu_\tau = \nu_Q = \alpha_{m,\tau} = \alpha_{m,Q} = 2.$

D Parameter values considered in chapter 7

D.A Nominal parameters of LIM

TABLE .1: *parameters of LIM*

Inductor resistance Rs [Ω]	11
Induced-part resistance Rr [Ω]	32.57
Inductor inductances Ls [H]	0.6376
3-phase magnetizing inductance Lm [H]	0.5175
Primary mass M [Kg]	20
Viscous friction D [m/s]	20
Pole-pairs p	3
Inductor length τ_m [m]	1.5
Pole pitch h [m]	0.1

D.B Parameter values of the two BAISMCs

Parameters values of the two BAISMCs:

- DISMC based on PBF: $\varepsilon_\nu = 10,\ \varepsilon_\psi = 10,\ \bar{F}_\nu = \bar{F}_\psi = 6.$

- CISMC based on PBF: $\varepsilon_\nu = 10$, $\varepsilon_\psi = 10$, $\bar{F}_\nu = \bar{F}_\psi = 1$.

D.C Parameter values of the two adaptive DHOSMCs based on growing gain strategy and dual layer strategy

Parameters values of the two adaptive DHOSMCs based on:

- Growing gain strategy: $\bar{\alpha}_\nu = 50$, $\bar{\alpha}_\psi = 50$, $\alpha_\nu(0) = 5$, $\alpha_\psi(0) = 5$, $\varepsilon_\nu^* = 0.1$, $\varepsilon_\psi^* = 0.2$.
- Dual layer strategy: $\bar{\alpha}_\nu = 50$, $\bar{\alpha}_\psi = 50$, $\alpha_\nu(0) = 5$, $\alpha_\psi(0) = 5$, $\varepsilon_\nu^* = 0.1$, $\varepsilon_\psi^* = 0.2$, $\varepsilon_\nu = 10$, $\varepsilon_\psi = 10$, $\bar{F}_\nu = \bar{F}_\psi = 1$.

Résumé :

Cette thèse porte sur le développement de nouvelles stratégies de commande et d'observation adaptatives par Modes Glissants (MG) et par Modes Glissants d'Ordres Supérieurs (MGOS). En effet, la mise en œuvre des commandes par MG et MGOS classiques nécessite la connaissance des limites supérieures des perturbations ou de leurs dérivées, souvent inconnues. Le premier apport de cette thèse est la synthèse d'une stratégie d'adaptation permettant d'assurer la convergence de la variable de glissement vers un voisinage prédéfini de zéro sans nécessiter d'informations sur les perturbations ou leurs dérivées et sans surestimation du gain. Cette stratégie est ensuite déclinée pour concevoir : deux commandes par MG d'ordre 1 et 2, une commande par mode glissant intégral, ainsi qu'une version du différenciateur de Levant. La deuxième contribution de la thèse est la mise au point de deux commandes adaptatives par MGOS discontinues. Ces deux algorithmes assurent un mode glissant d'ordre n en s'affranchissant de la connaissance de la limite supérieure de la perturbation et de sa dérivée. Enfin, afin de montrer l'efficacité des algorithmes proposés, ils sont appliqués avec succès à travers des simulations pour la commande d'un système de conversion de l'énergie éolienne et la commande d'un moteur à induction linéaire pour la cogénération.

Mots clés : Mode glissant, modes glissant d'ordre supérieur, super-twisting adaptataif, fonction barrière de Lyapunov, systèmes de conversion de l'énergie.

Abstract:

This thesis deals with the development of novel strategies to adapt higher order sliding mode controllers and observers. The implementation of classics first order and higher order sliding mode controllers requires the knowledge of the upper bound of the disturbance or its derivative, which are often not known. The first contribution of this thesis is the design of an adaptive strategy that can ensure the convergence of the sliding variable to a predefined neighborhood of zero without requiring any information of the disturbance or its derivative and without overestimating the adaptive gain. This adaptive strategy is then declined for the design of the first order, second order and integral sliding mode controllers, and for the Levant's differentiator. The second contribution of the thesis is the development of two adaptive strategies for discontinuous higher order sliding mode control. The proposed two algorithms can provide the achievement of n-order sliding mode despite disturbances with unknown upper bounds or with unknown upper bounds of their derivatives. Finally, in order to show the effectiveness of the proposed algorithms, they are successfully applied through simulations to control the wind energy conversion system and the linear induction motor system for cogeneration.

Keywords: adaptive sliding mode, adaptive super-twisting, adaptive higher order sliding mode, Barrier Lyapunov Function, energy conversion system.

SPIM

■ École doctorale SPIM - Université de Technologie Belfort-Montbéliard
F - 90010 Belfort Cedex ■ tél. +33 (0)3 84 58 31 39
■ ed-spim@univ-fcomte.fr ■ www.ed-spim.univ-fcomte.fr

utbm
université de technologie
Belfort-Montbéliard